SUPPORTING INFORMATION

Transformations of diphenylphosphinothioic acid tertiary amides mediated by the directed ortho metallation

Hajar el Hajjouji,[a] *Eva Belmonte,*[a] *Jesús García-López,*[a] *Ignacio Fernández,*[a] *María José Iglesias,*[a] *Laura Roces,*[b,c] *Santiago García-Granda,*[b] *Anas El Laghdach,*[d] *and Fernando López Ortiz,**[,a]

[a] Área de Química Orgánica, Universidad de Almería, Carretera de Sacramento, 04120, Almería. Spain.
[b] Departamento de Química Física y Analítica, Universidad de Oviedo, Avda. Julián Clavería 8, 33006 , Spain.
[c] Servicios Científico Técnicos, Universidad de Oviedo, 33006 Oviedo, Spain.
[d]Département de Chimie, Faculté des Sciences, Université Abdelmalek Essaâdi, BP. 2121, MhannechII, 93002 Tétouan, Maroc.

Contents

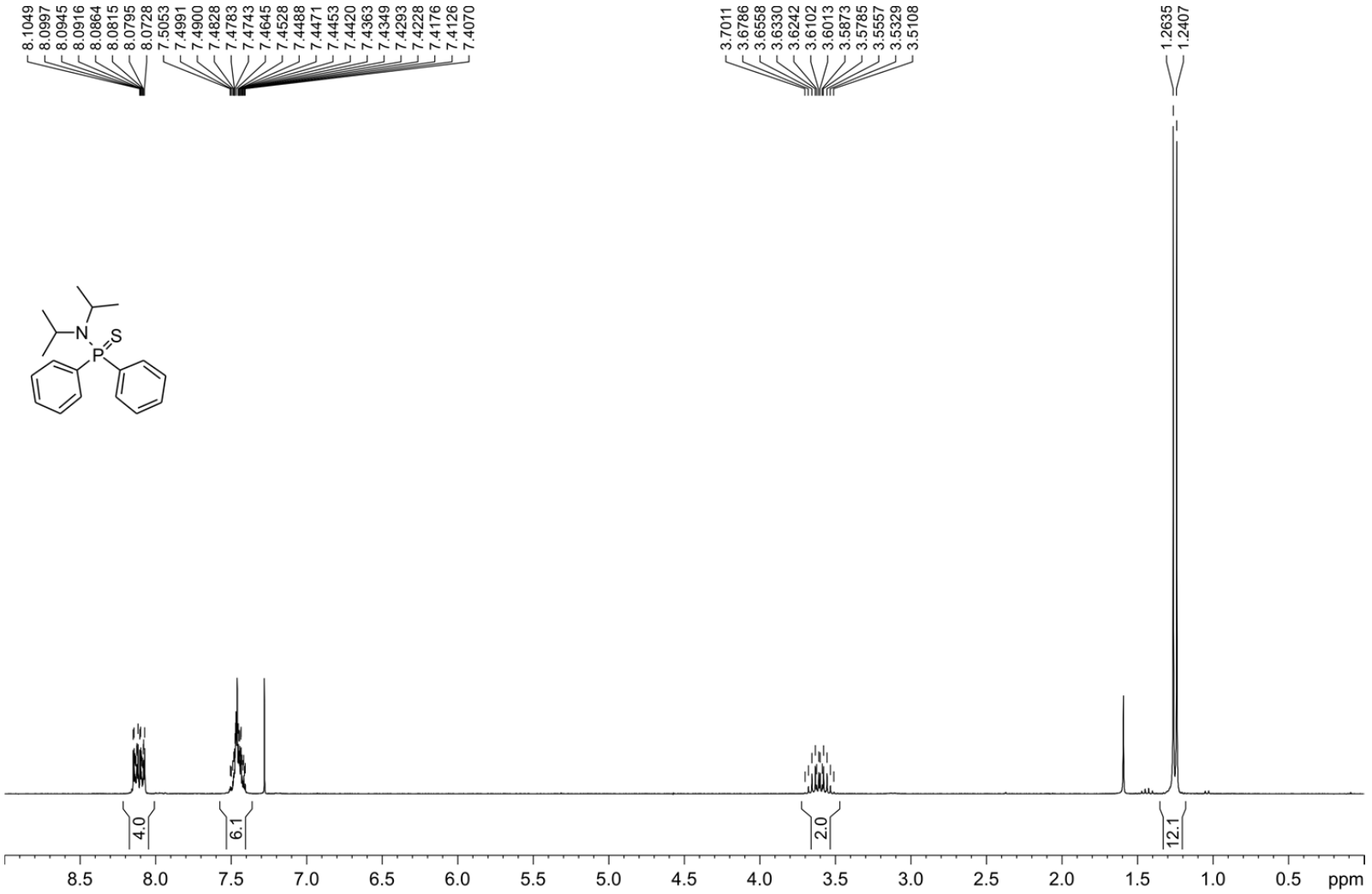

Figure S1. ^{1}H NMR spectrum (300.13 MHz) of **7** in $CDCl_3$.

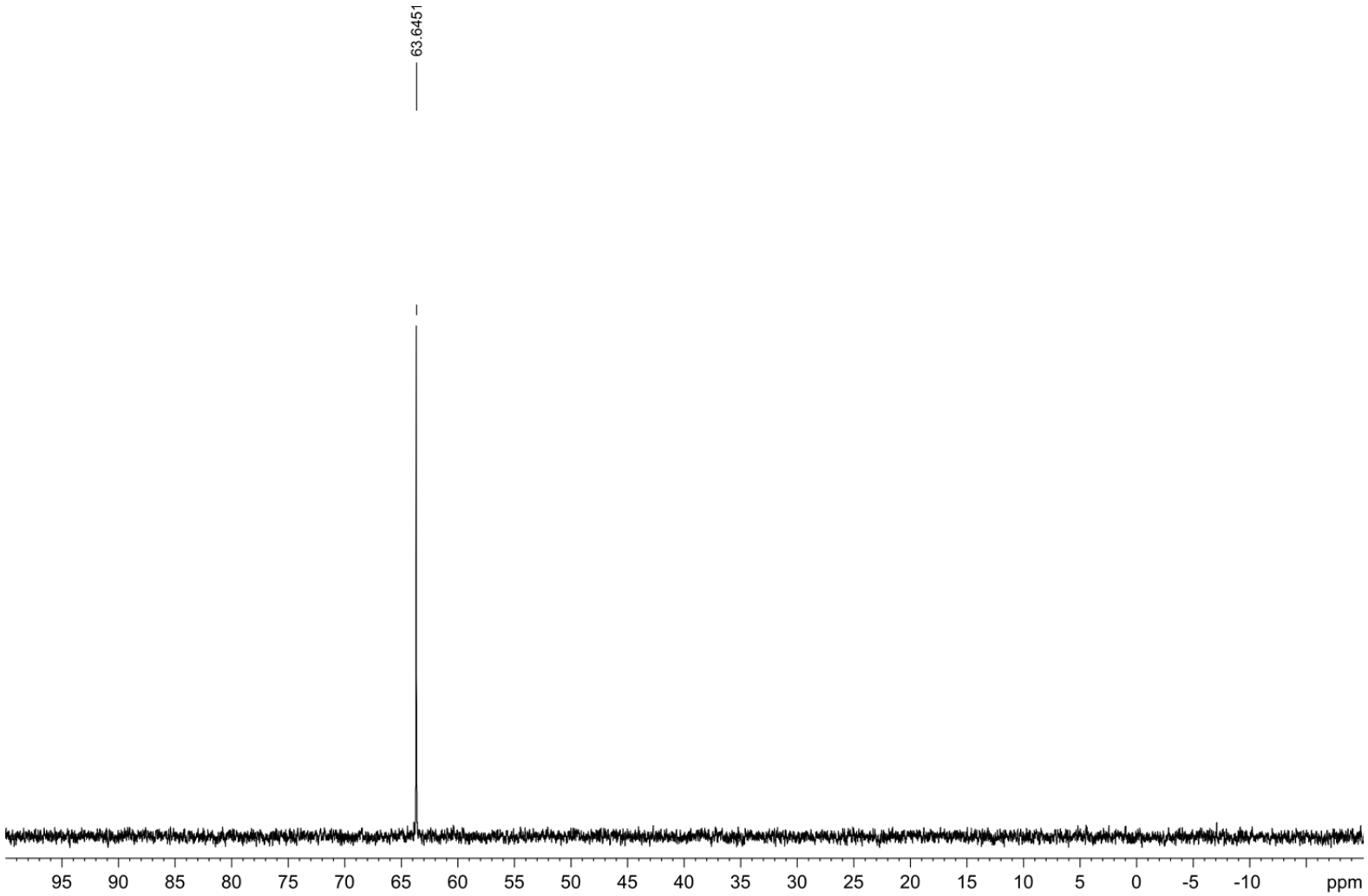

Figure S2. ^{31}P NMR spectrum (121.47 MHz) of **7** in $CDCl_3$.

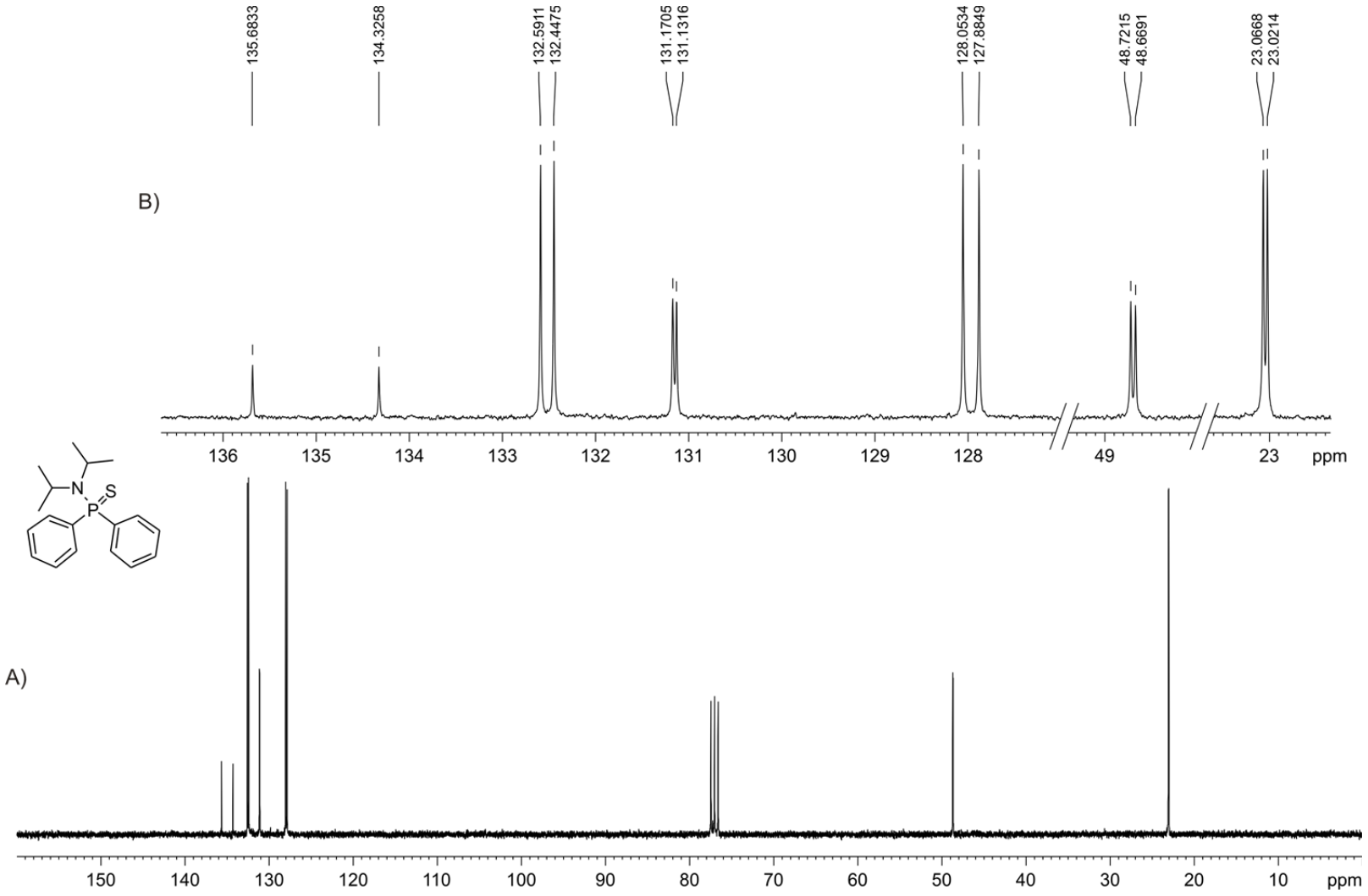

Figure S3. A) ^{13}C NMR spectrum (75.47 MHz) of **7** in $CDCl_3$. B) Expansion of A).

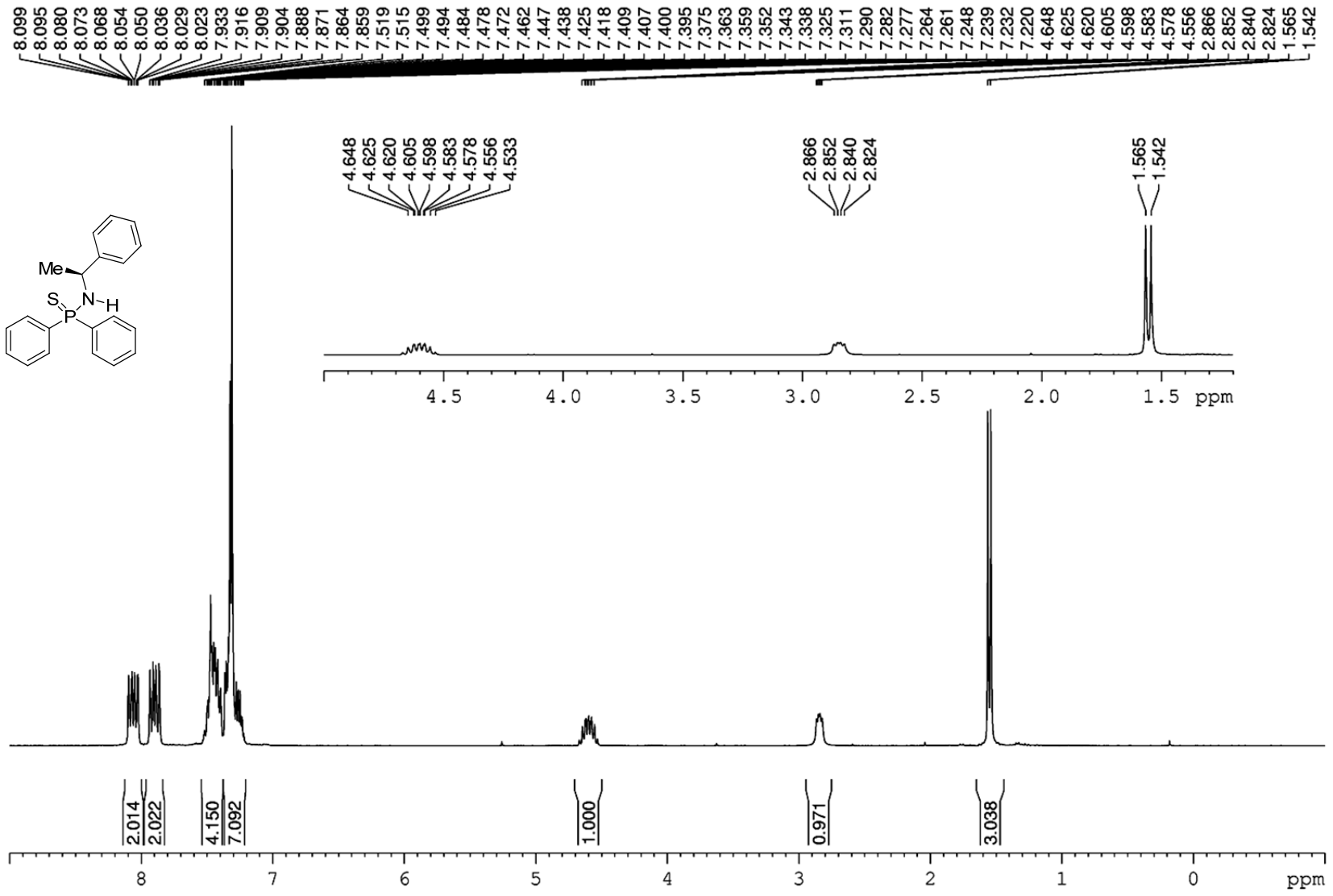

Figure S4. ^{1}H NMR spectrum (300.13 MHz) of **23** in $CDCl_3$.

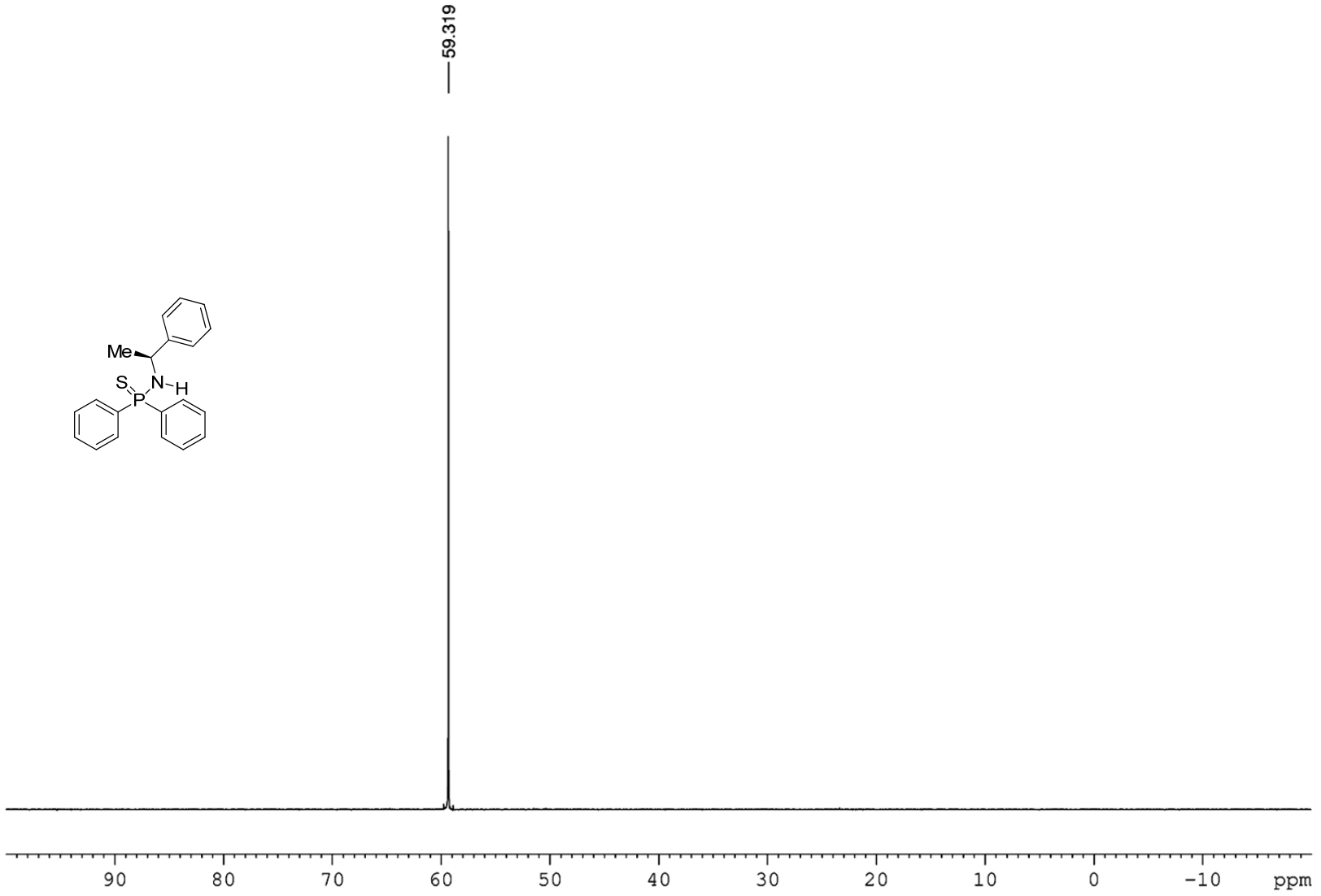

Figure S5. ^{31}P NMR spectrum (121.47 MHz) of **23** in $CDCl_3$.

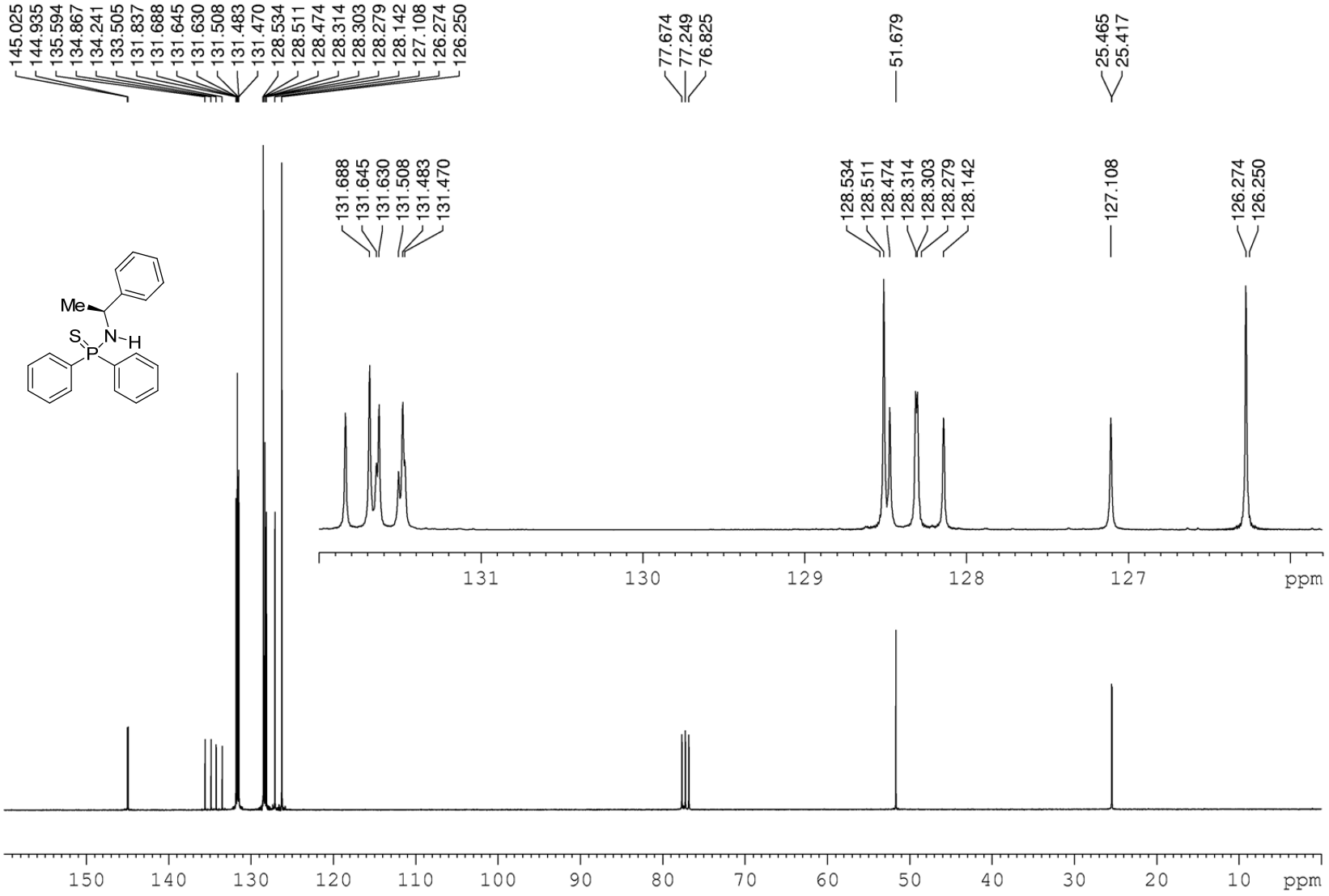

Figure S6. ^{13}C NMR spectrum (75.47 MHz) of **23** in $CDCl_3$.

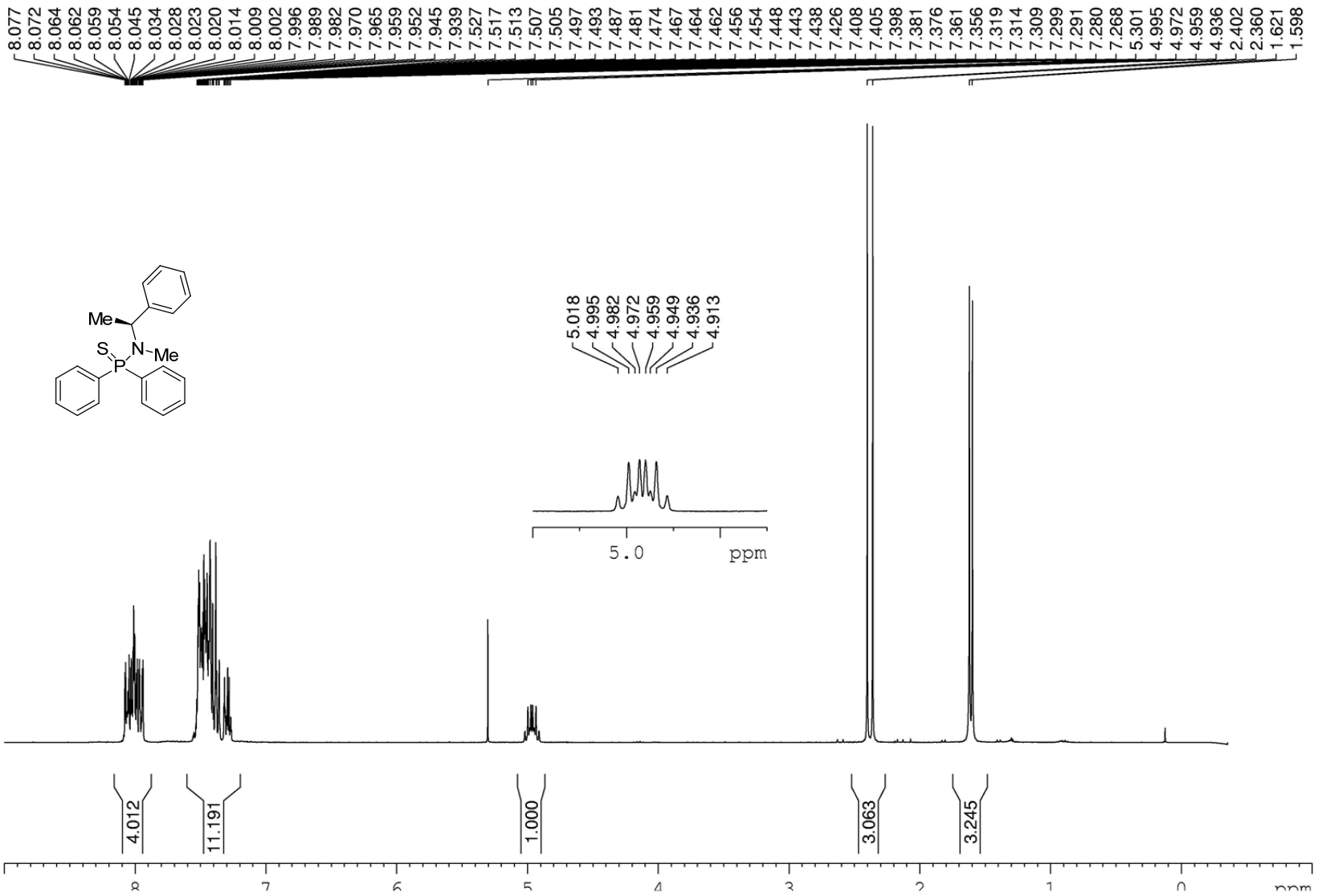

Figure S7. ^{1}H NMR spectrum (300.13 MHz) of **24** in $CDCl_3$.

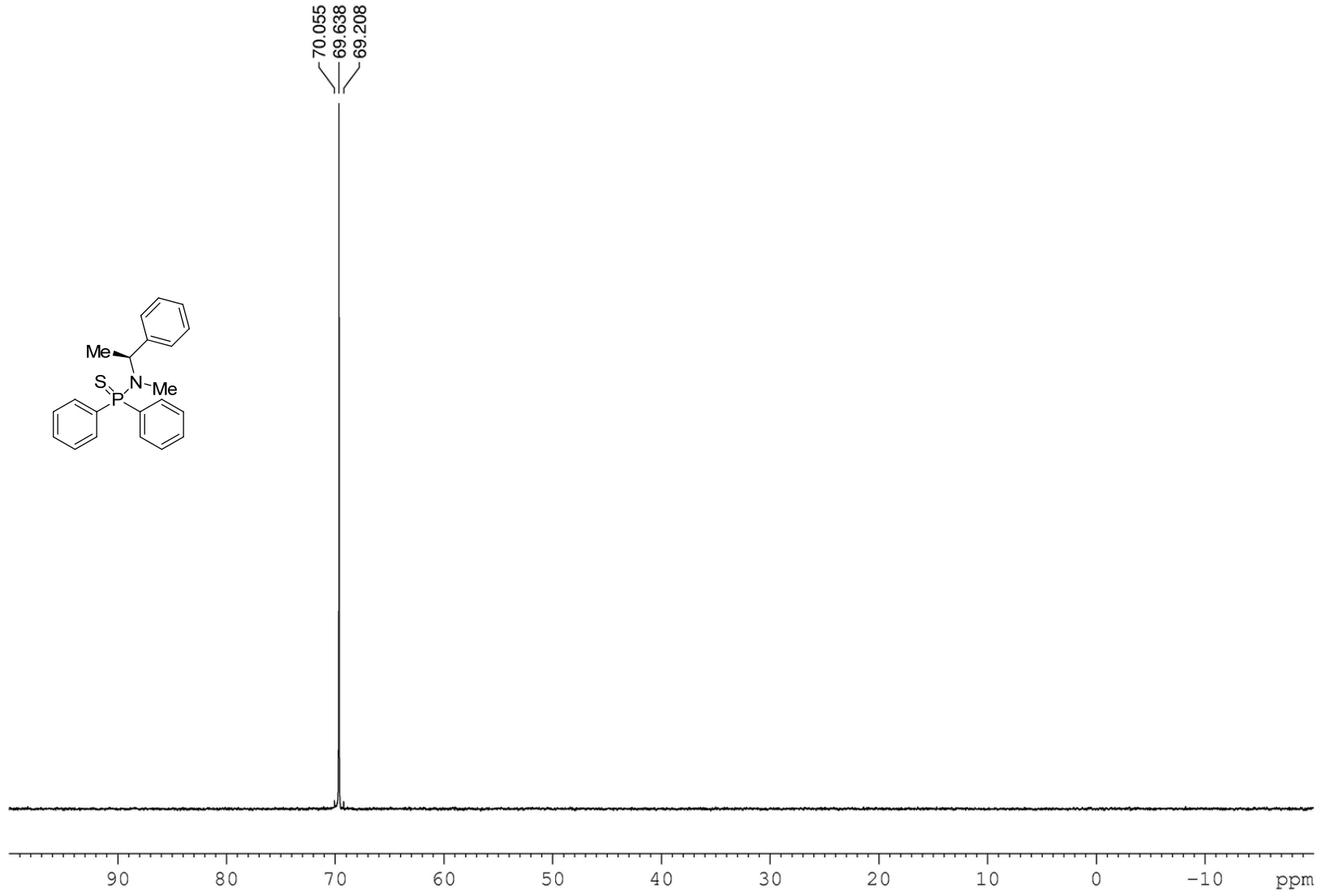

Figure S8. ^{31}P NMR spectrum (121.47 MHz) of **24** in $CDCl_3$.

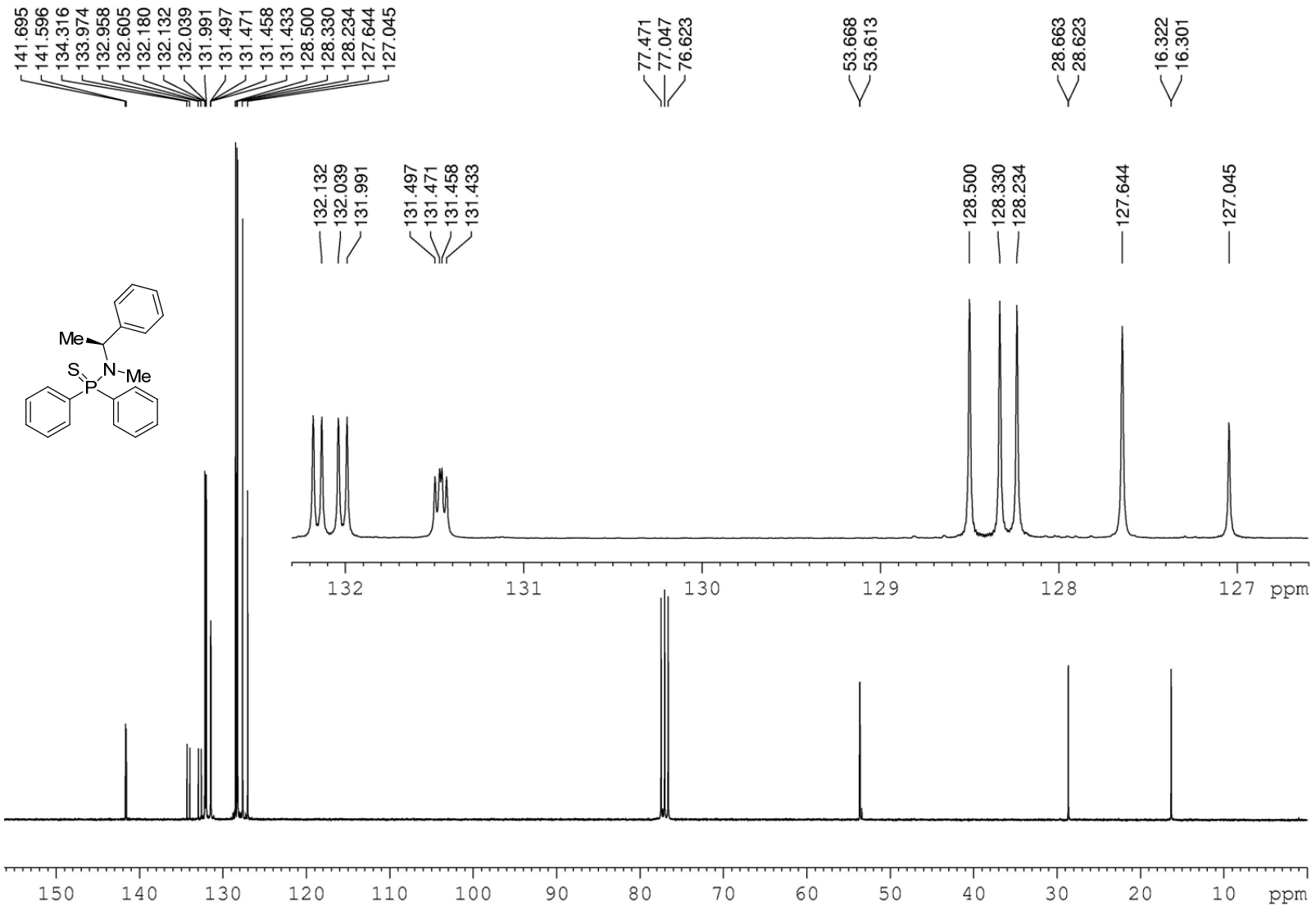

Figure S9. ^{13}C NMR spectrum (75.47 MHz) of **24** in $CDCl_3$.

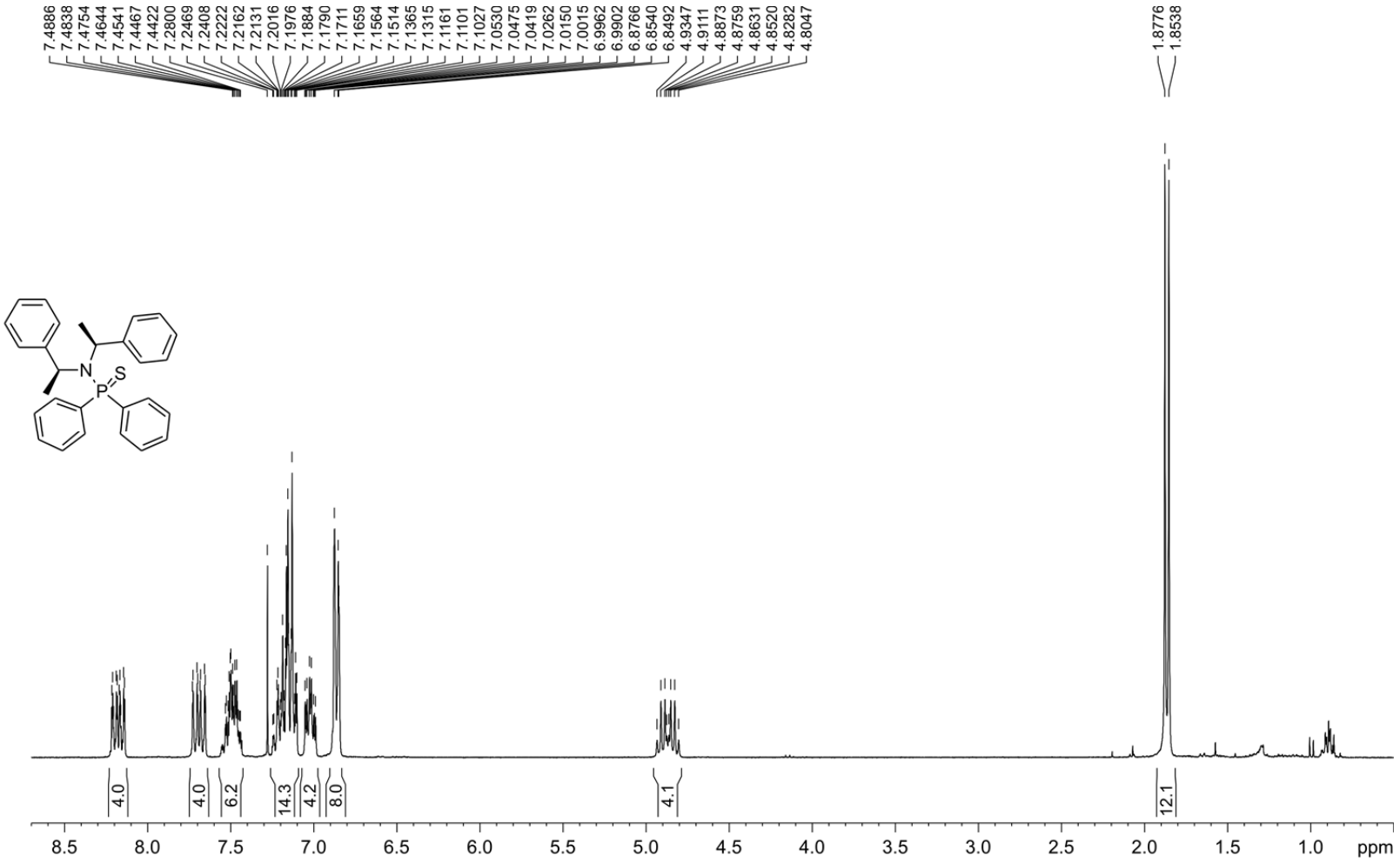

Figure S10. ^{1}H NMR spectrum (300.13 MHz) of **26** in $CDCl_3$.

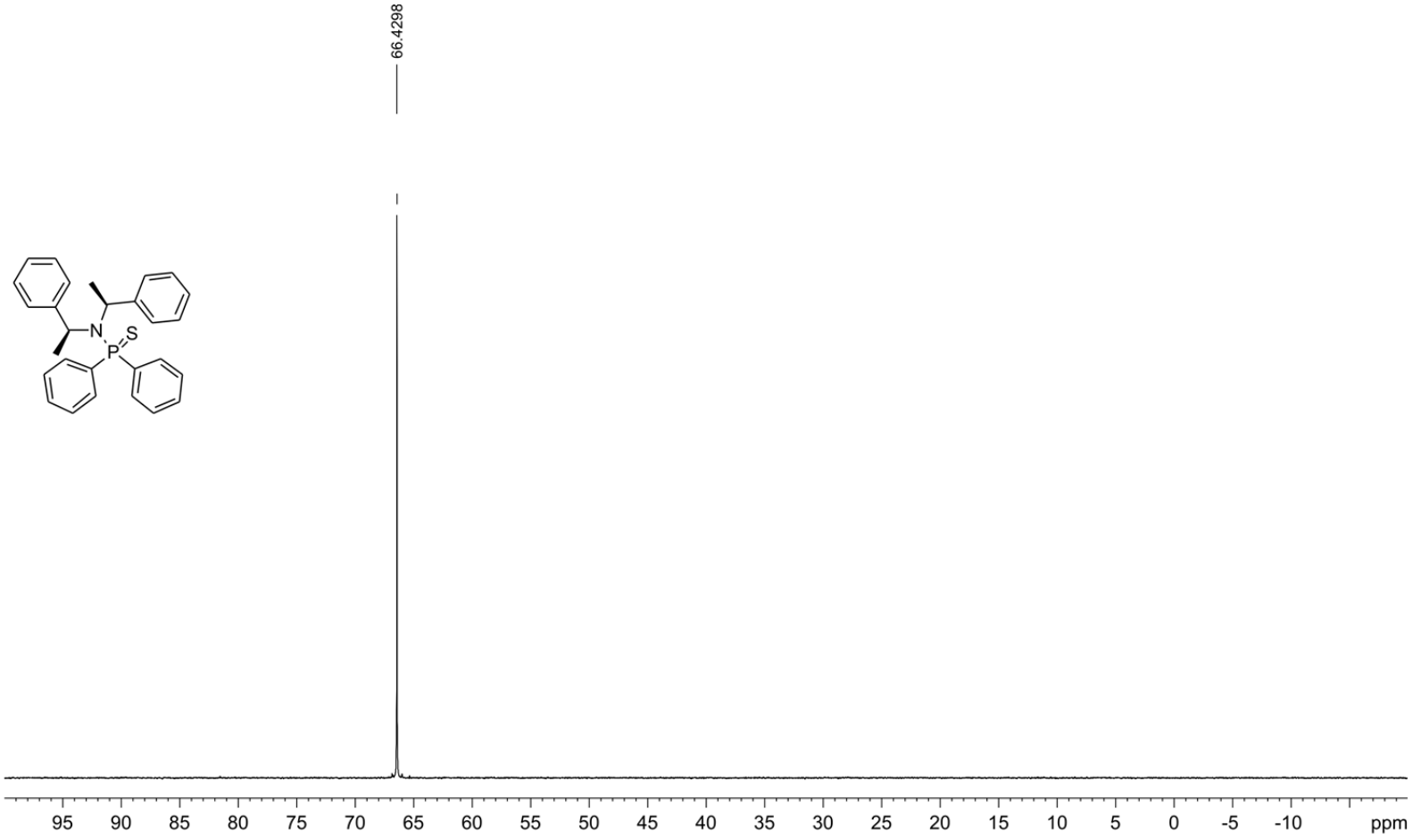

Figure S11. ^{31}P NMR spectrum (121.47 MHz) of **26** in $CDCl_3$.

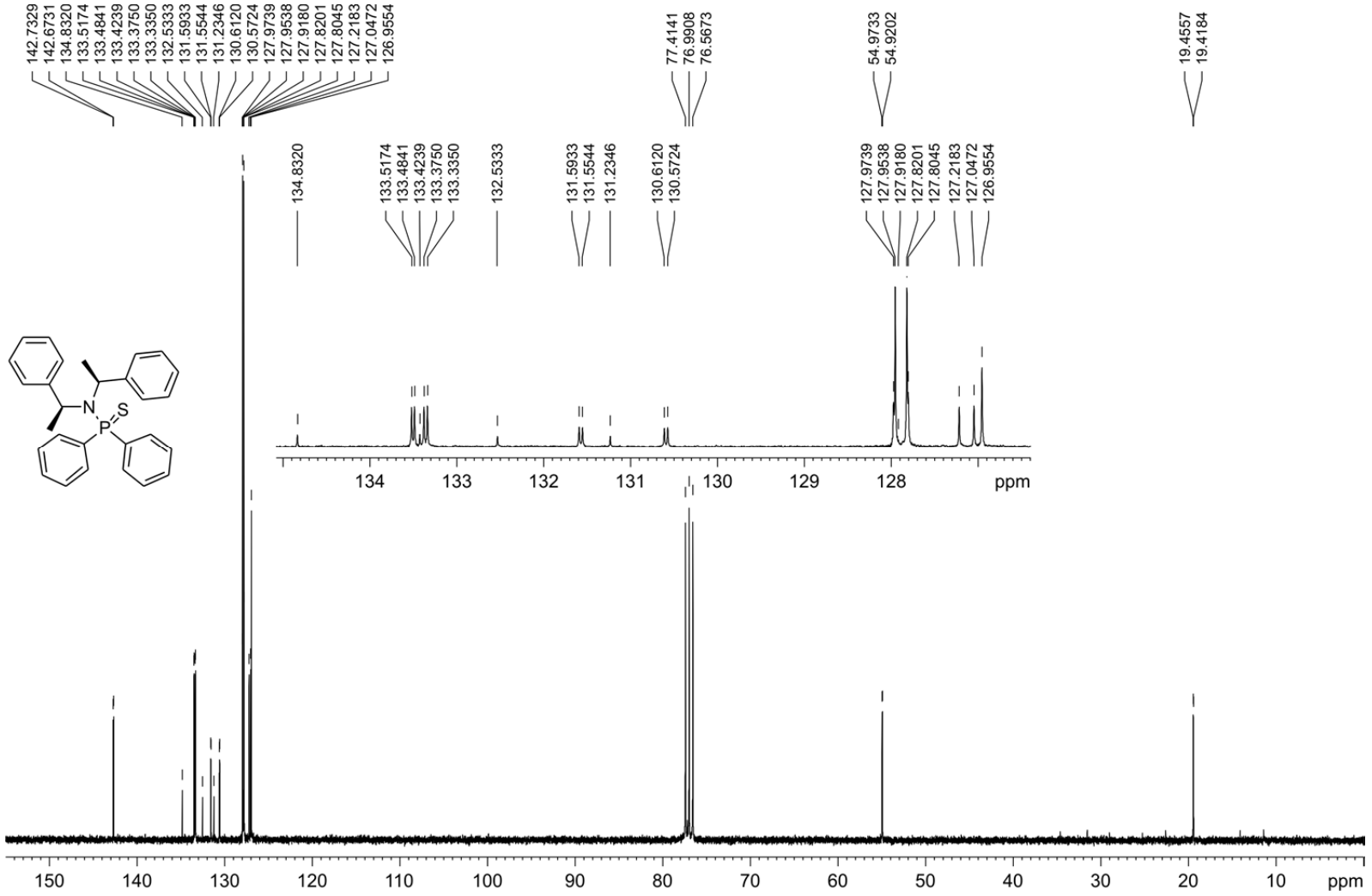

Figure S12. ^{13}C NMR spectrum (75.47 MHz) of **26** in $CDCl_3$.

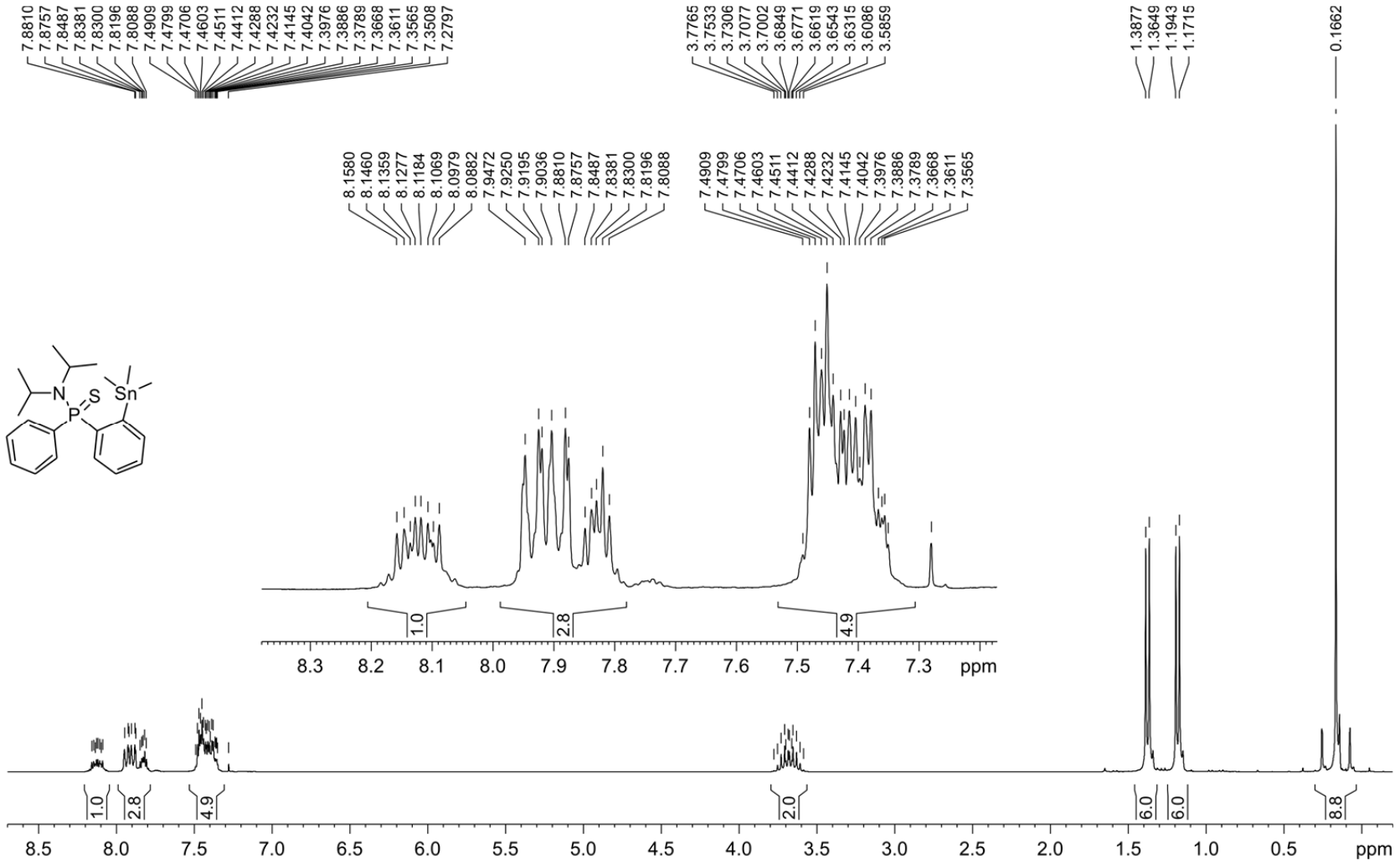

Figure S13. ^{1}H NMR spectrum (300.13 MHz) of **9** in $CDCl_3$.

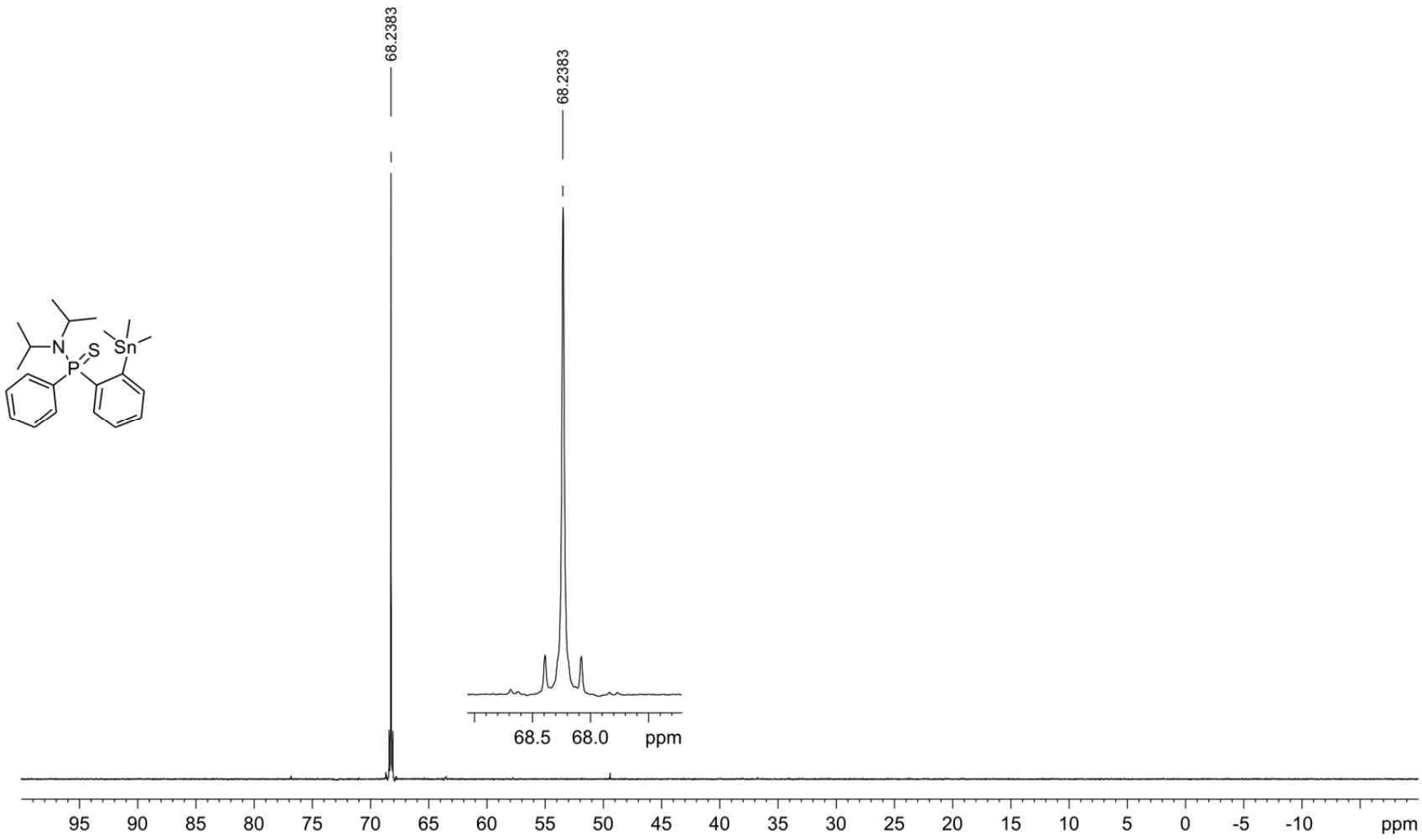

Figure S14. ^{31}P NMR spectrum (121.47 MHz) of **9** in $CDCl_3$.

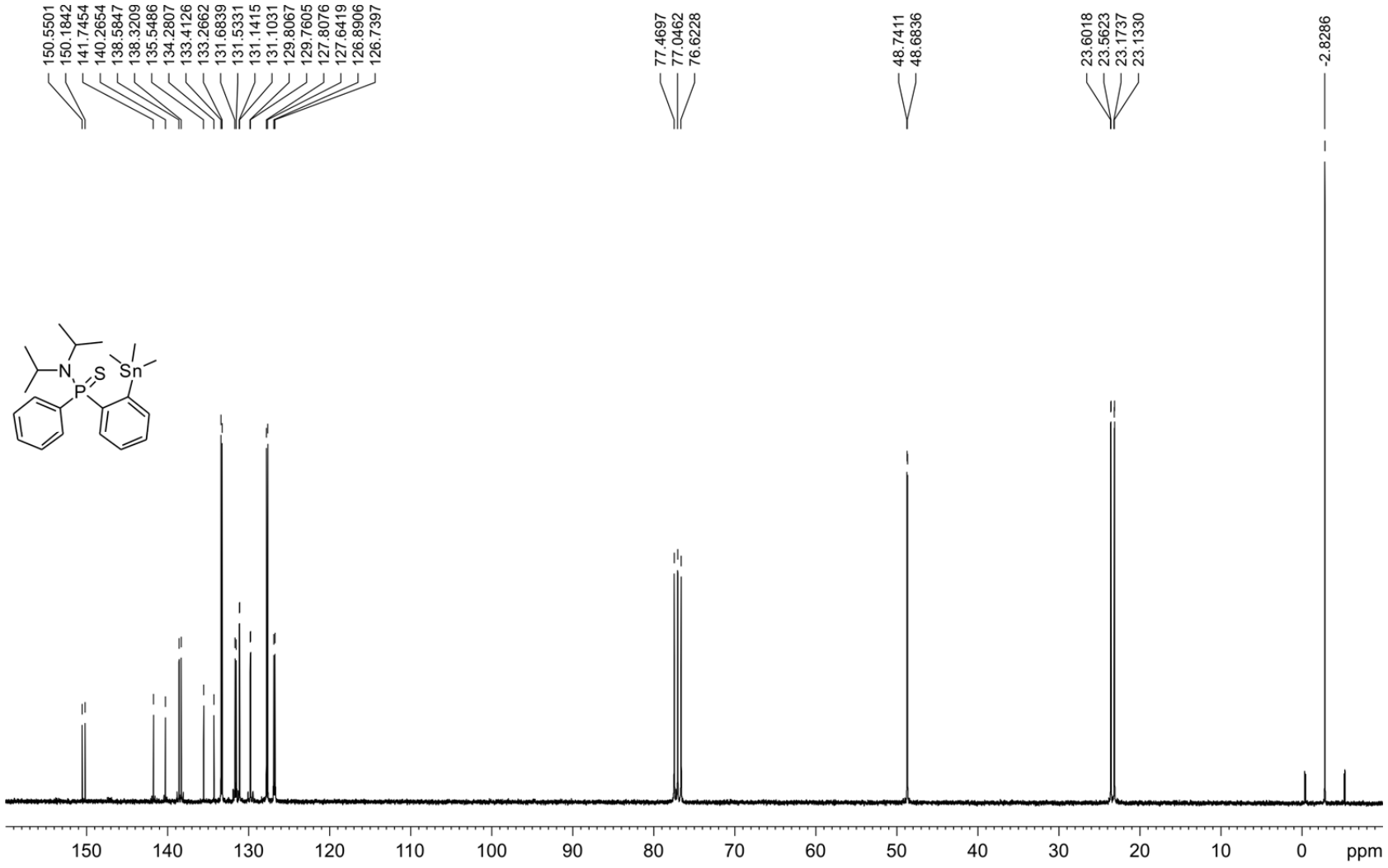

Figure S15. ^{13}C NMR spectrum (75.47 MHz) of **9** in $CDCl_3$.

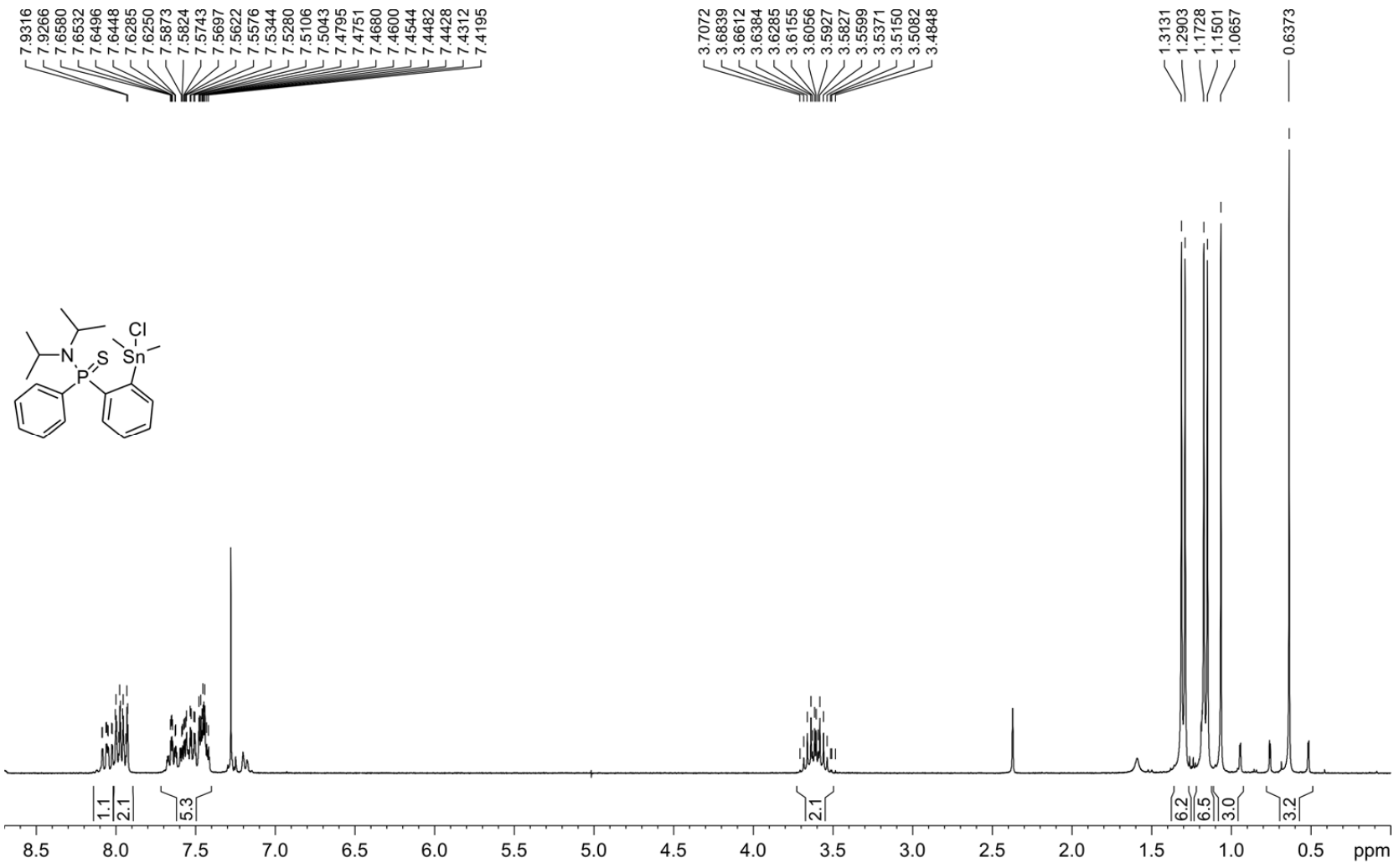

Figure S16. ^{1}H NMR spectrum (300.13 MHz) of **10** in $CDCl_3$.

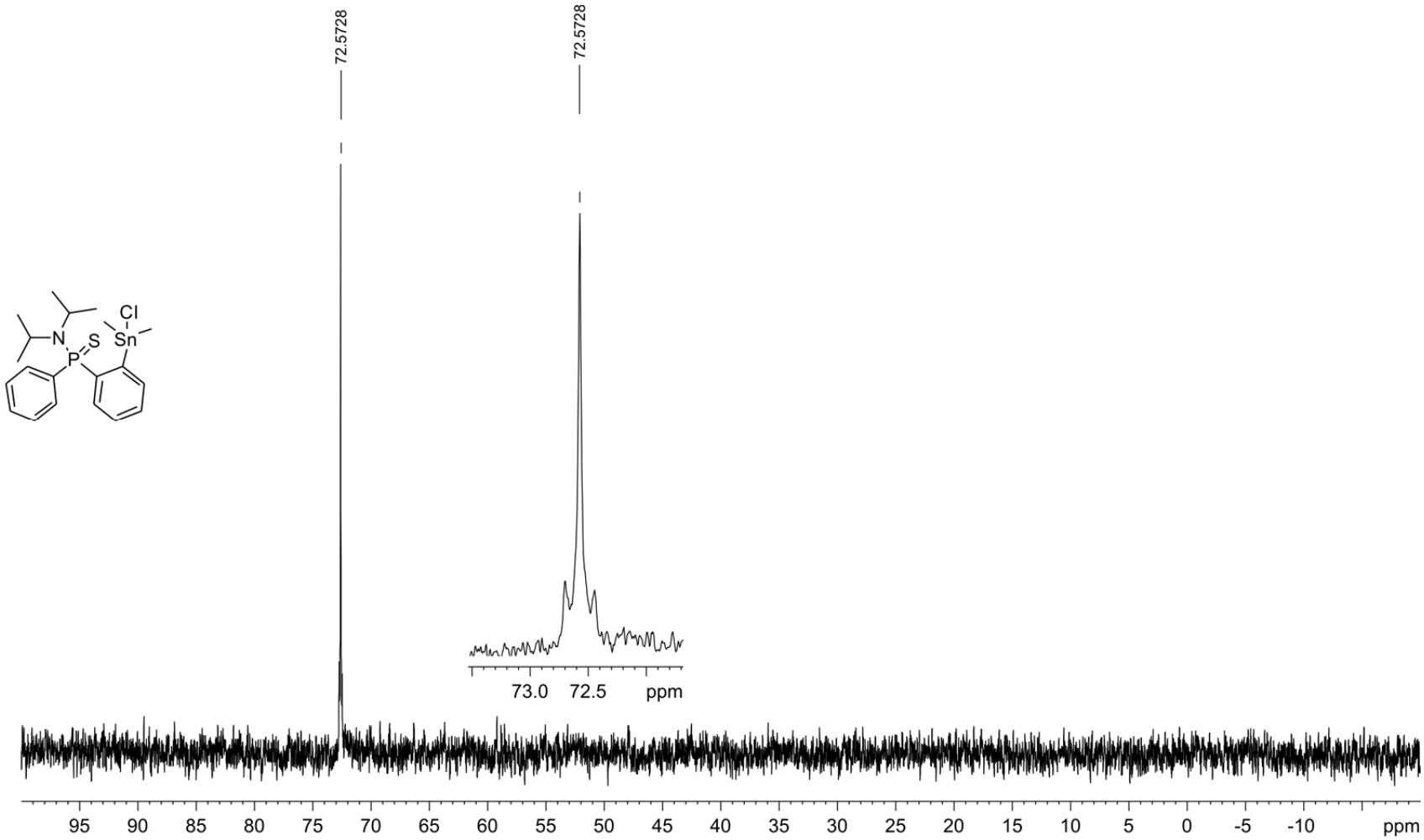

Figure S17. ^{31}P NMR spectrum (121.47 MHz) of **10** in $CDCl_3$.

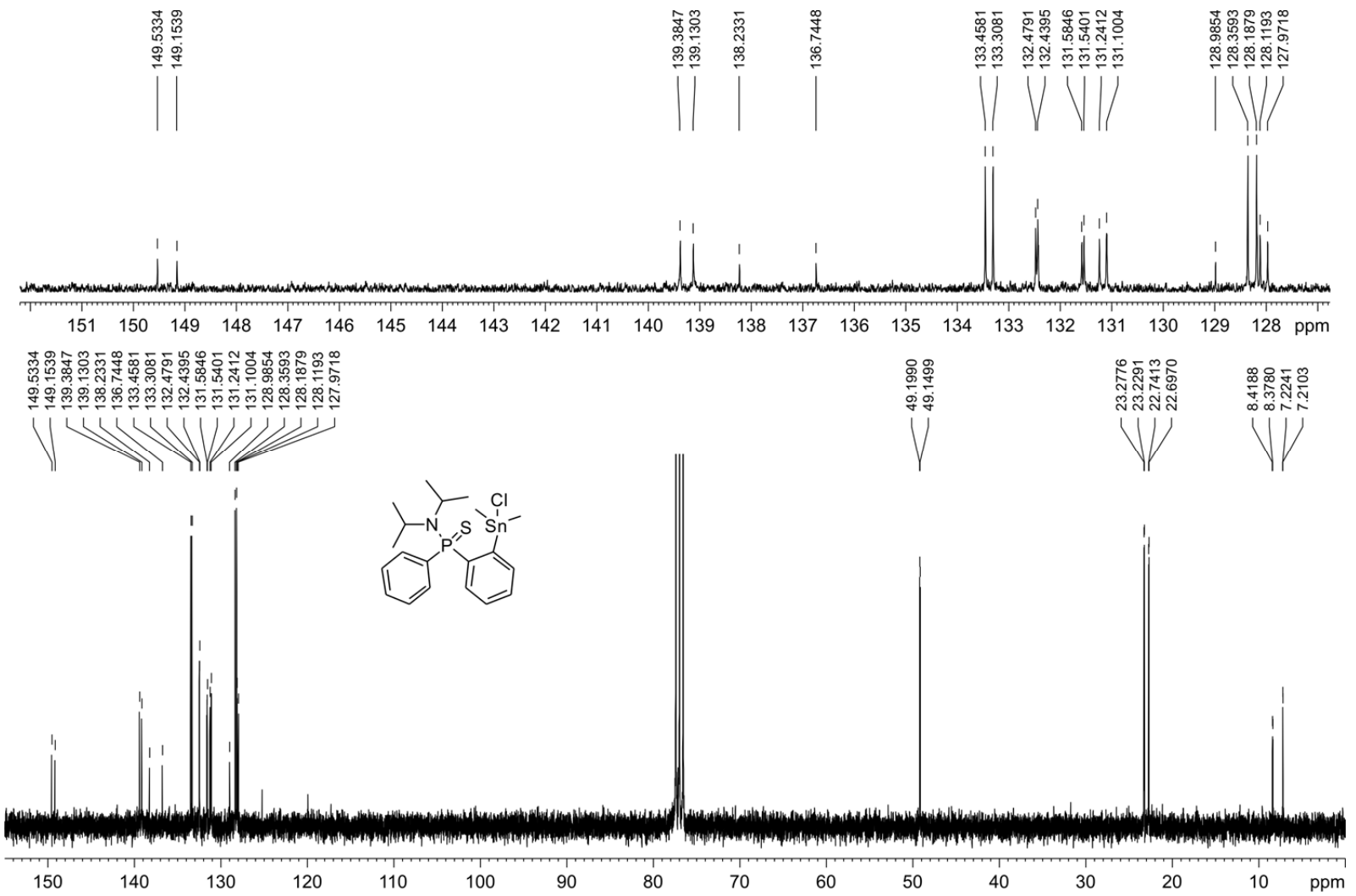

Figure S18. ^{13}C NMR spectrum (75.47 MHz) of **10** in $CDCl_3$.

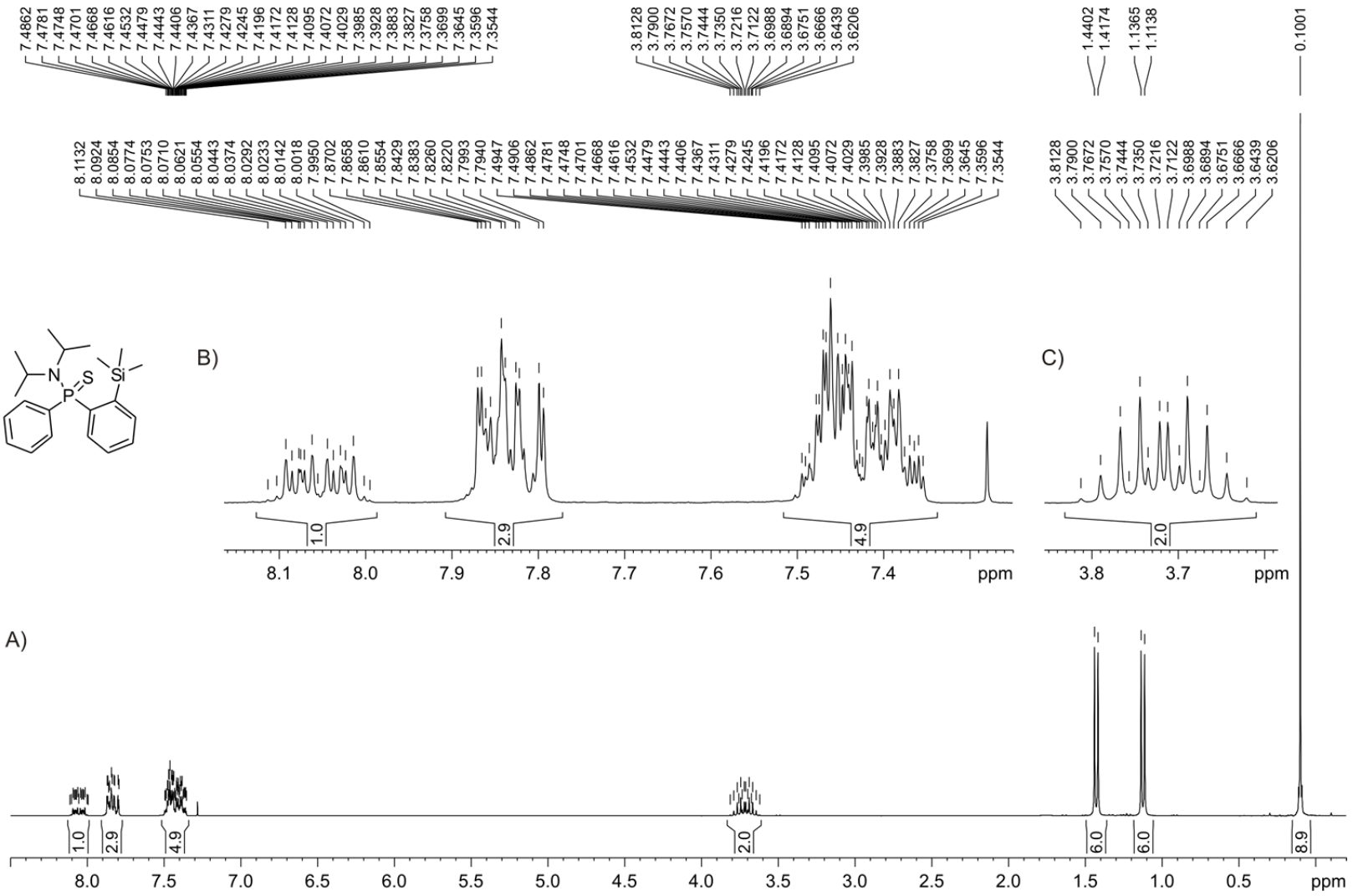

Figure S19. ^{1}H NMR spectrum (300.13 MHz) of **11** in $CDCl_3$.

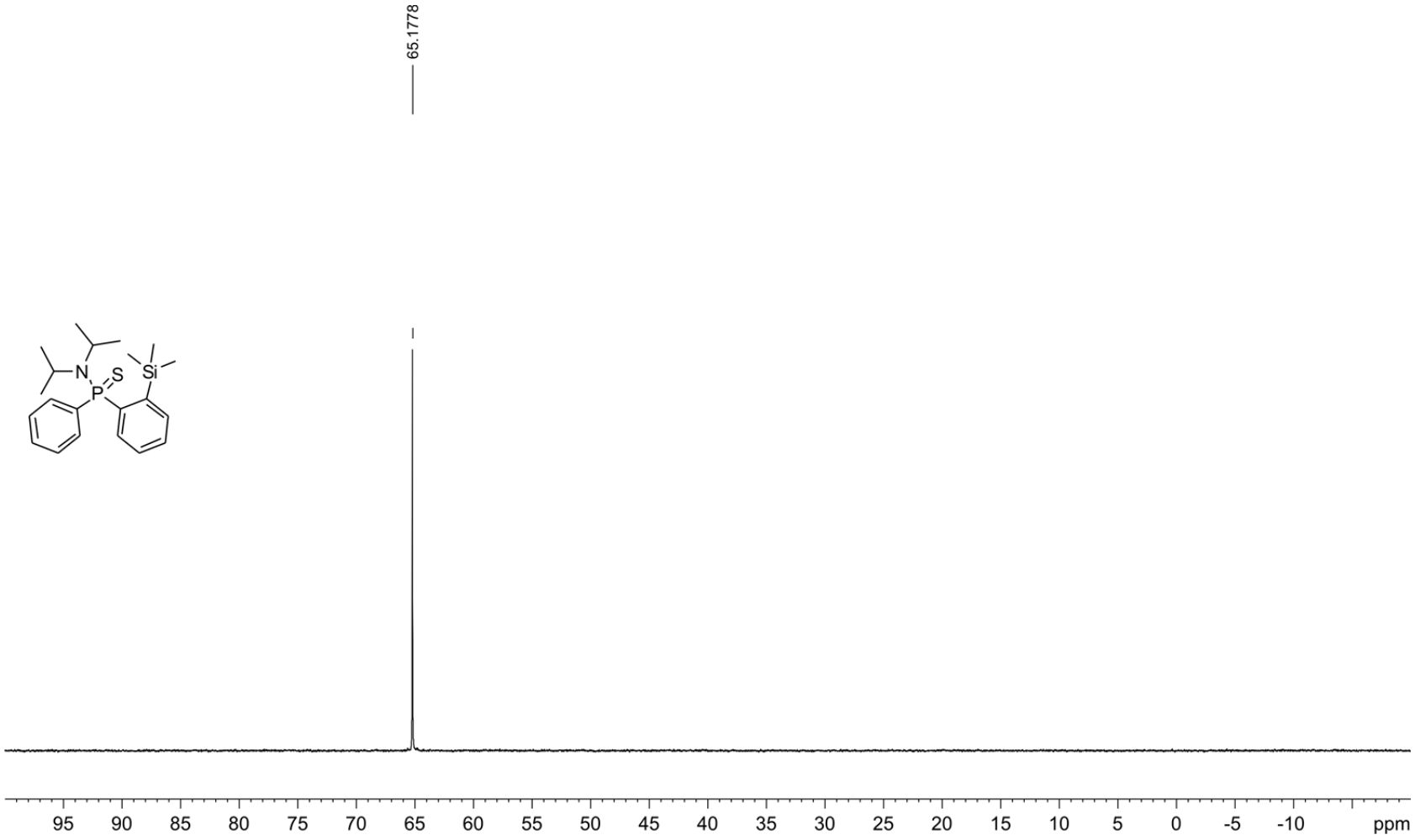

Figure S20. ^{31}P NMR spectrum (121.47 MHz) of **11** in $CDCl_3$.

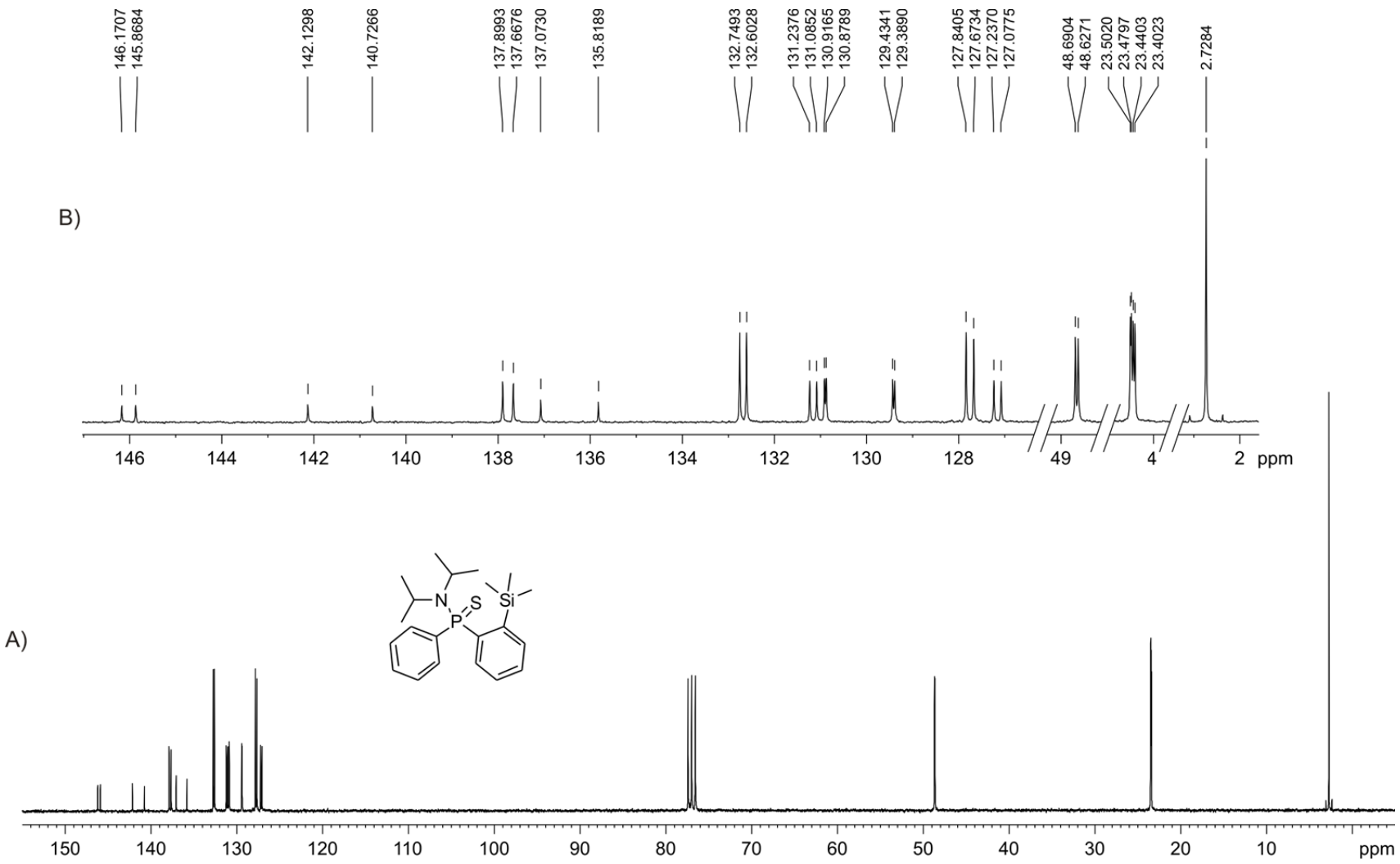

Figure S21. ^{13}C NMR spectrum (75.47 MHz) of **11** in $CDCl_3$.

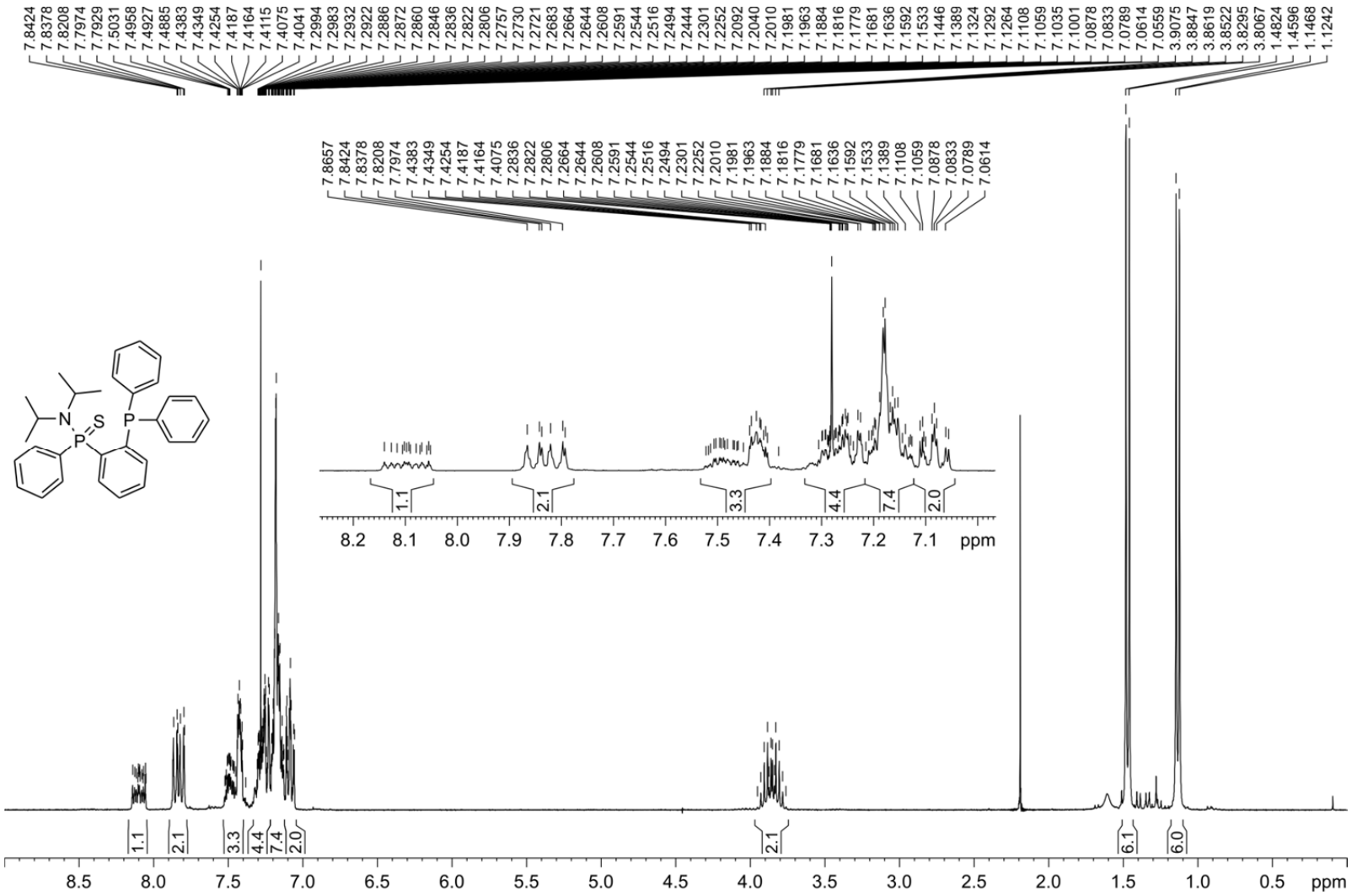

Figure S22. ^{1}H NMR spectrum (300.13 MHz) of **12** in $CDCl_3$.

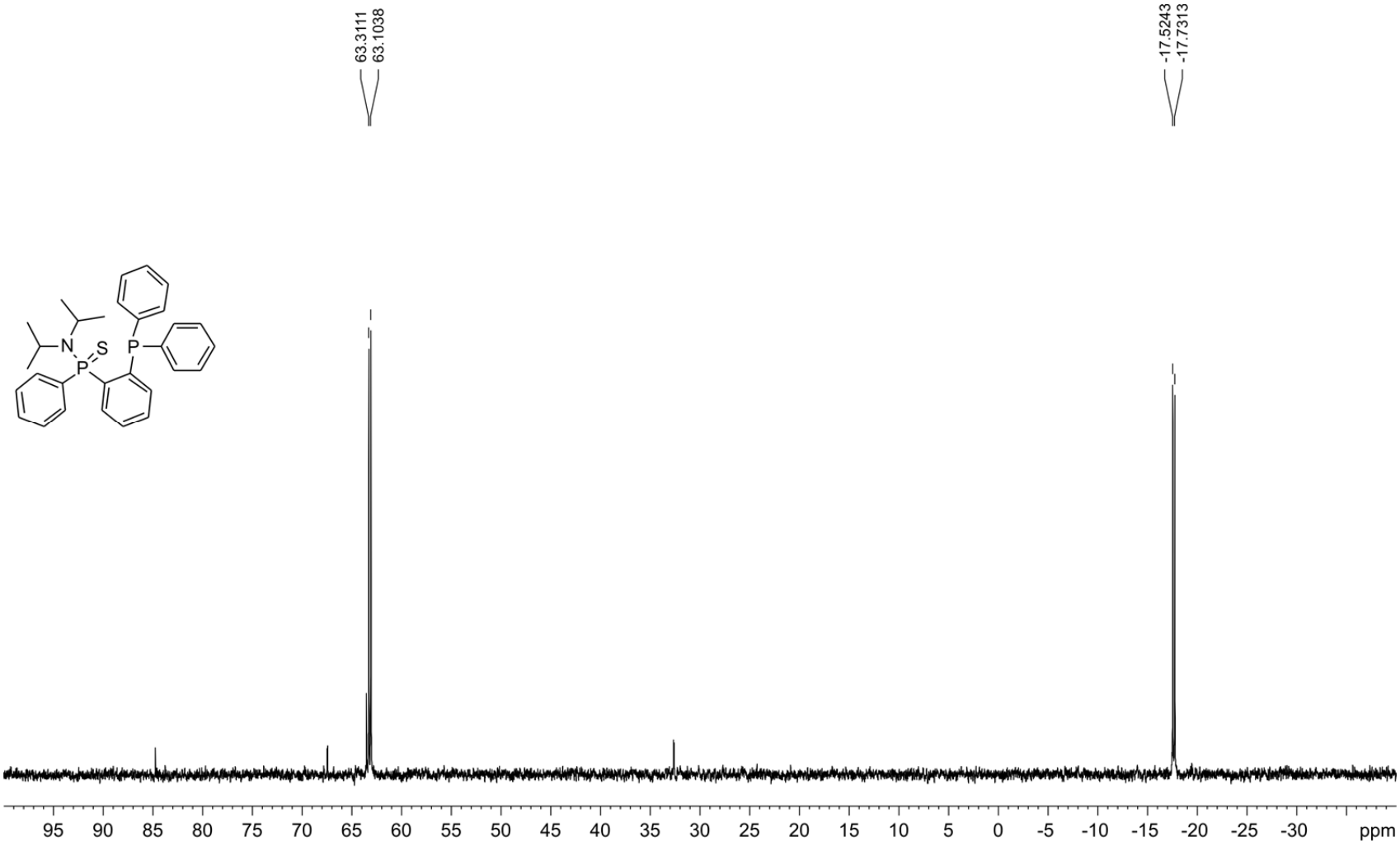

Figure S23. ^{31}P NMR spectrum (121.47 MHz) of **11** in $CDCl_3$.

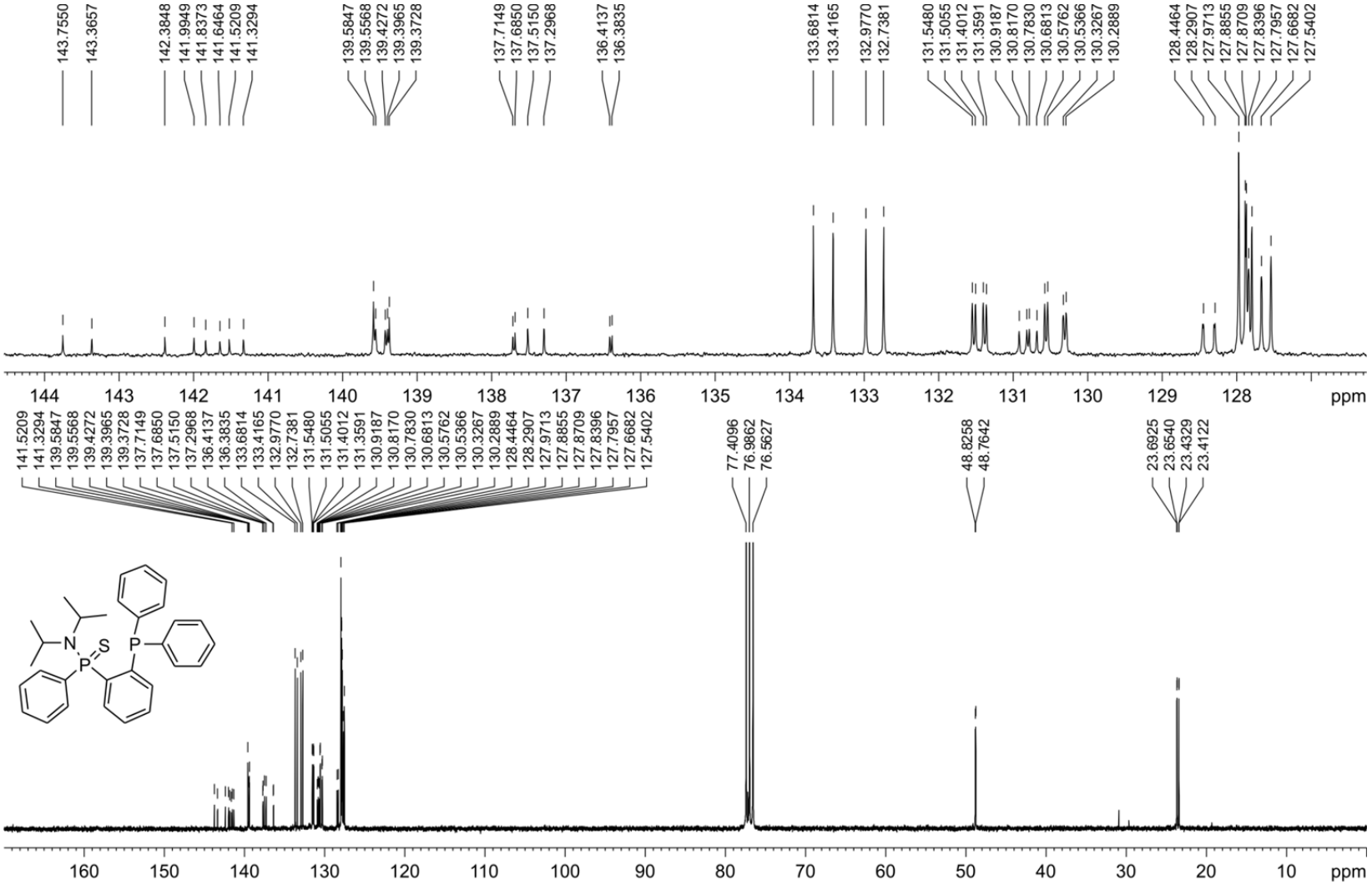

Figure S24. ^{13}C NMR spectrum (75.47 MHz) of **12** in $CDCl_3$.

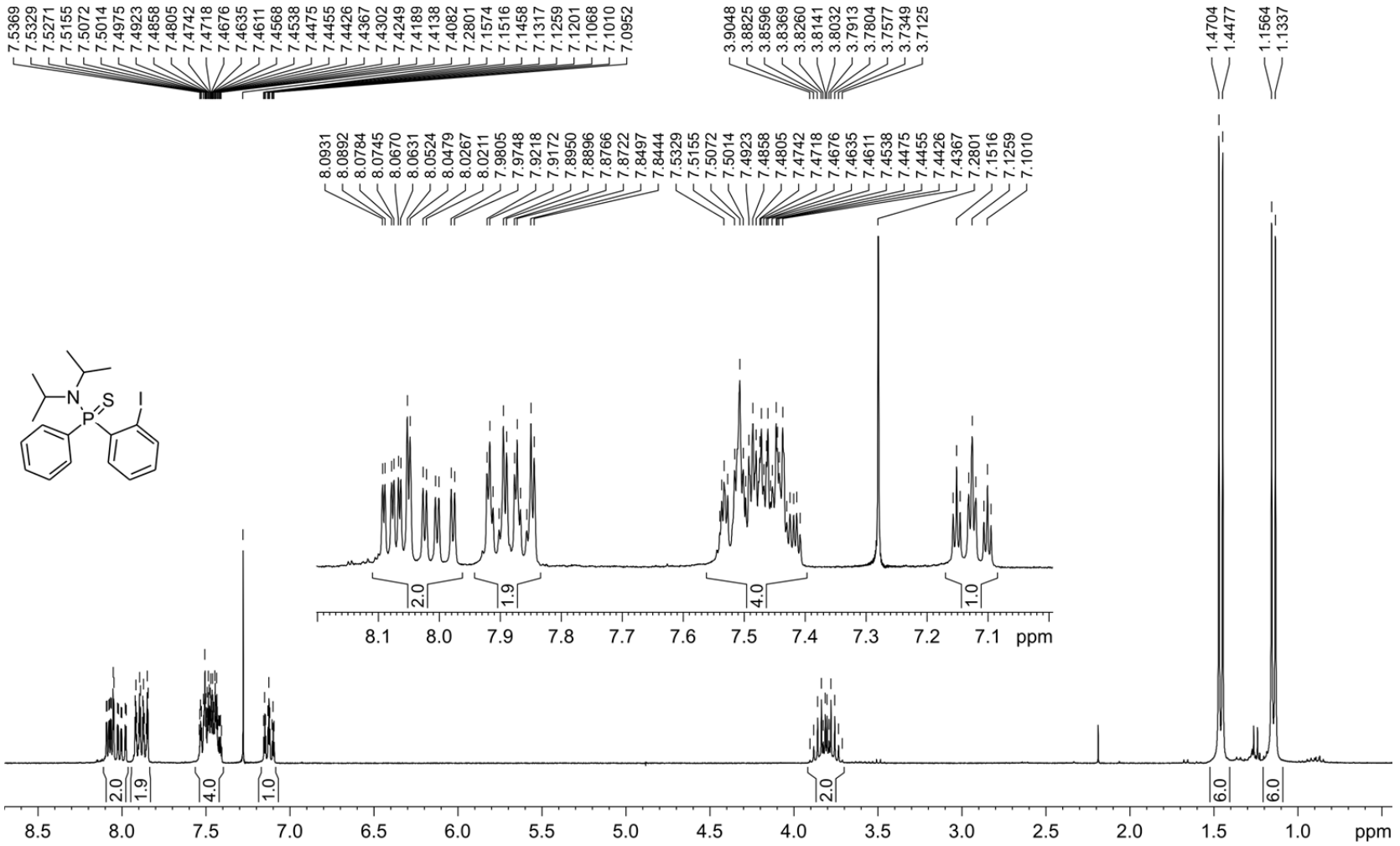

Figure S25. ^{1}H NMR spectrum (300.13 MHz) of **13** in $CDCl_3$.

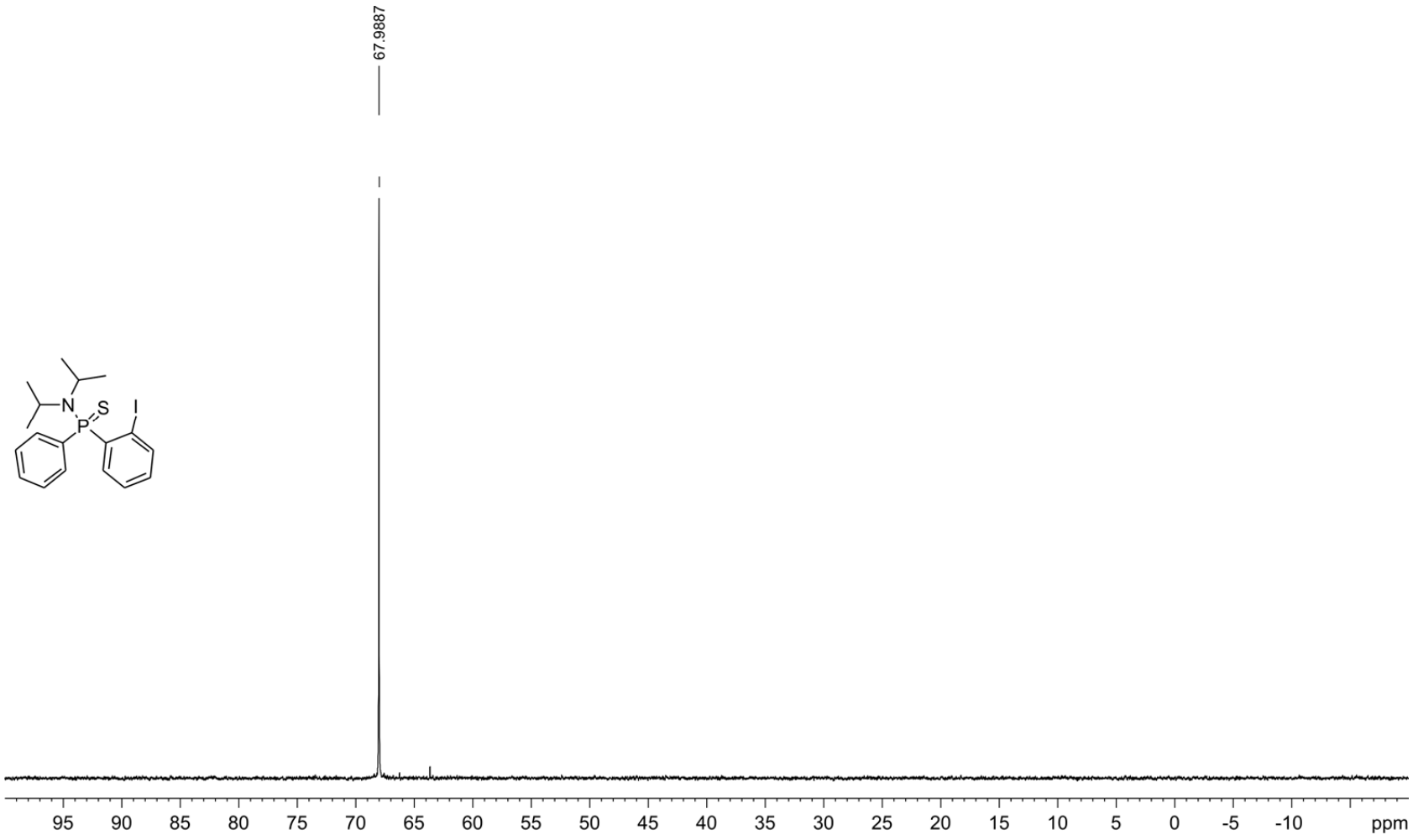

Figure S26. ^{31}P NMR spectrum (121.47 MHz) of **13** in $CDCl_3$.

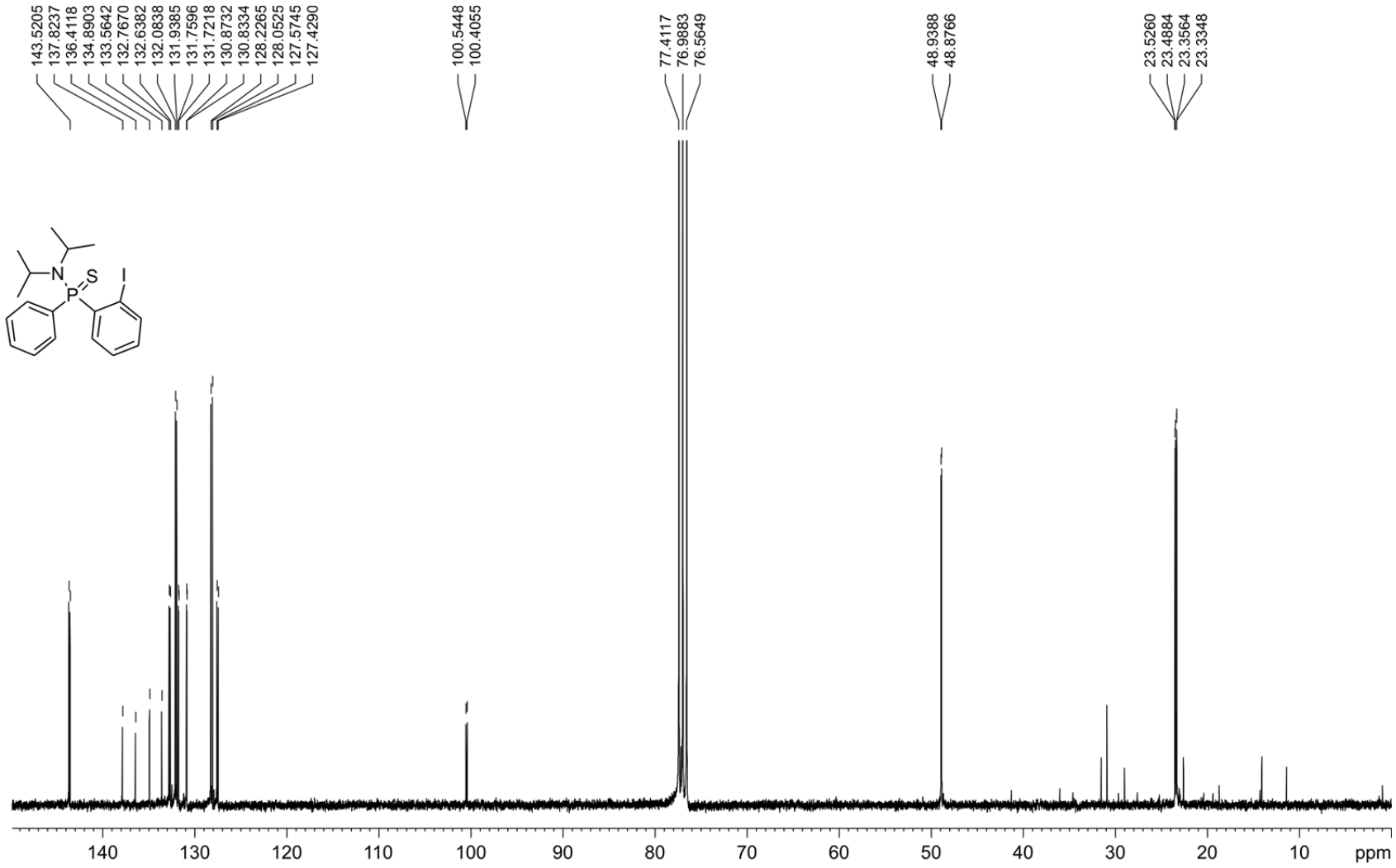

Figure S27. ^{13}C NMR spectrum (75.47 MHz) of **13** in $CDCl_3$.

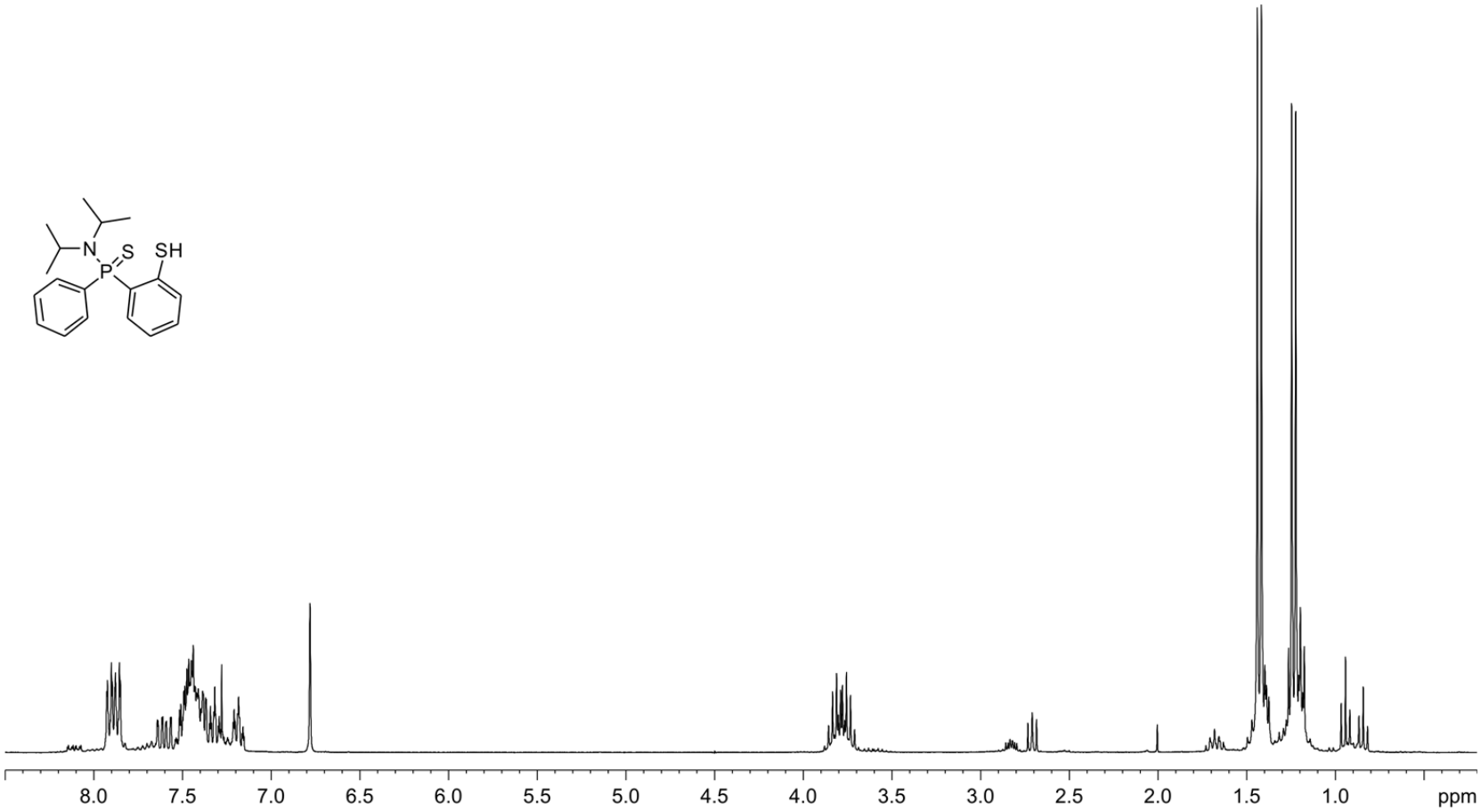

Figure S28. ^{1}H NMR spectrum (300.13 MHz) of the crude reaction affording **14** in $CDCl_3$.

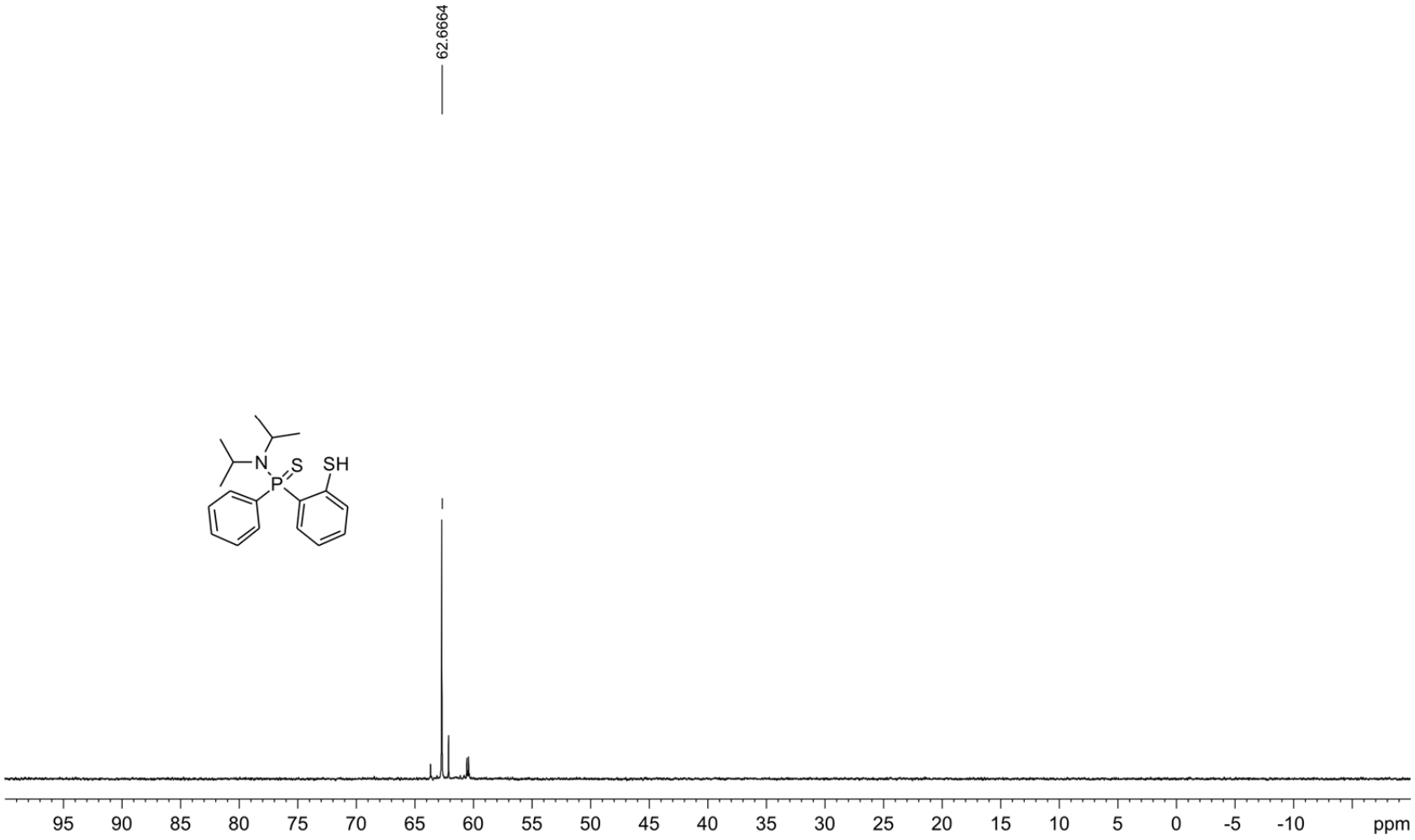

Figure S29. ^{31}P NMR spectrum (121.47 MHz) of the crude reaction affording **14** in $CDCl_3$.

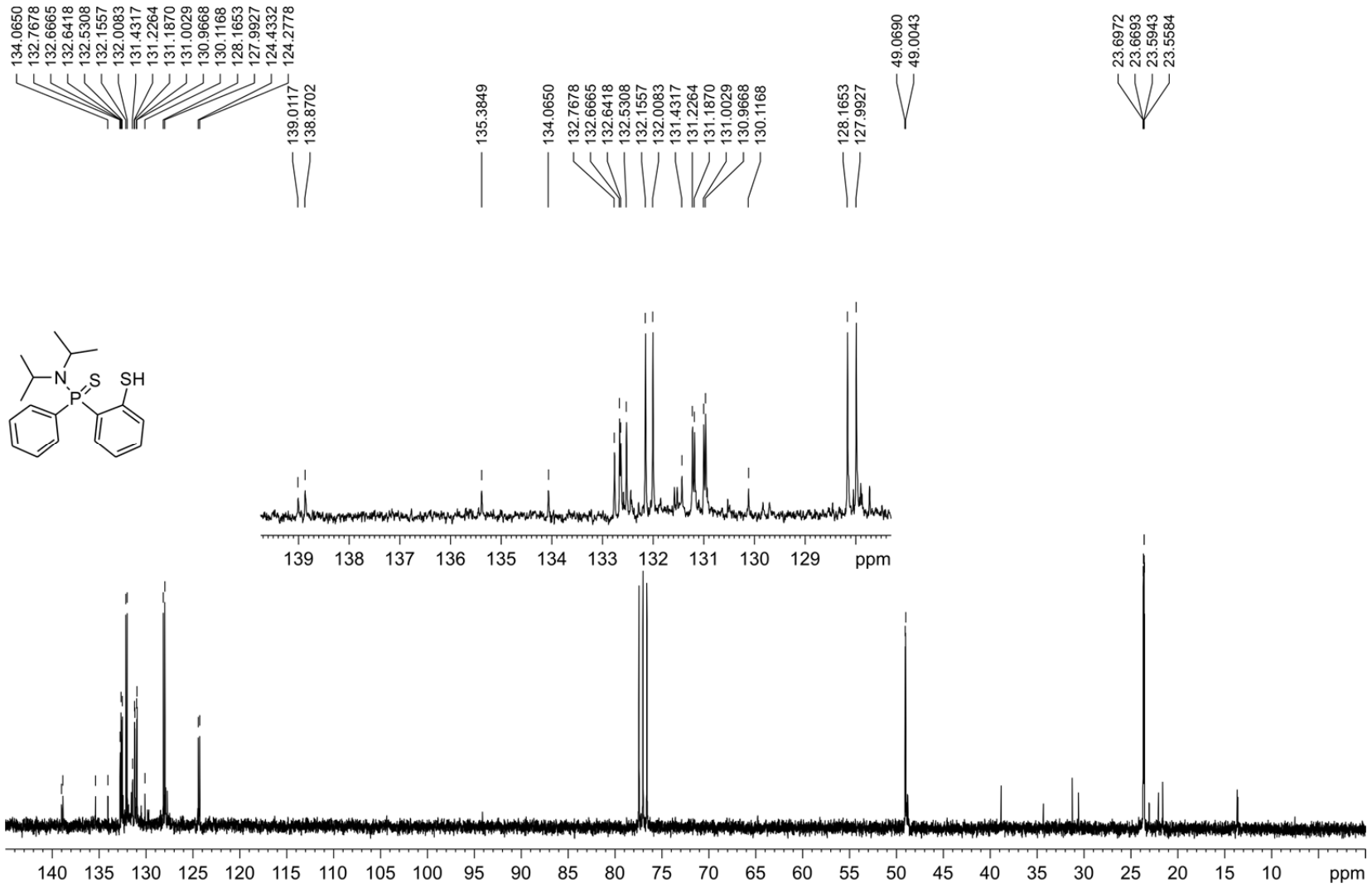

Figure S30. ^{13}C NMR spectrum (75.47 MHz) of the crude reaction affording **14** in $CDCl_3$.

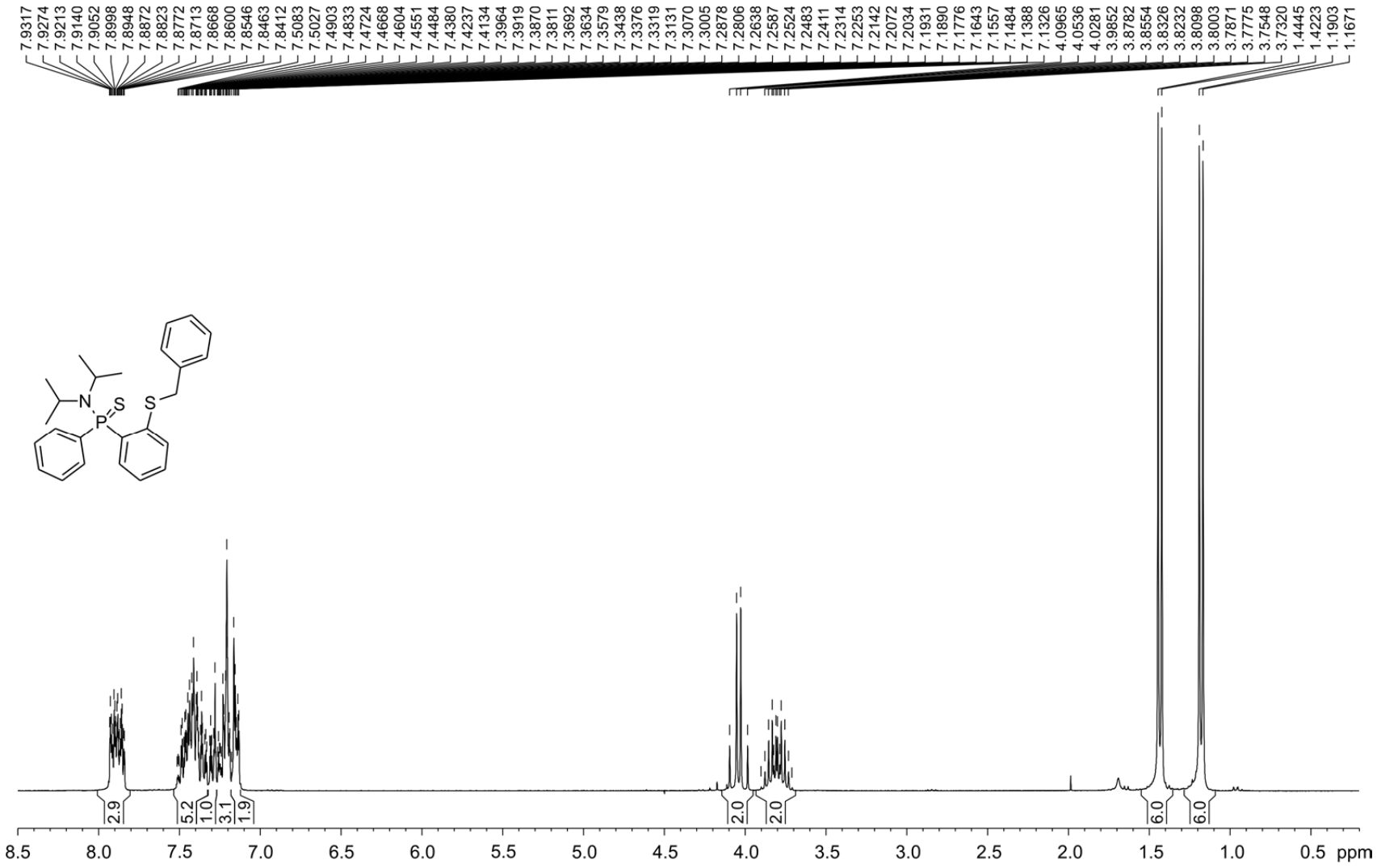

Figure S31. ^{1}H NMR spectrum (300.13 MHz) of **15** in $CDCl_3$.

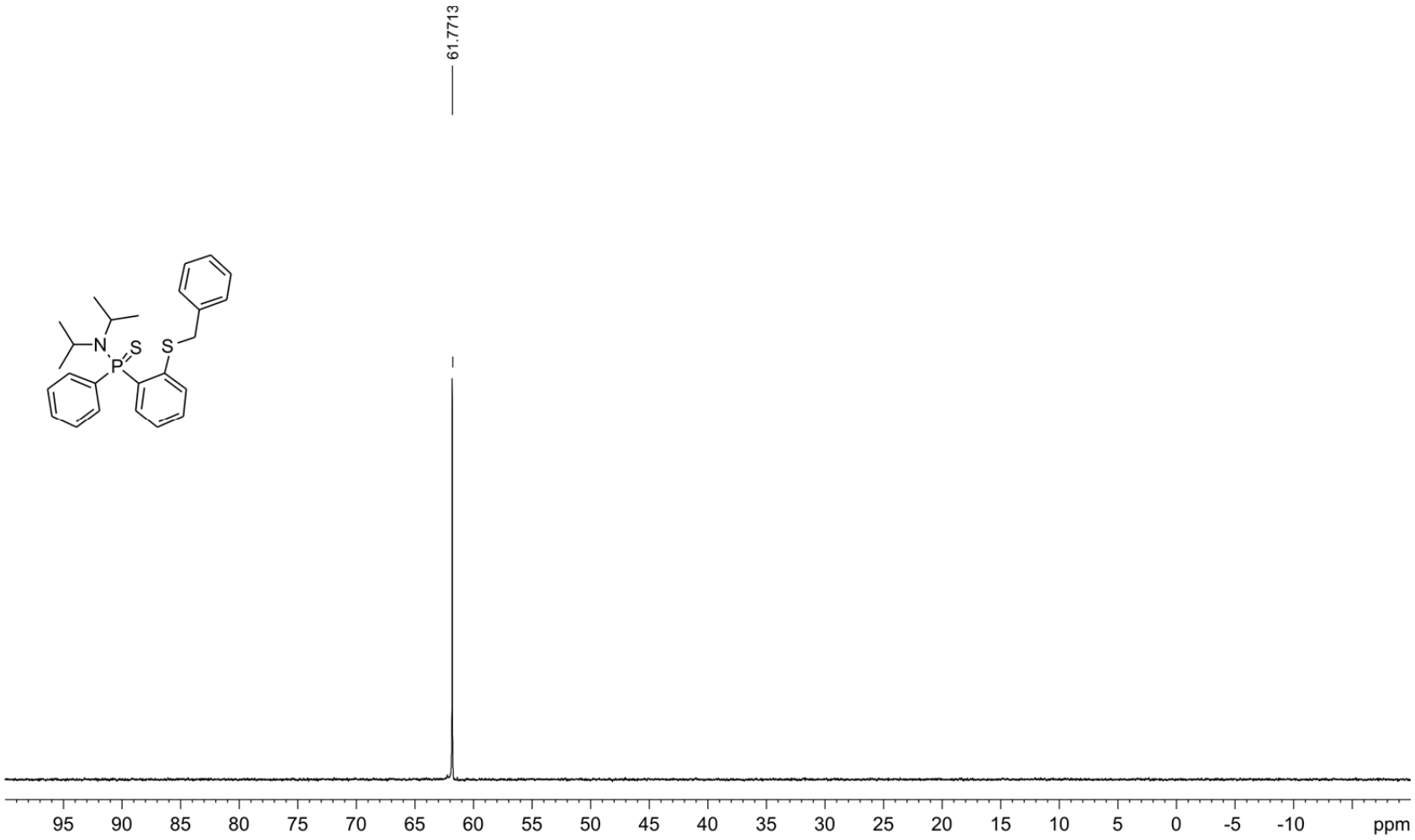

Figure S32. ^{31}P NMR spectrum (121.47 MHz) of **15** in $CDCl_3$.

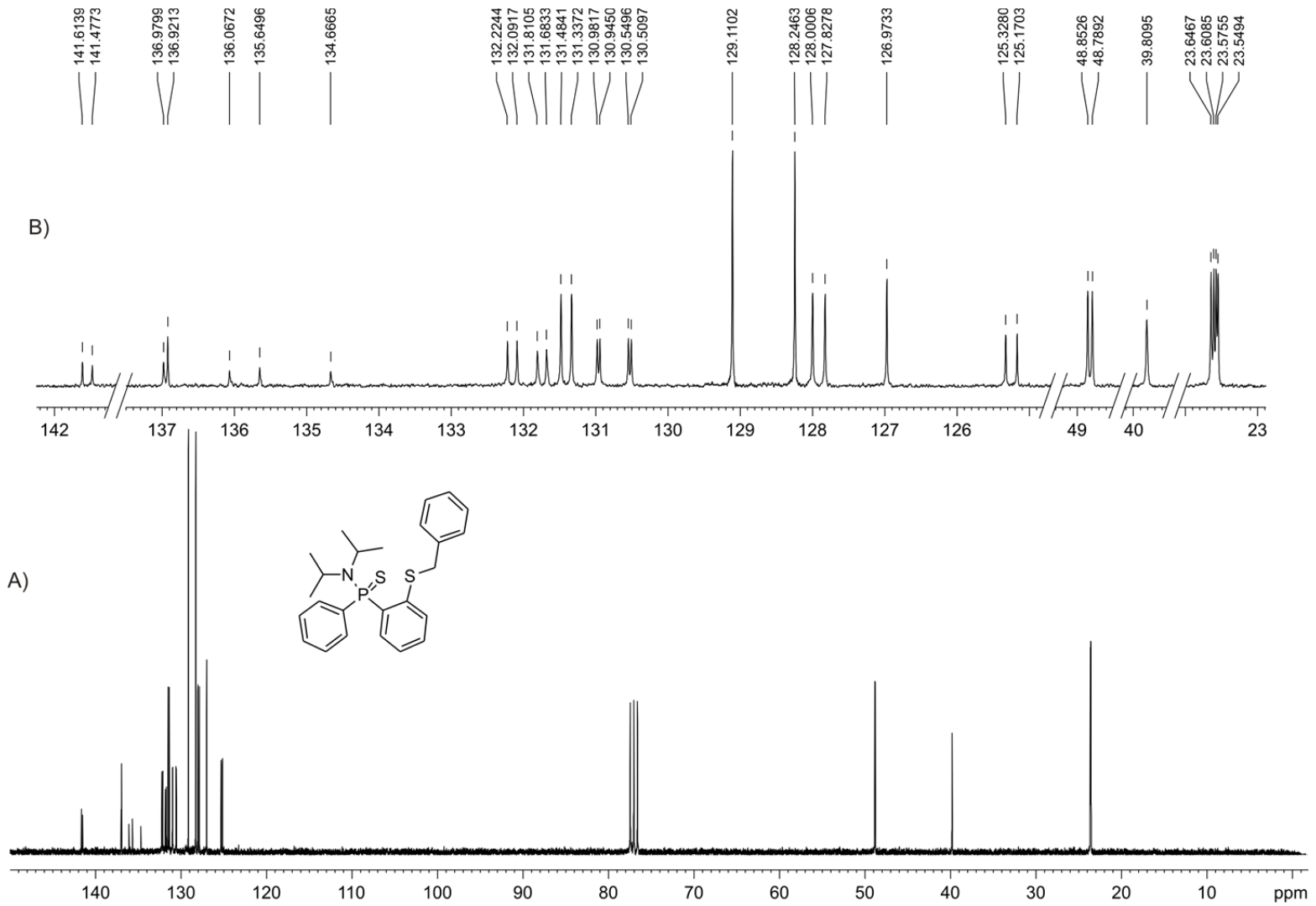

Figure S33. ^{13}C NMR spectrum (75.47 MHz) of **15** in $CDCl_3$.

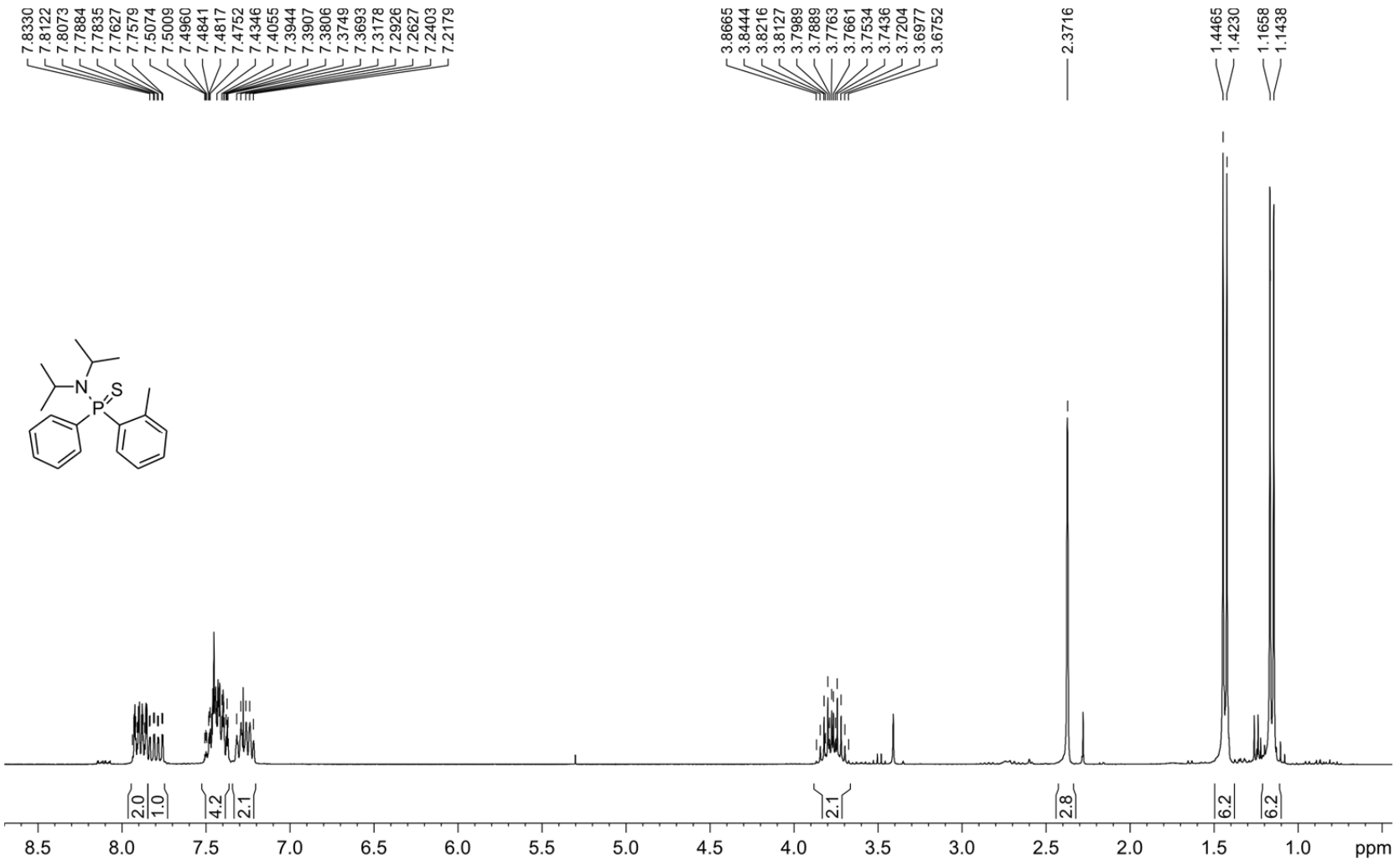

Figure S34. ^{1}H NMR spectrum (300.13 MHz) of **16** in $CDCl_3$.

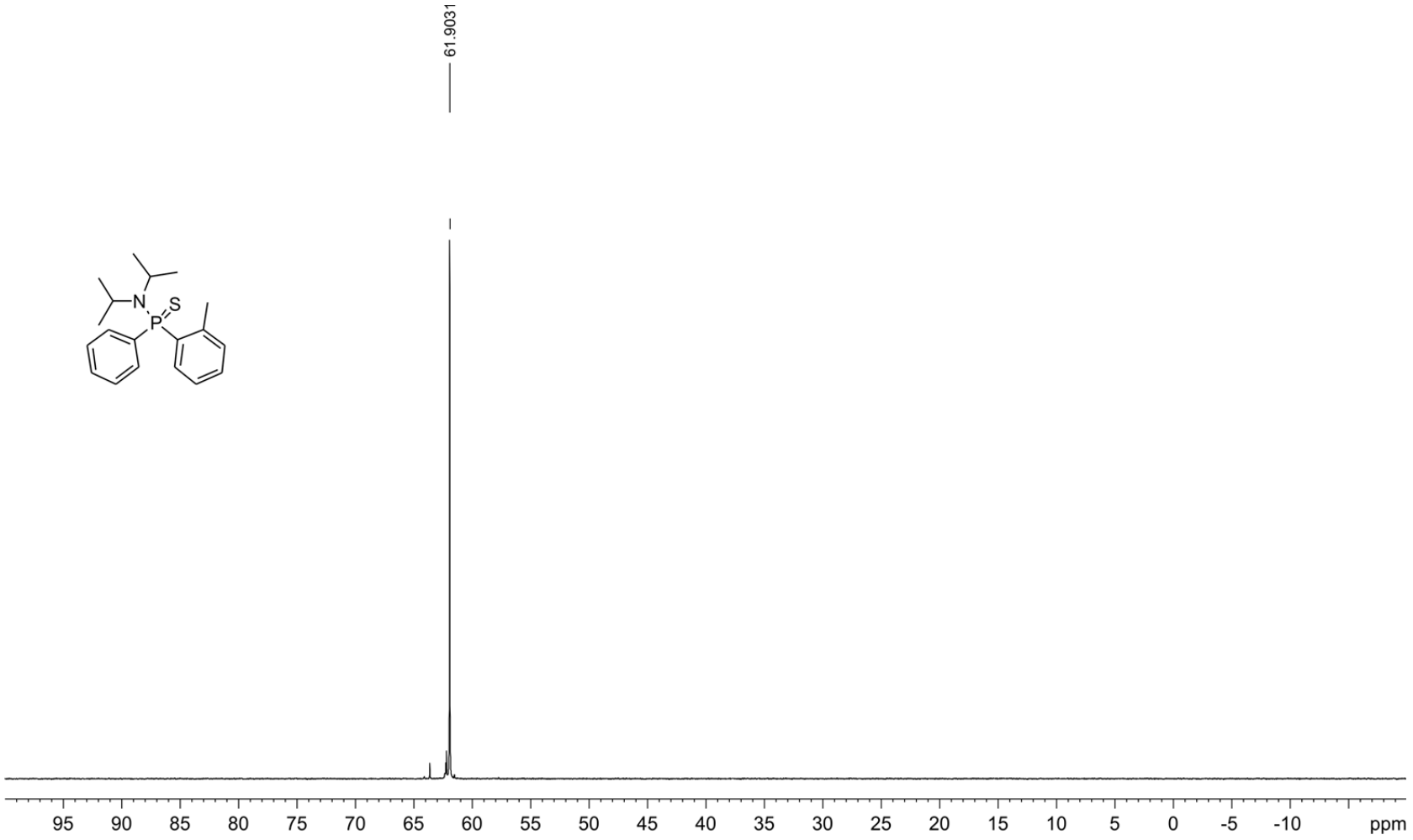

Figure S35. ^{31}P NMR spectrum (121.47 MHz) of **16** in $CDCl_3$.

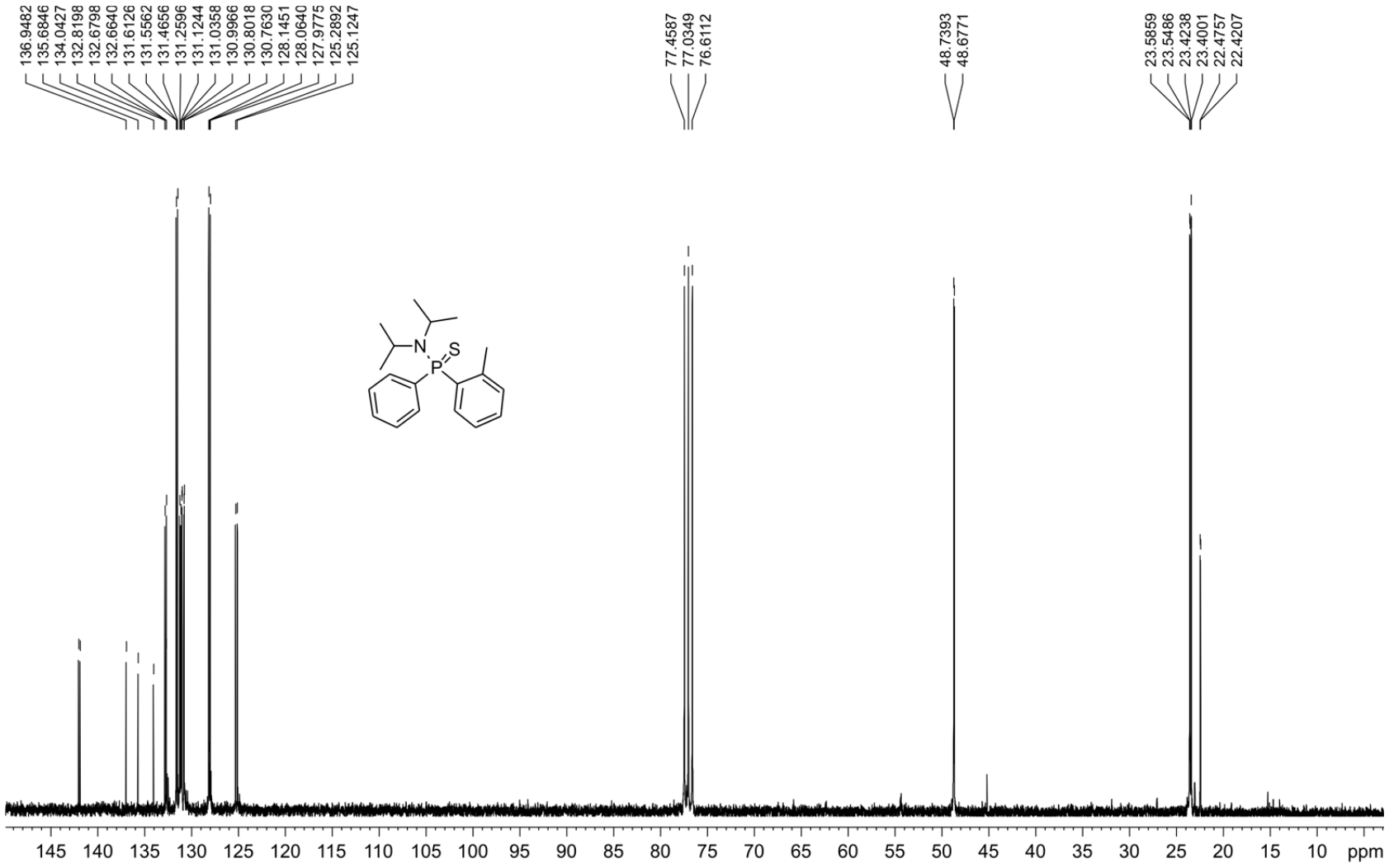

Figure S36. ^{13}C NMR spectrum (75.47 MHz) of **16** in $CDCl_3$.

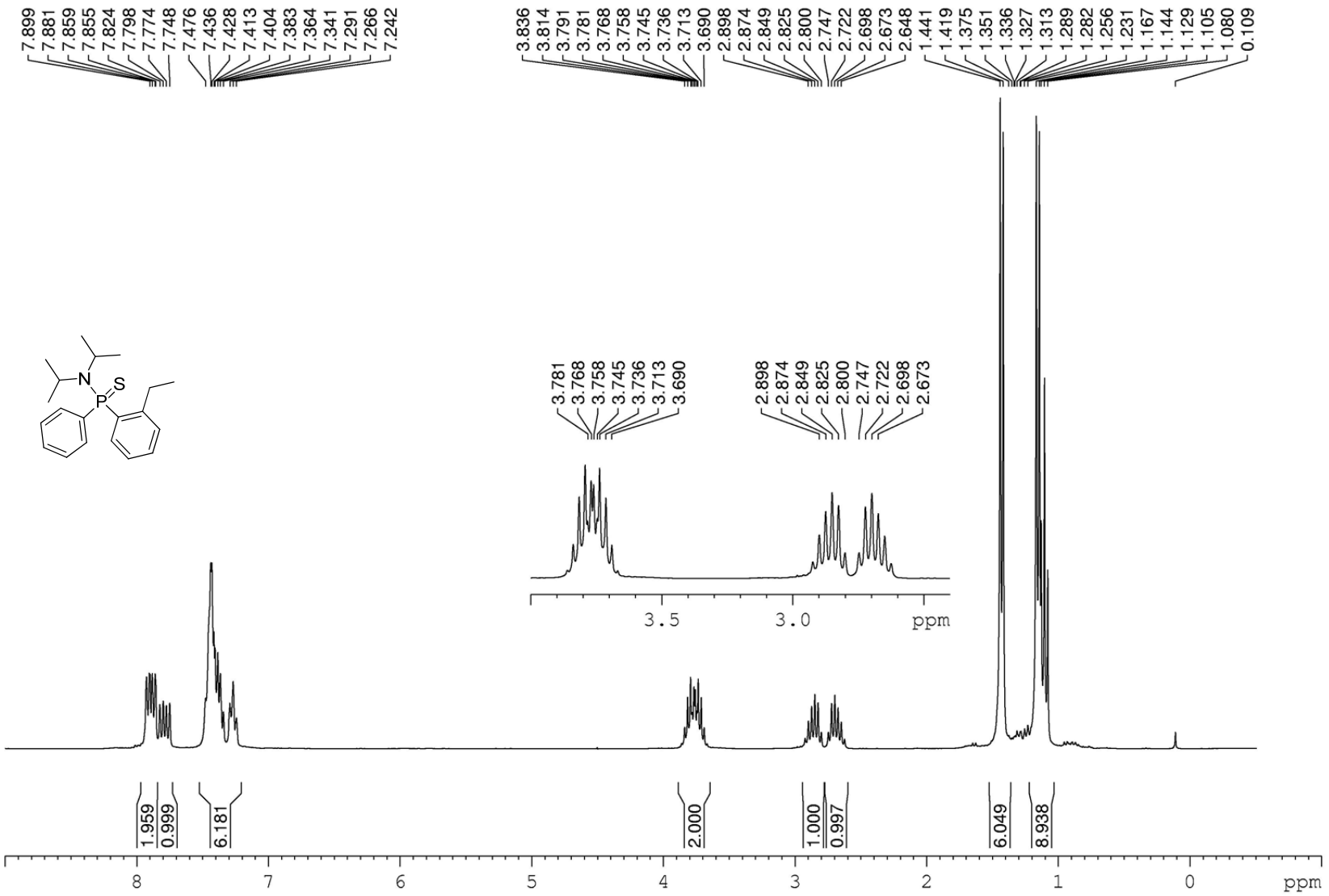

Figure S37. ^{1}H NMR spectrum (300.13 MHz) of **17** in $CDCl_3$.

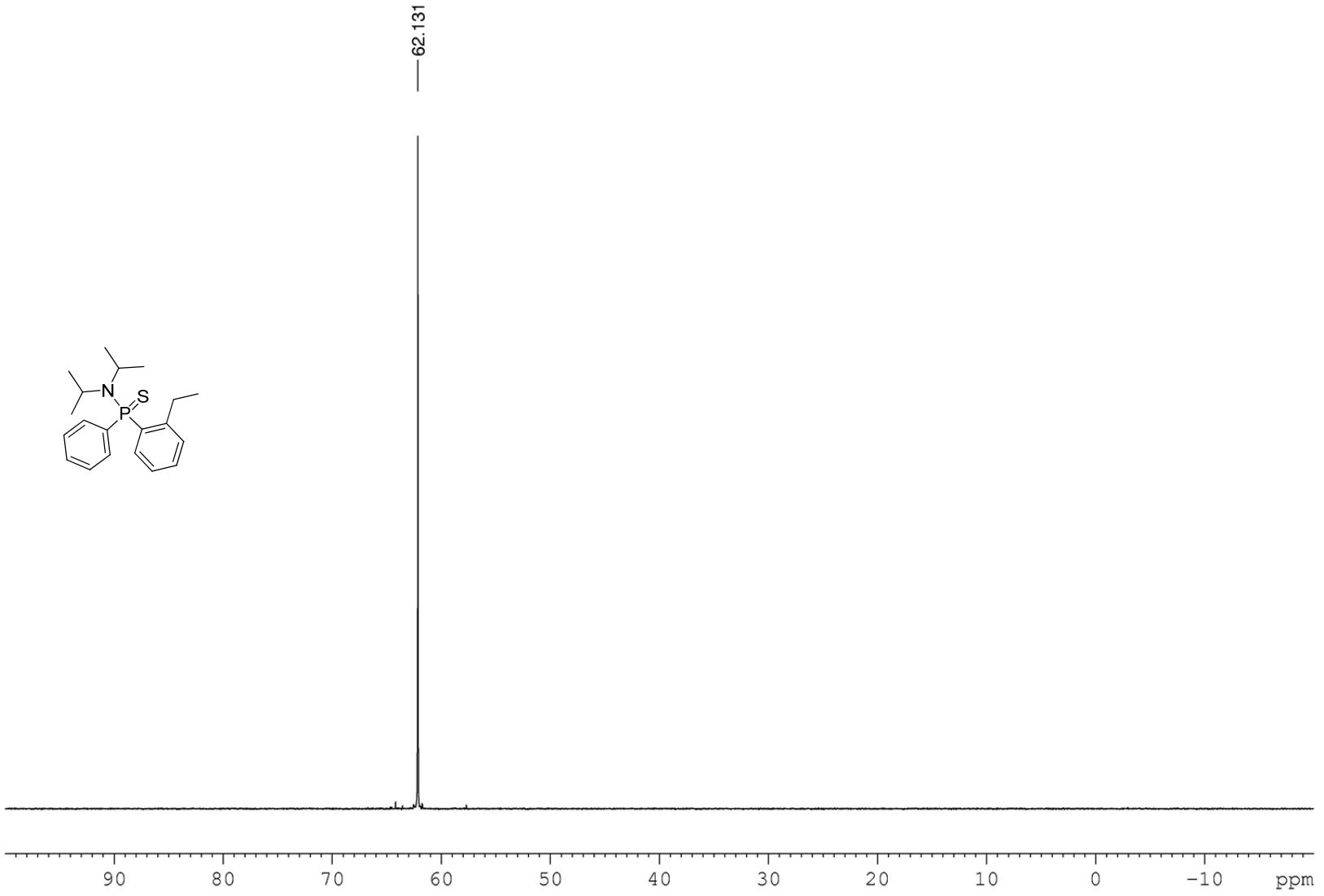

Figure S38. ^{31}P NMR spectrum (121.47 MHz) of **17** in $CDCl_3$.

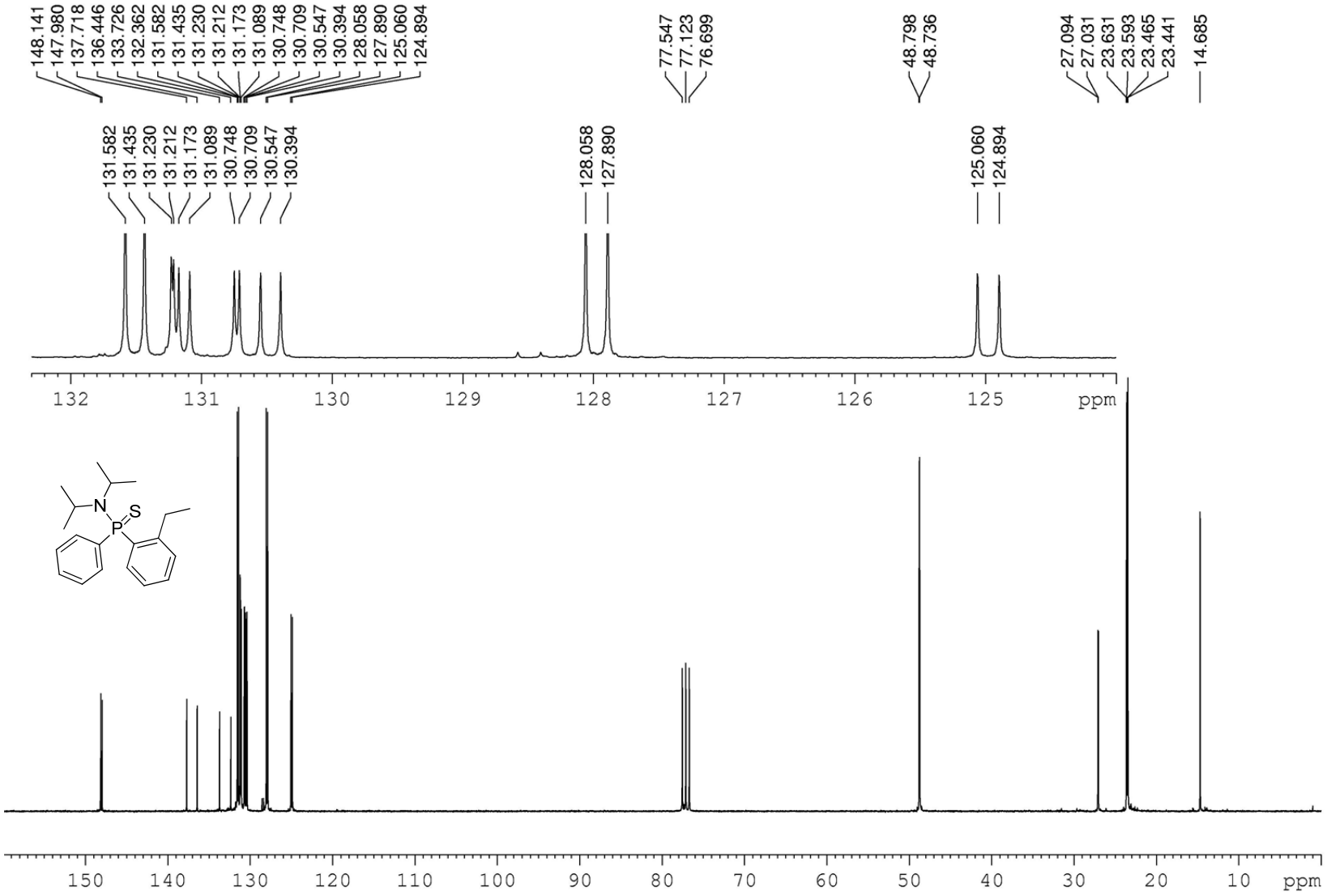

Figure S39. ^{13}C NMR spectrum (75.47 MHz) of **17** in $CDCl_3$.

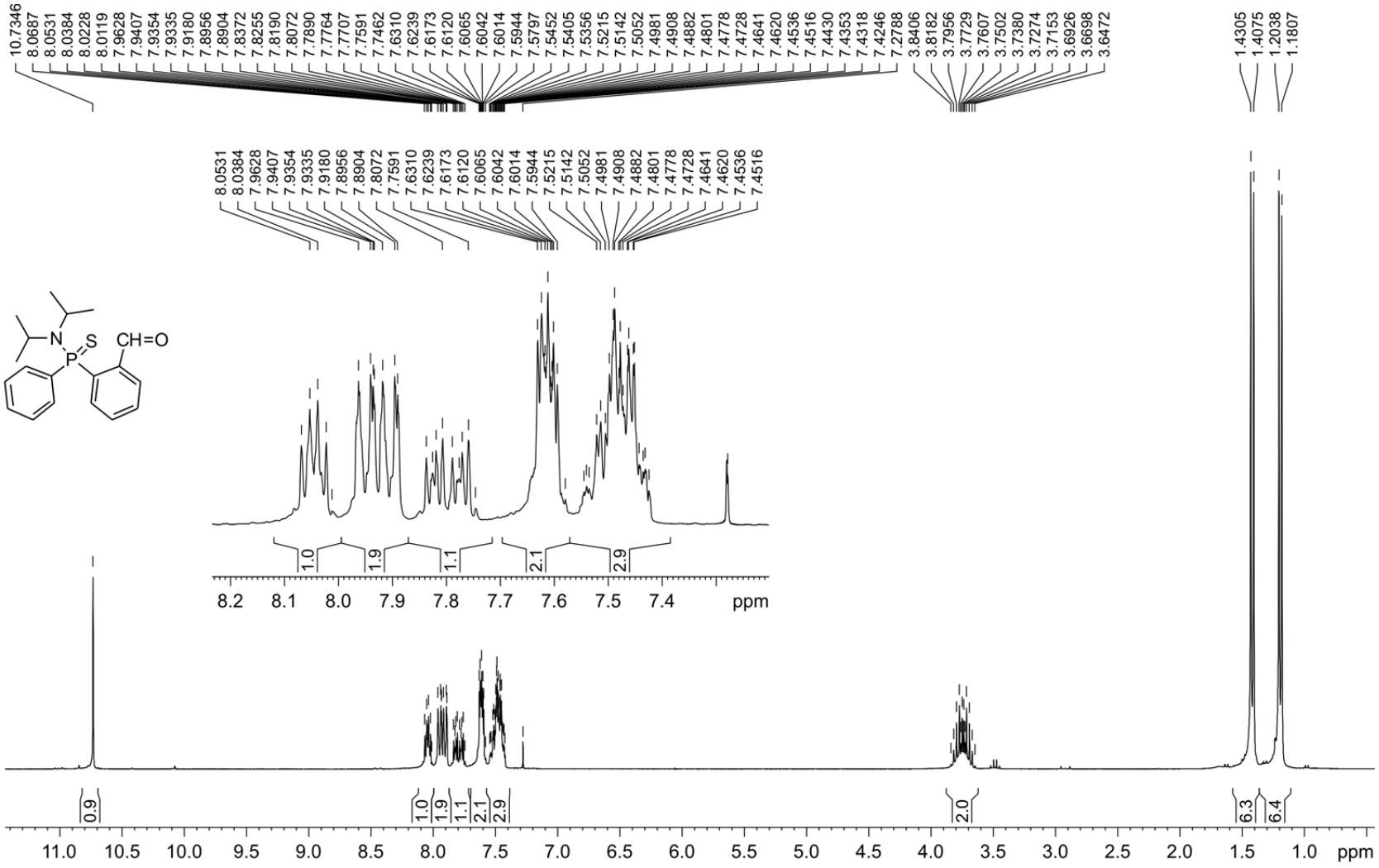

Figure S40. ^{1}H NMR spectrum (300.13 MHz) of **18** in $CDCl_3$.

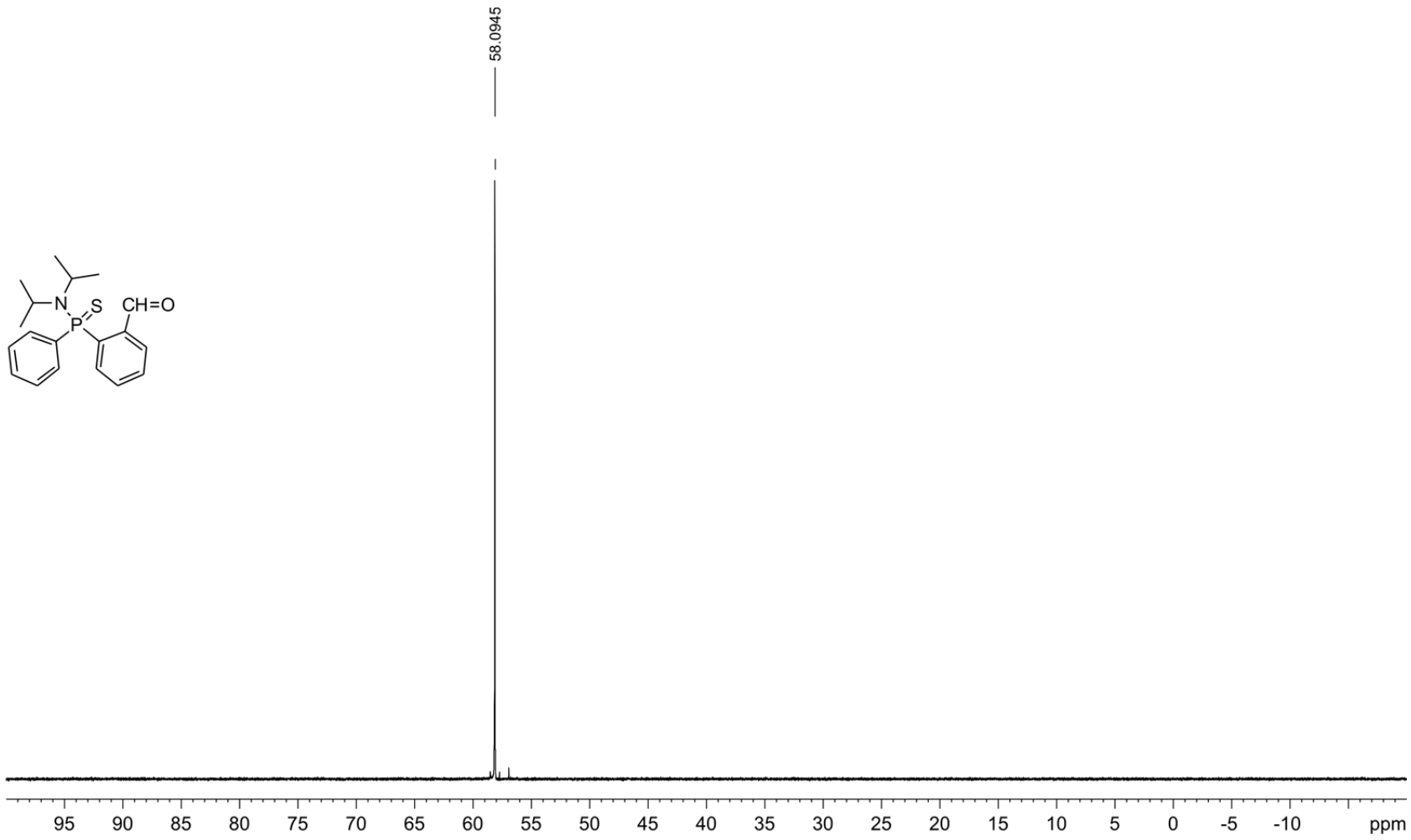

Figure S41. ^{31}P NMR spectrum (121.47 MHz) of **18** in $CDCl_3$.

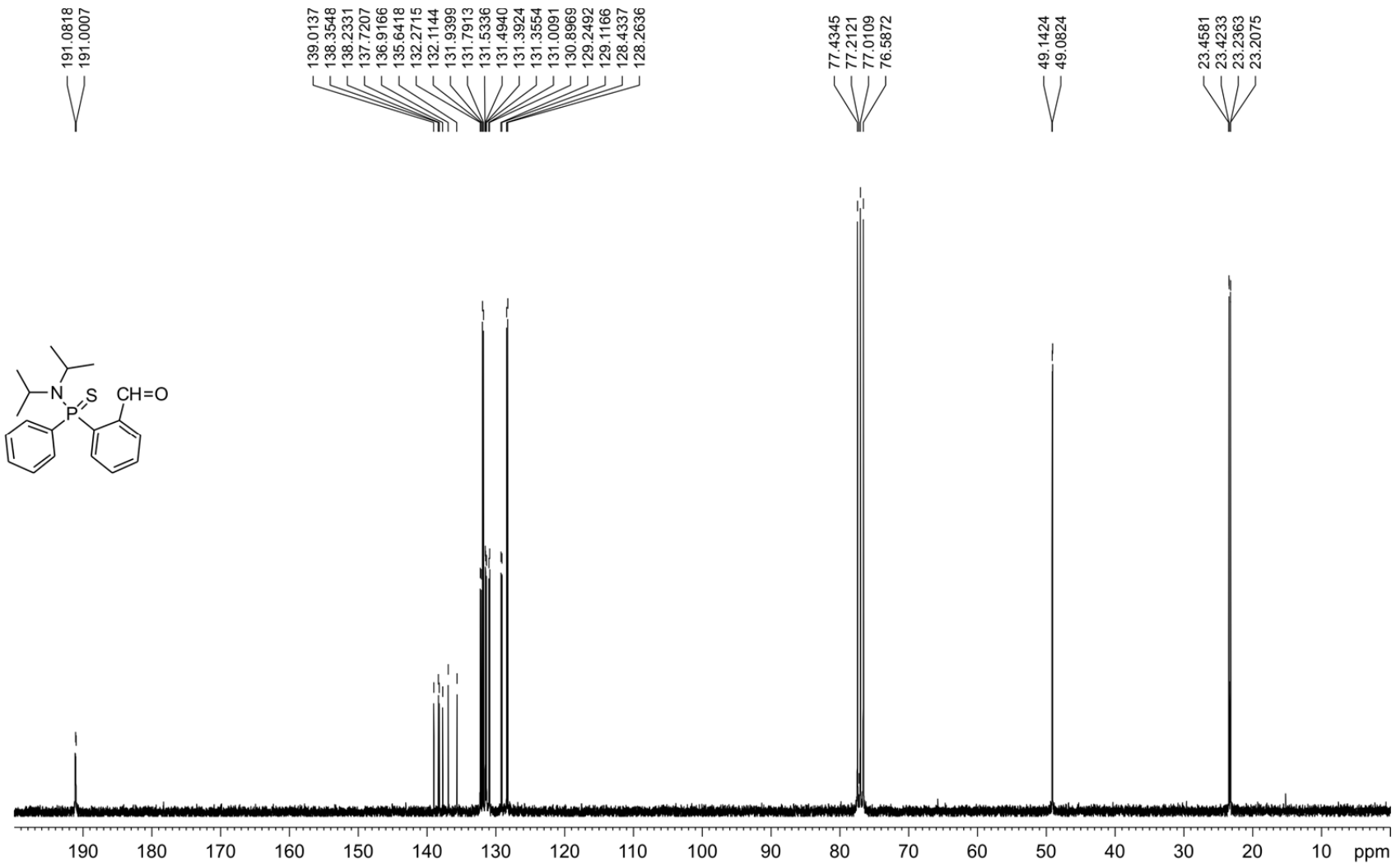

Figure S42. ^{13}C NMR spectrum (75.47 MHz) of **18** in $CDCl_3$.

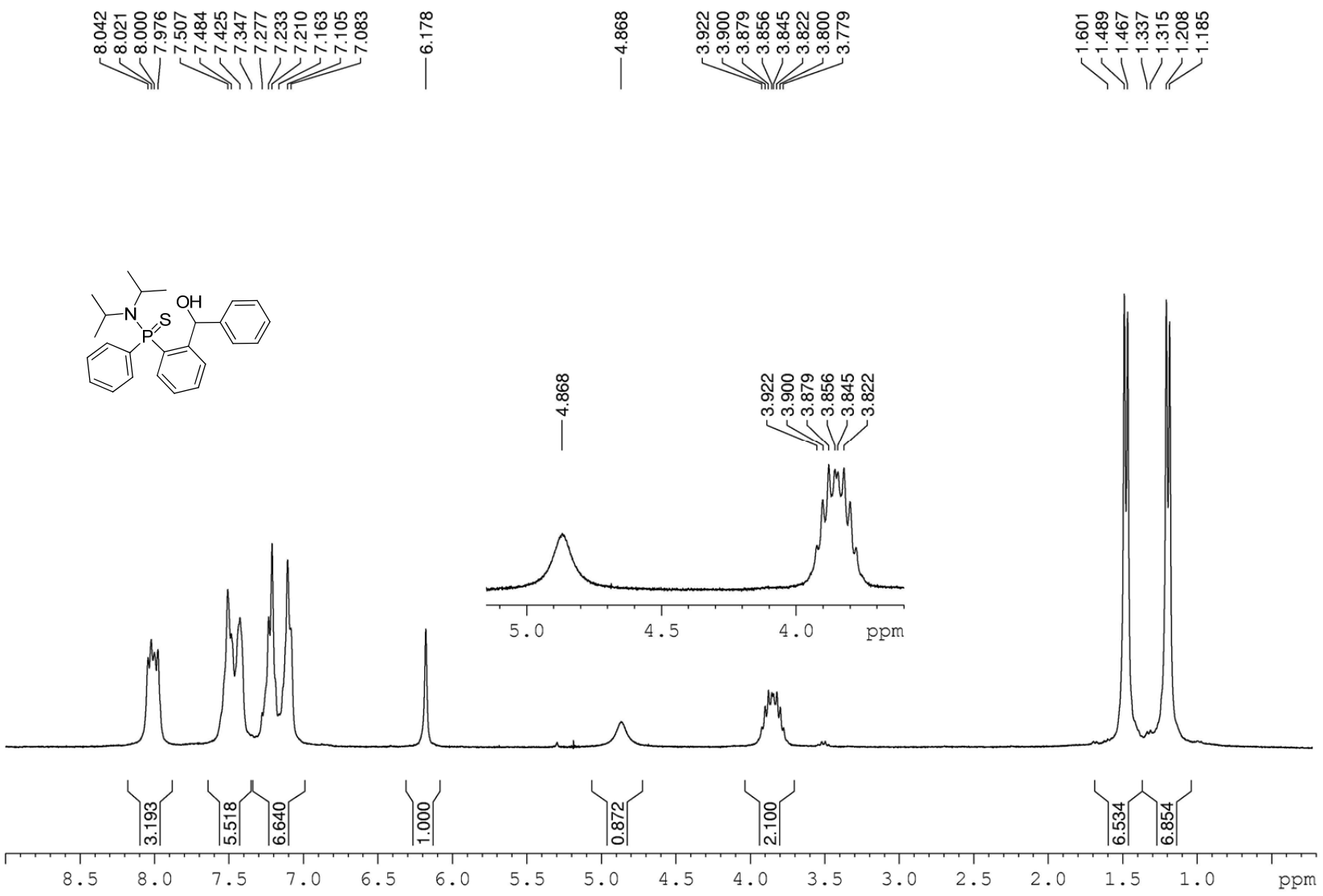

Figure S43. ^{1}H NMR spectrum (300.13 MHz) of **19** in $CDCl_3$.

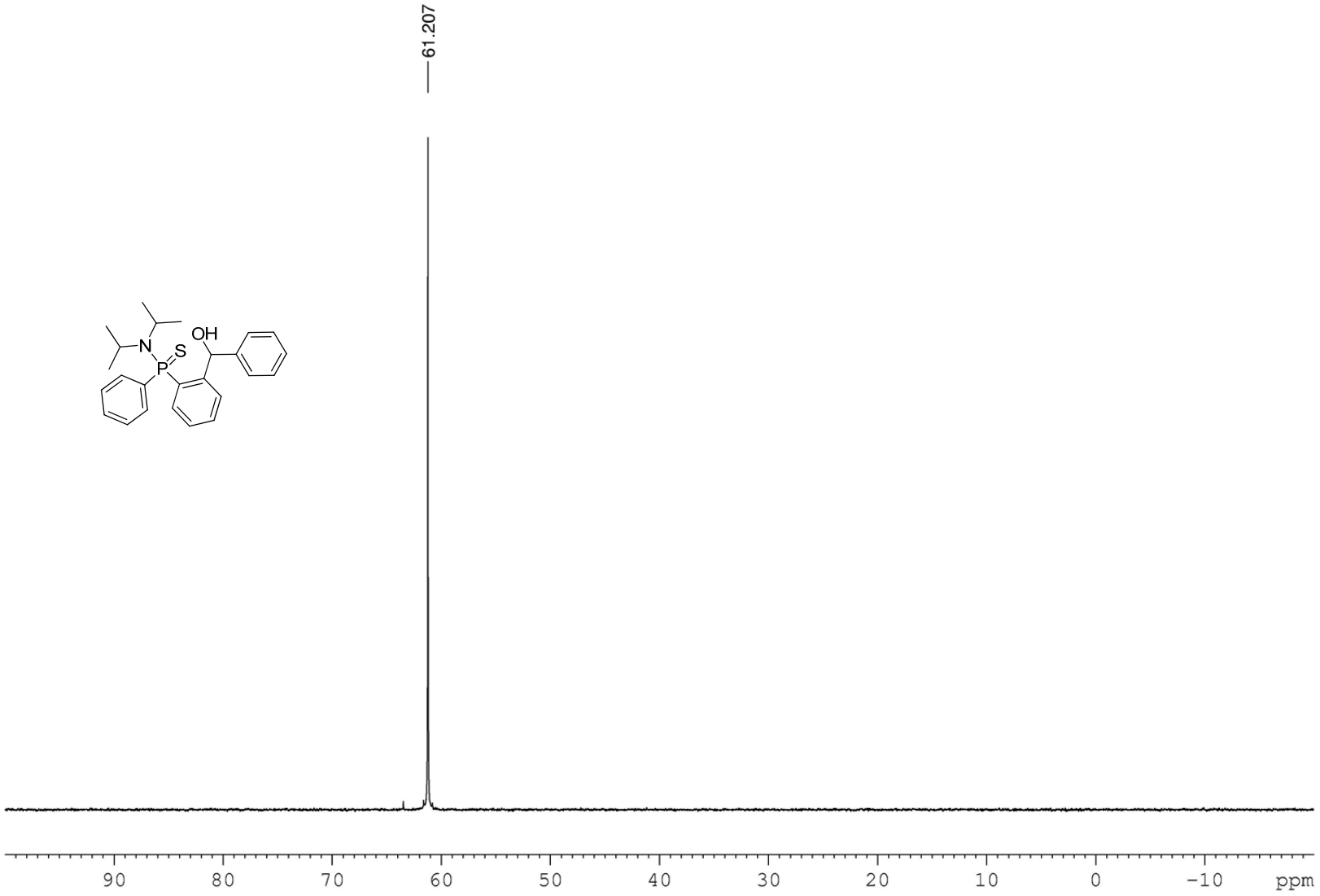

Figure S44. ^{31}P NMR spectrum (121.47 MHz) of **19** in $CDCl_3$.

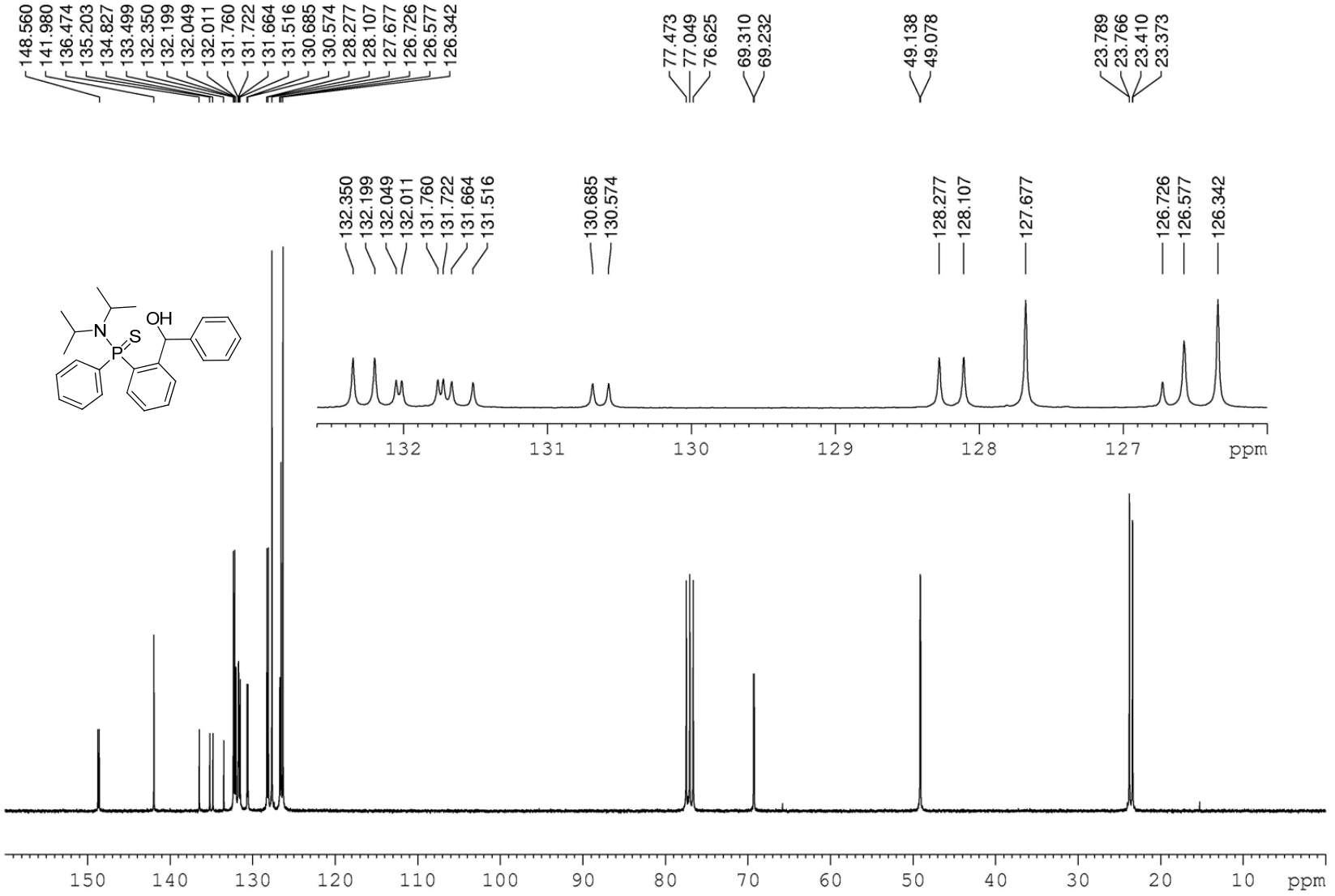

Figure S45. ^{13}C NMR spectrum (75.47 MHz) of **19** in $CDCl_3$.

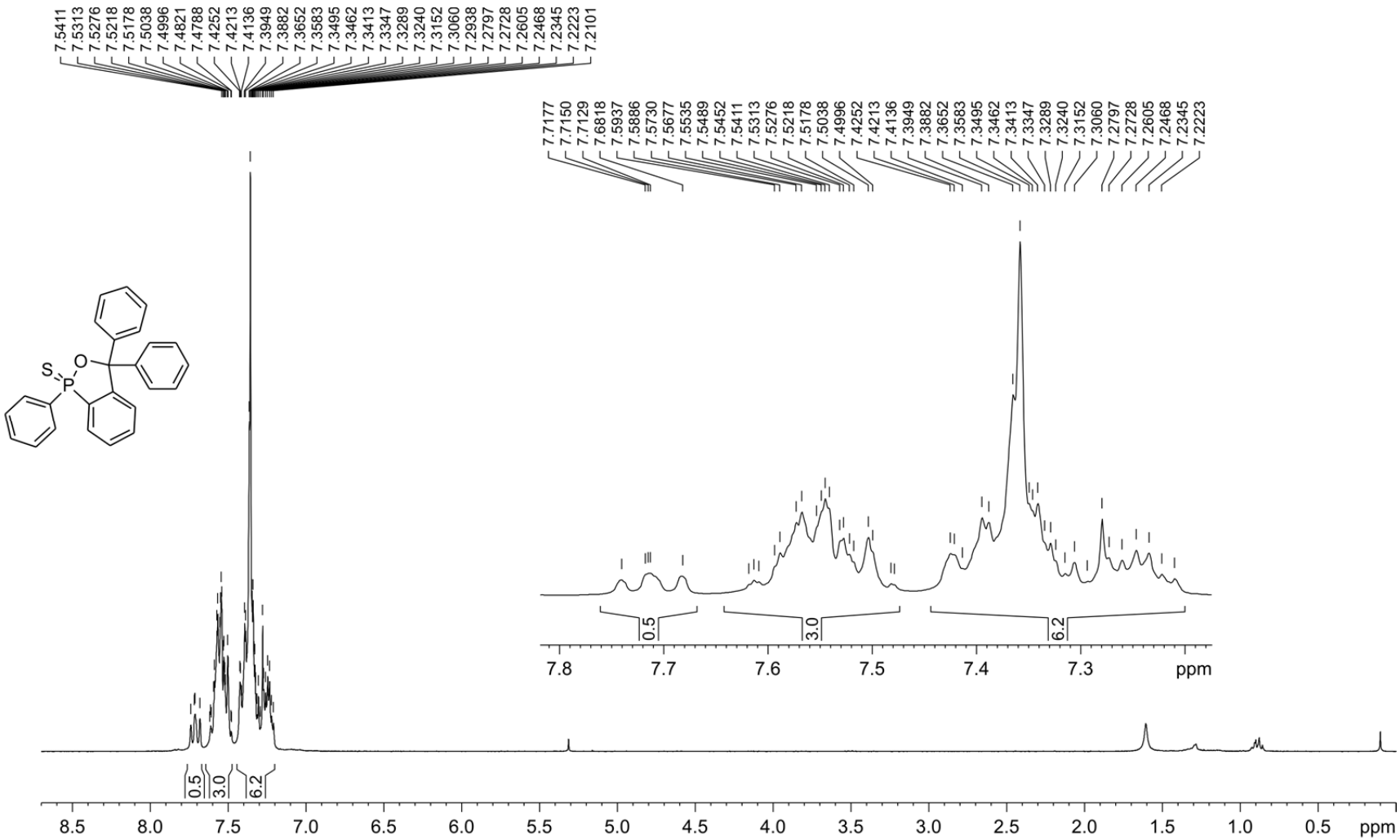

Figure S46. ^{1}H NMR spectrum (300.13 MHz) of **20** in $CDCl_3$.

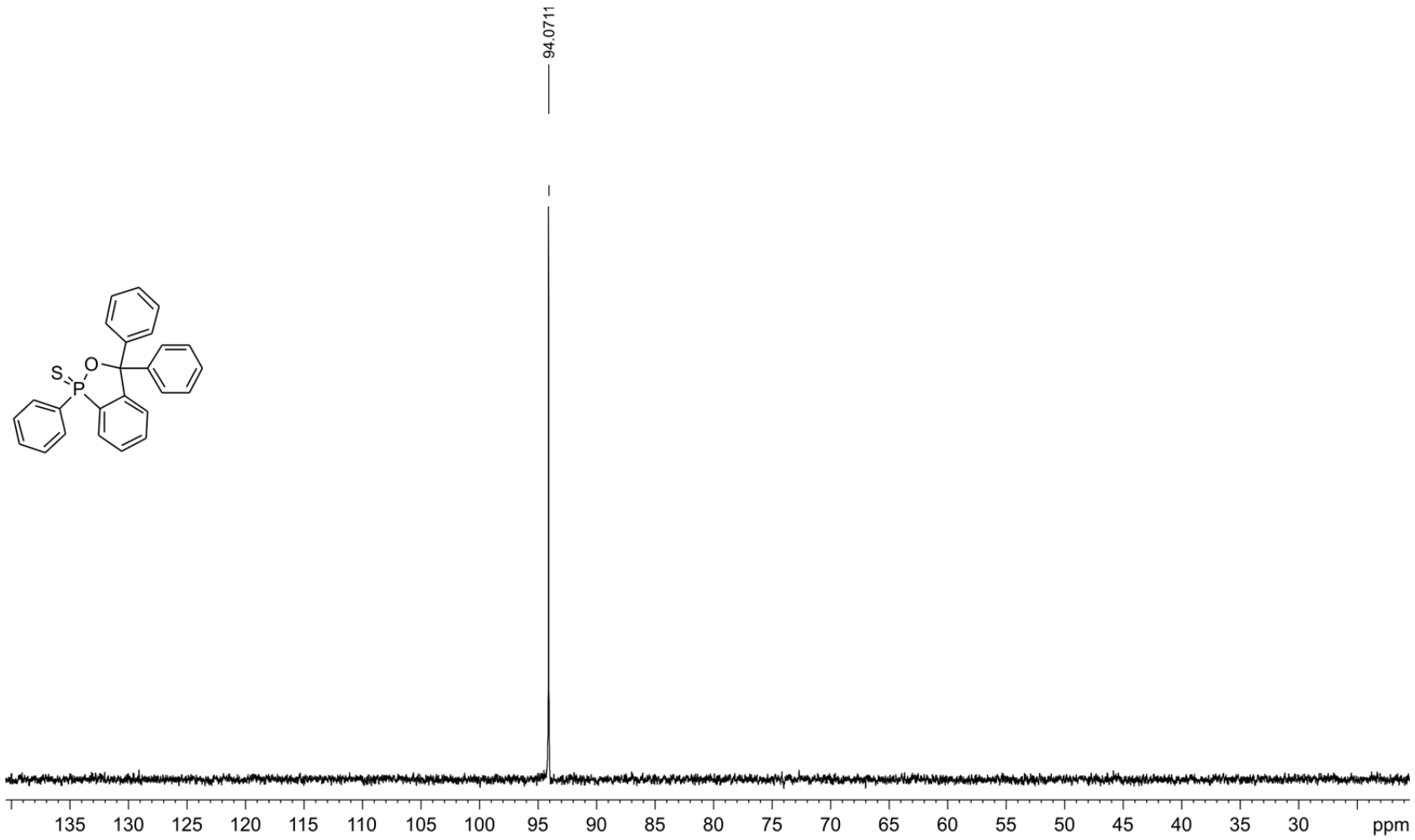

Figure S47. ^{31}P NMR spectrum (121.47 MHz) of **20** in $CDCl_3$.

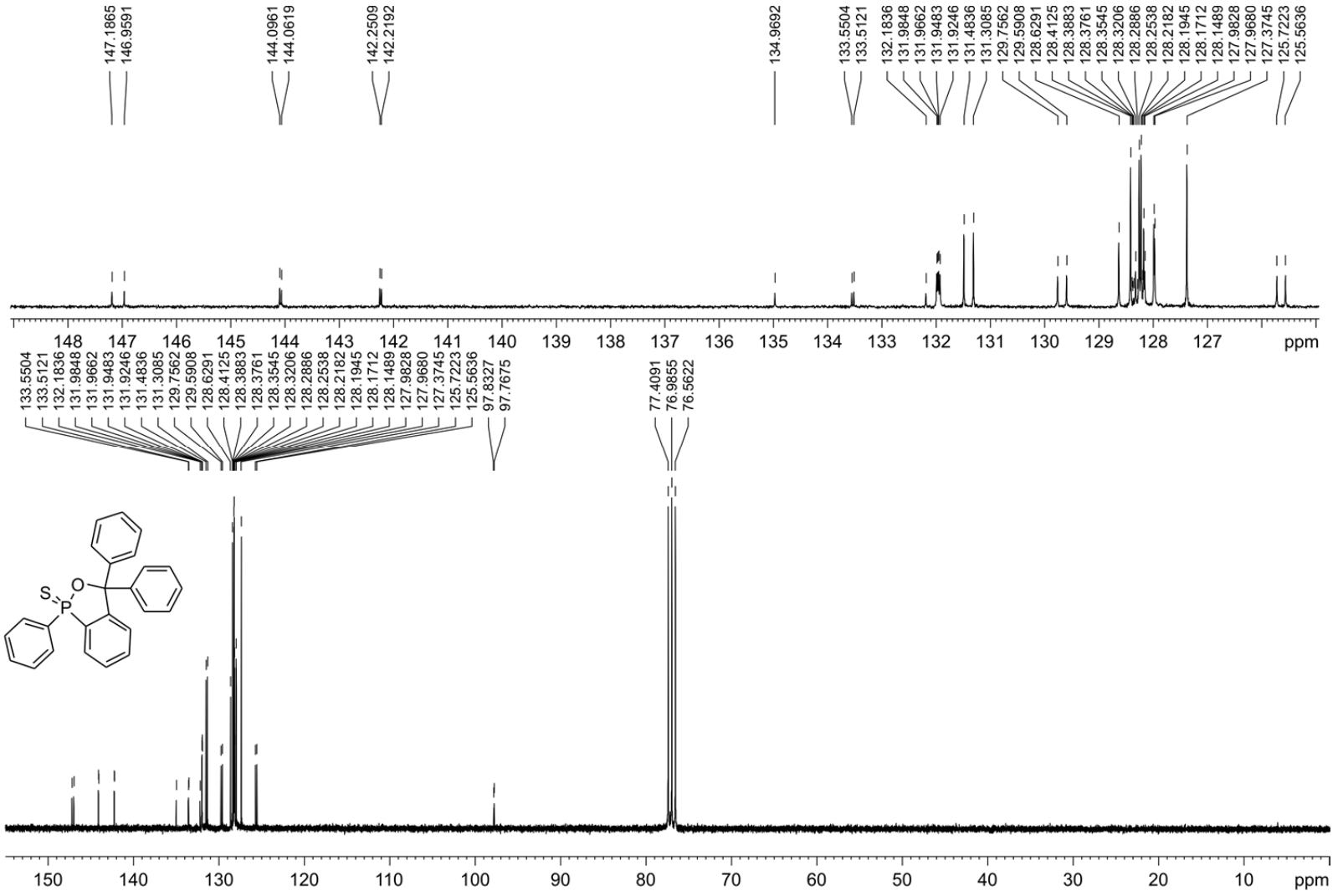

Figure S48. ^{13}C NMR spectrum (75.47 MHz) of **20** in $CDCl_3$.

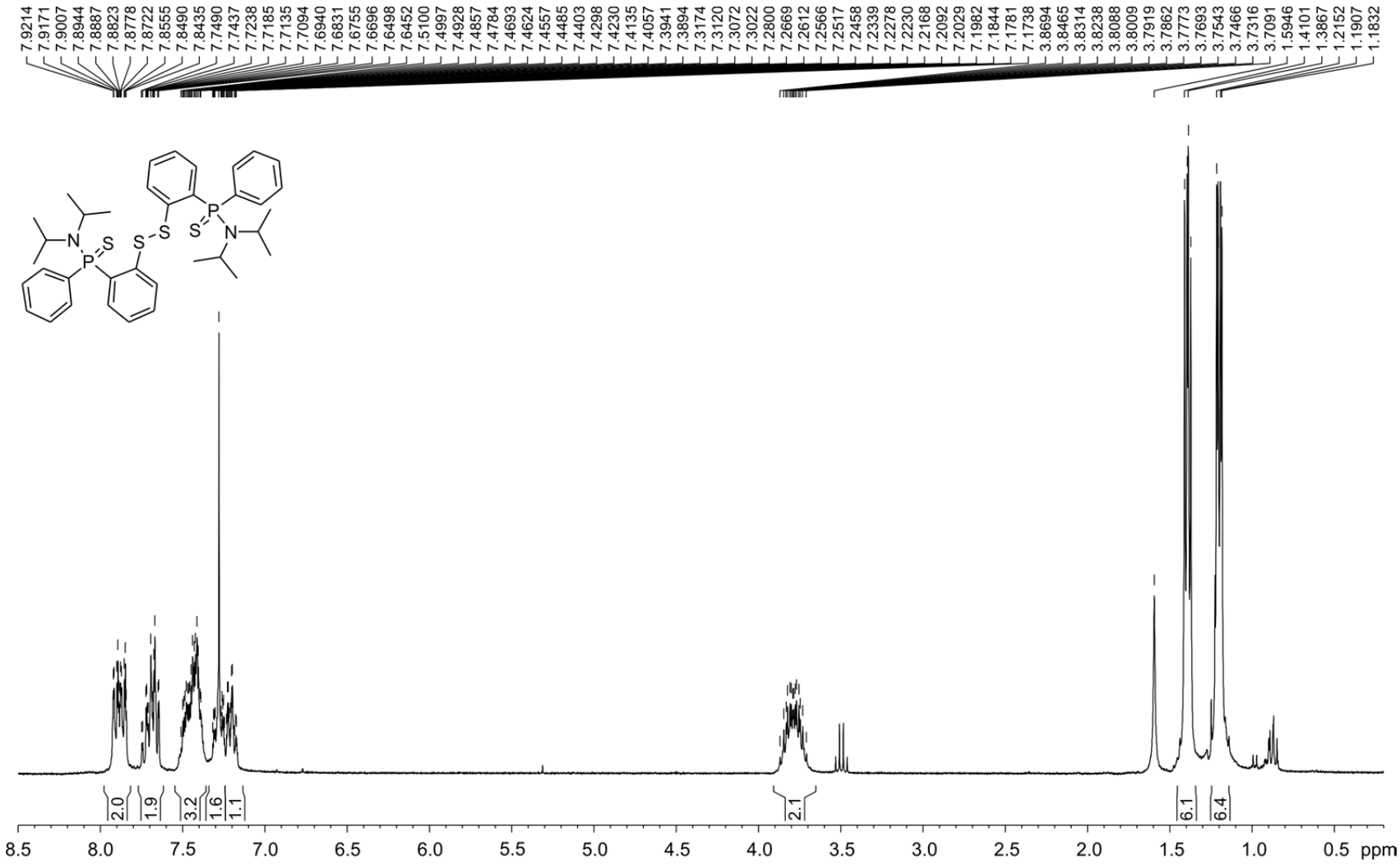

Figure S49. ^{1}H NMR spectrum (300.13 MHz) of **21** in $CDCl_3$.

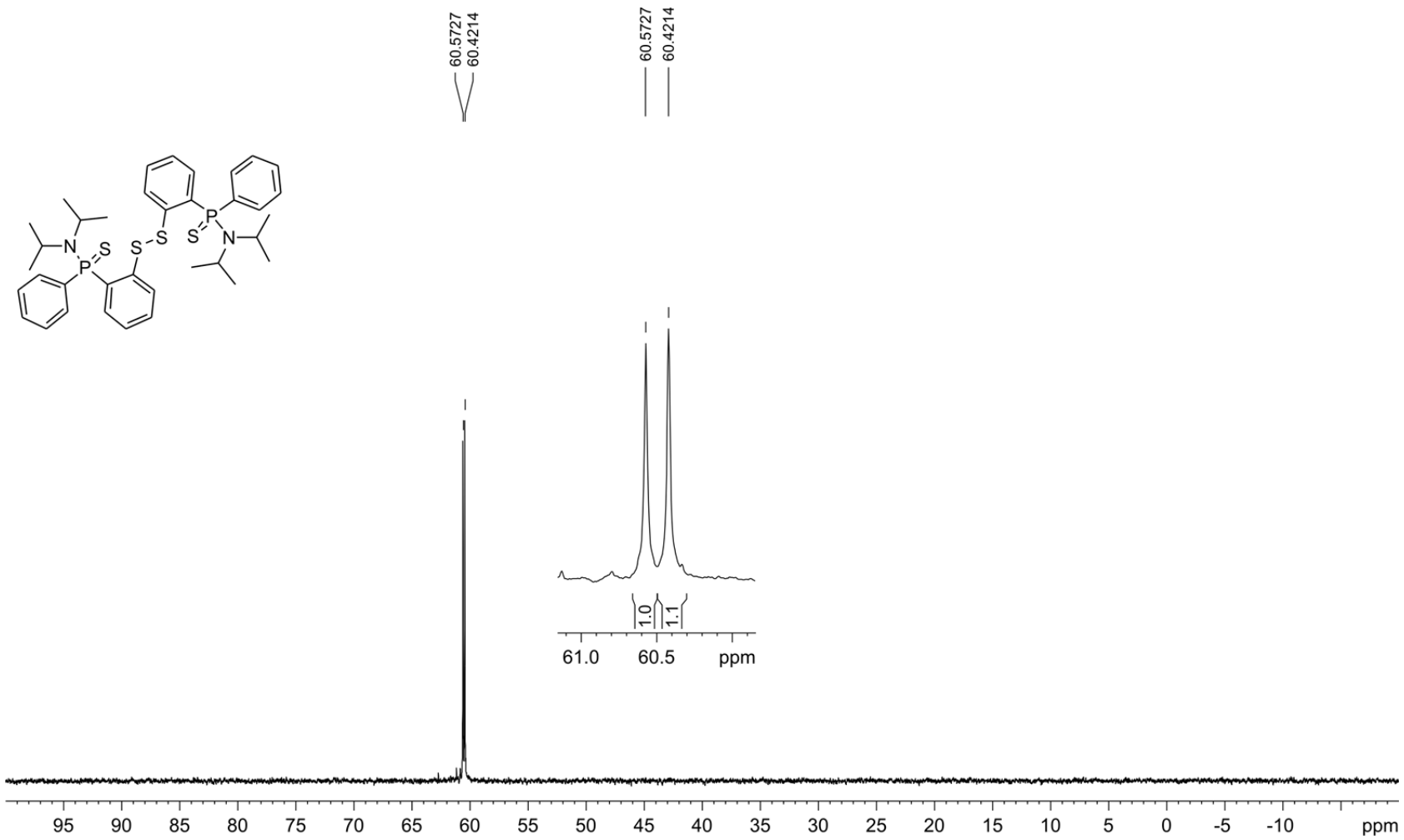

Figure S50. ^{31}P NMR spectrum (121.47 MHz) of **21** in $CDCl_3$.

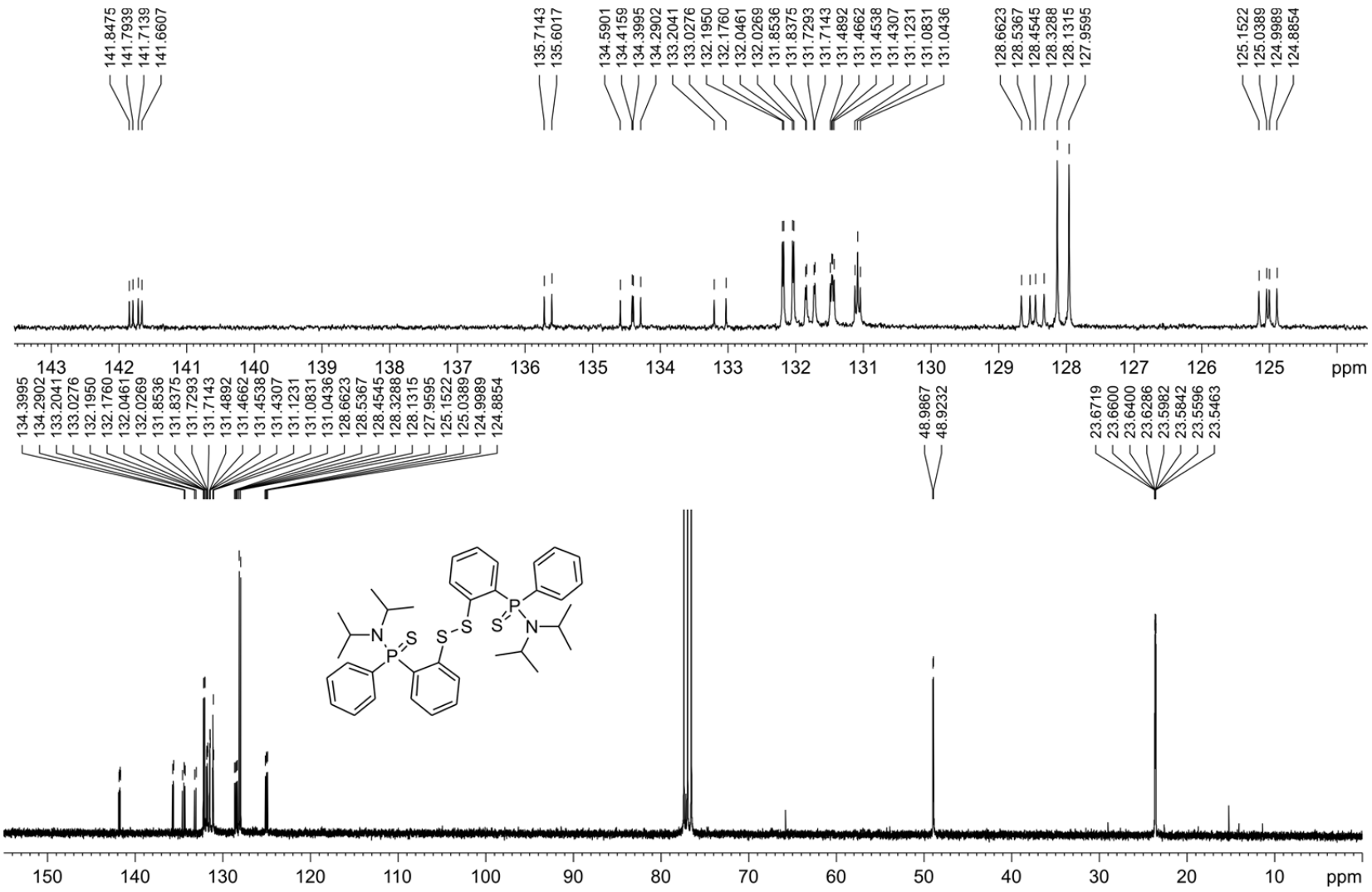

Figure S51. ^{13}C NMR spectrum (75.47 MHz) of **21** in $CDCl_3$.

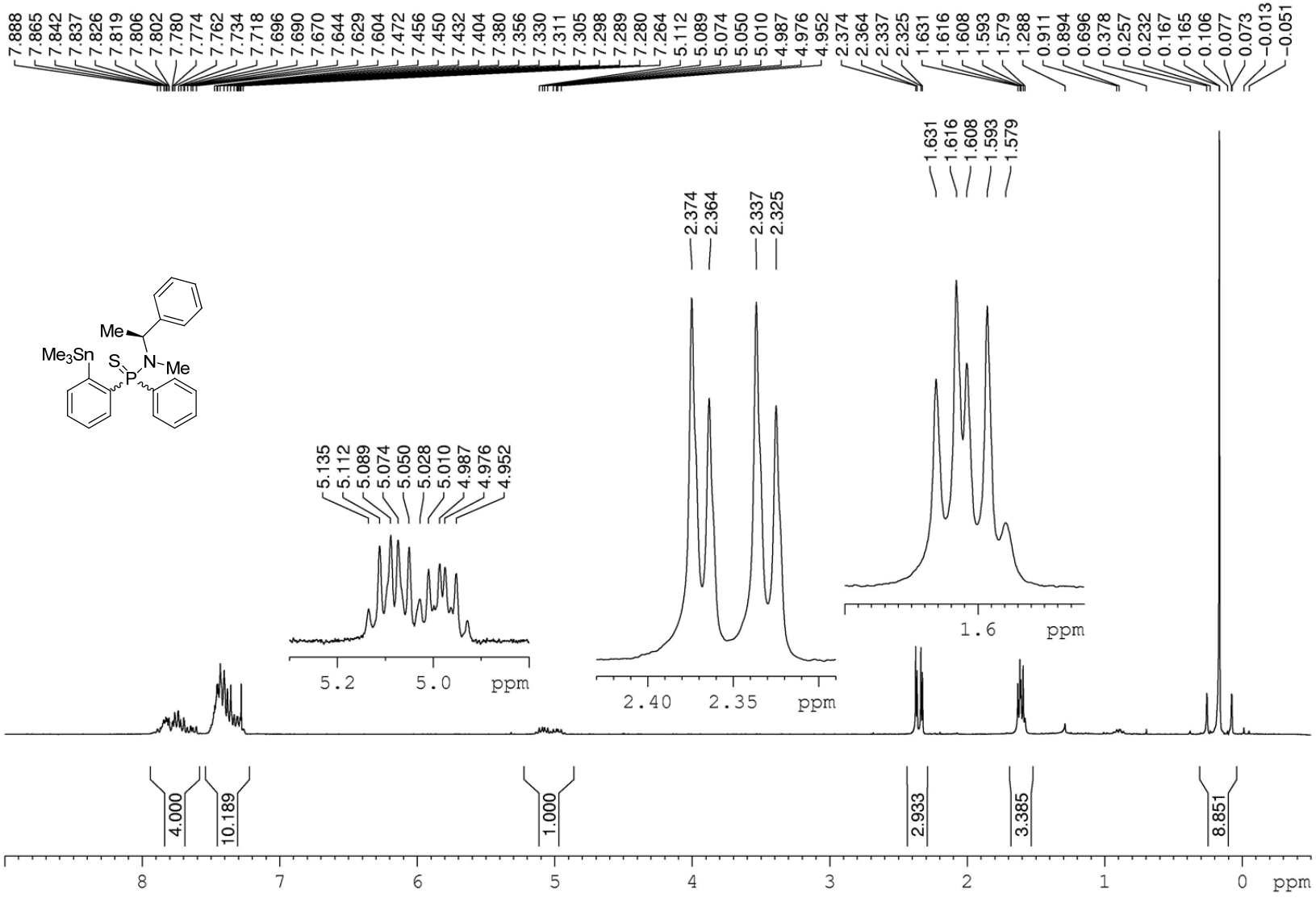

Figure S52. ^{1}H NMR spectrum (300.13 MHz) of **27** in $CDCl_3$.

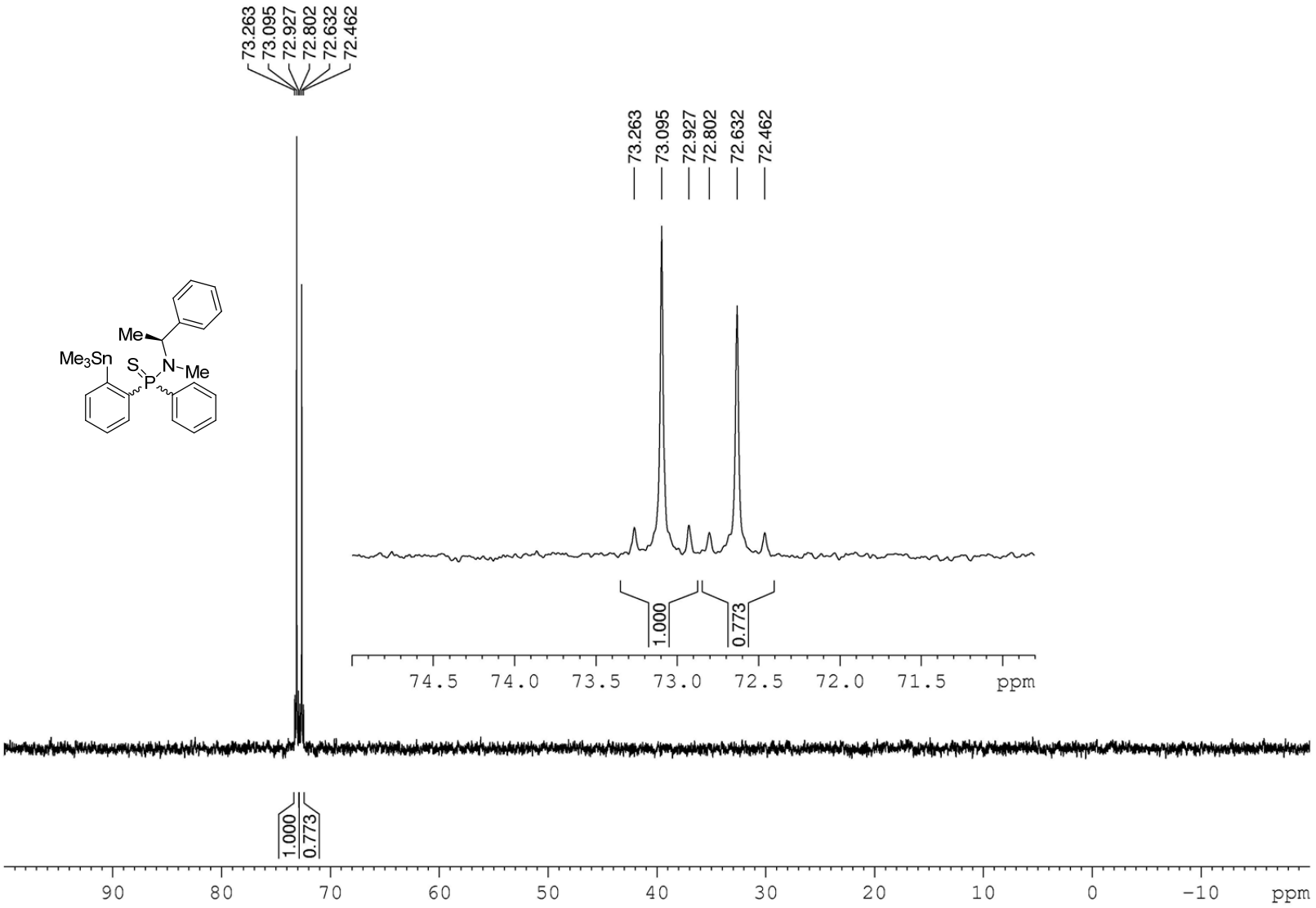

Figure S53. ^{31}P NMR spectrum (121.47 MHz) of **27** in $CDCl_3$.

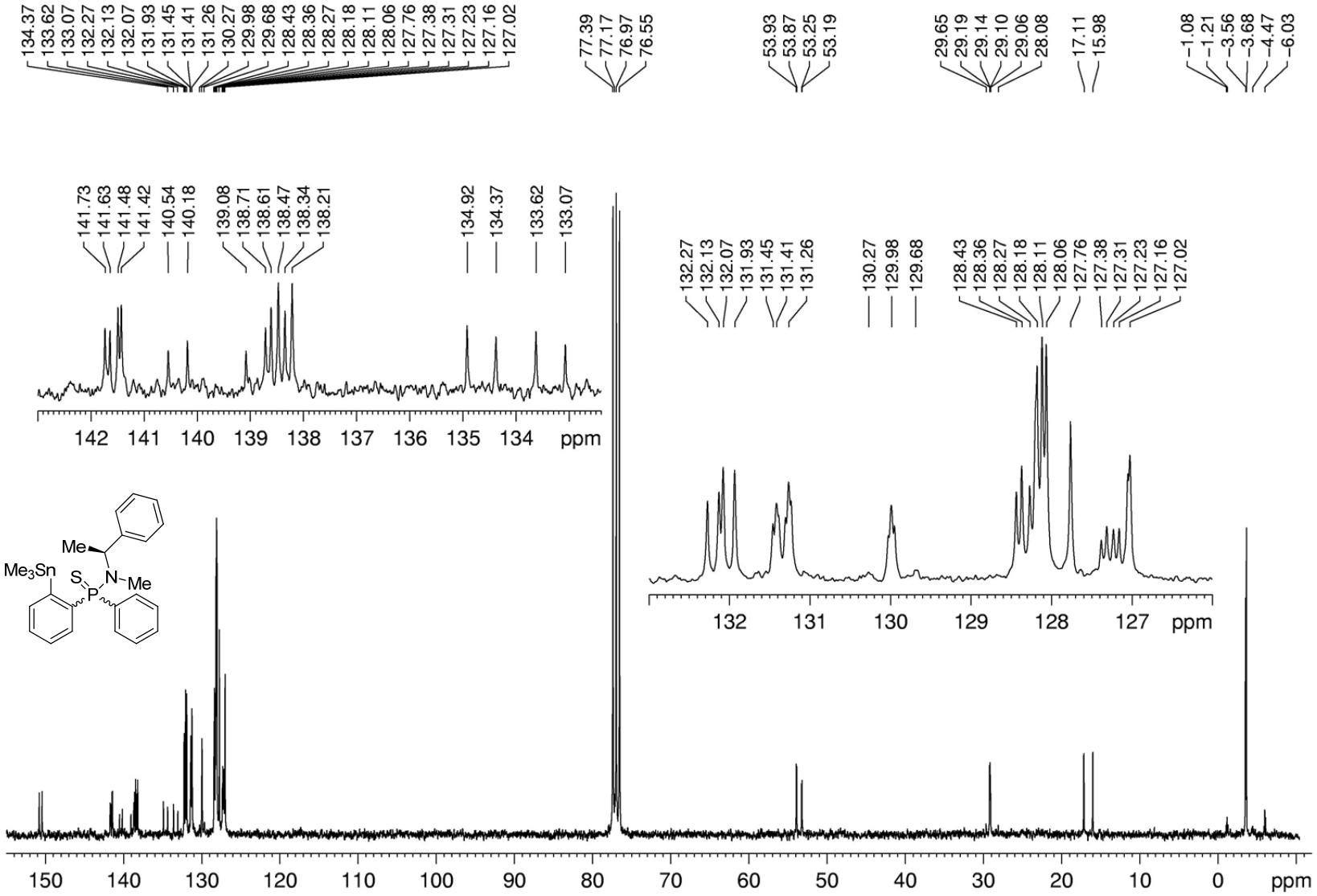

Figure S54. ^{13}C NMR spectrum (75.47 MHz) of **27** in $CDCl_3$.

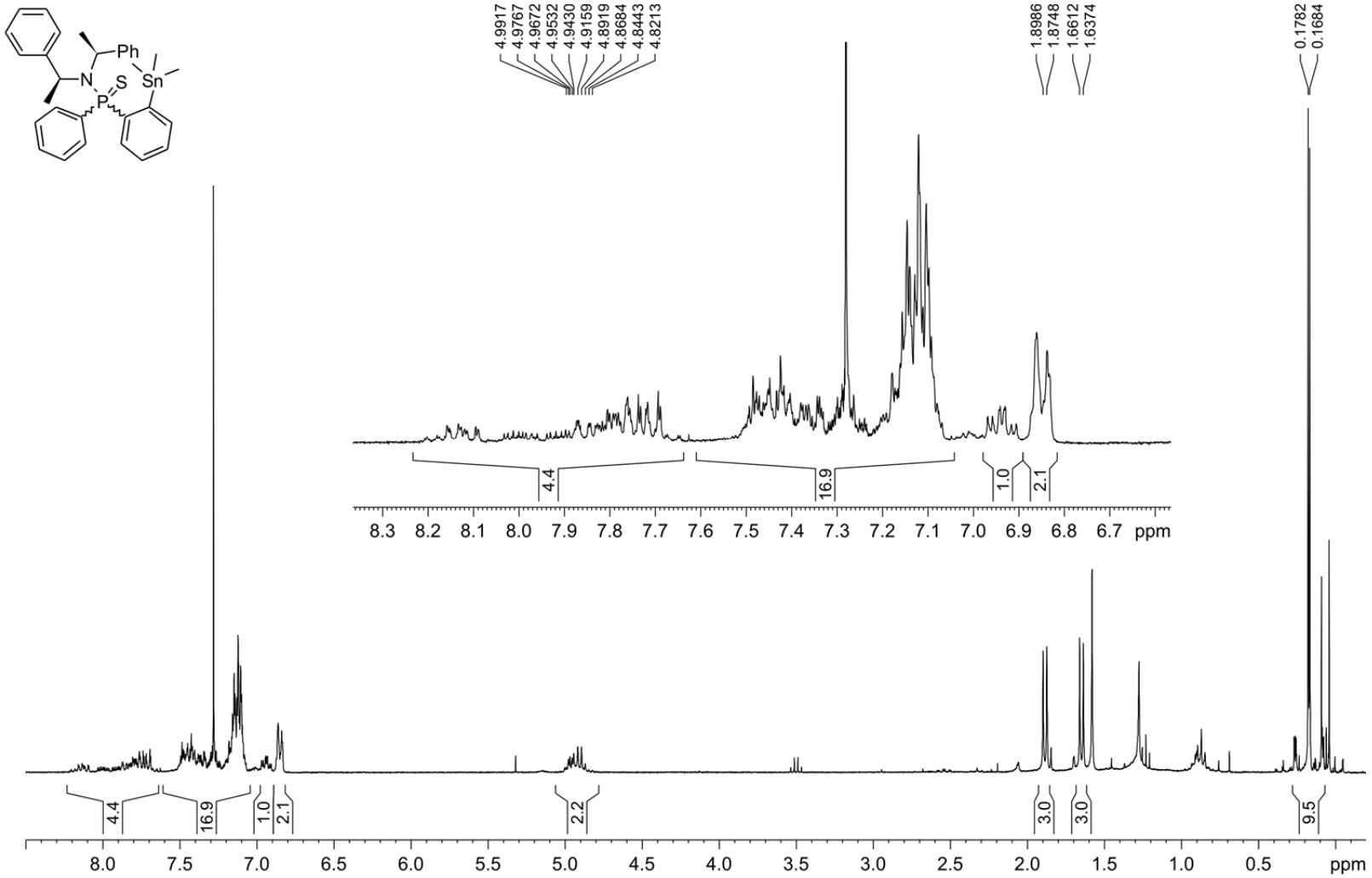

Figure S55. ^{1}H NMR spectrum (300.13 MHz) of **29** in $CDCl_3$.

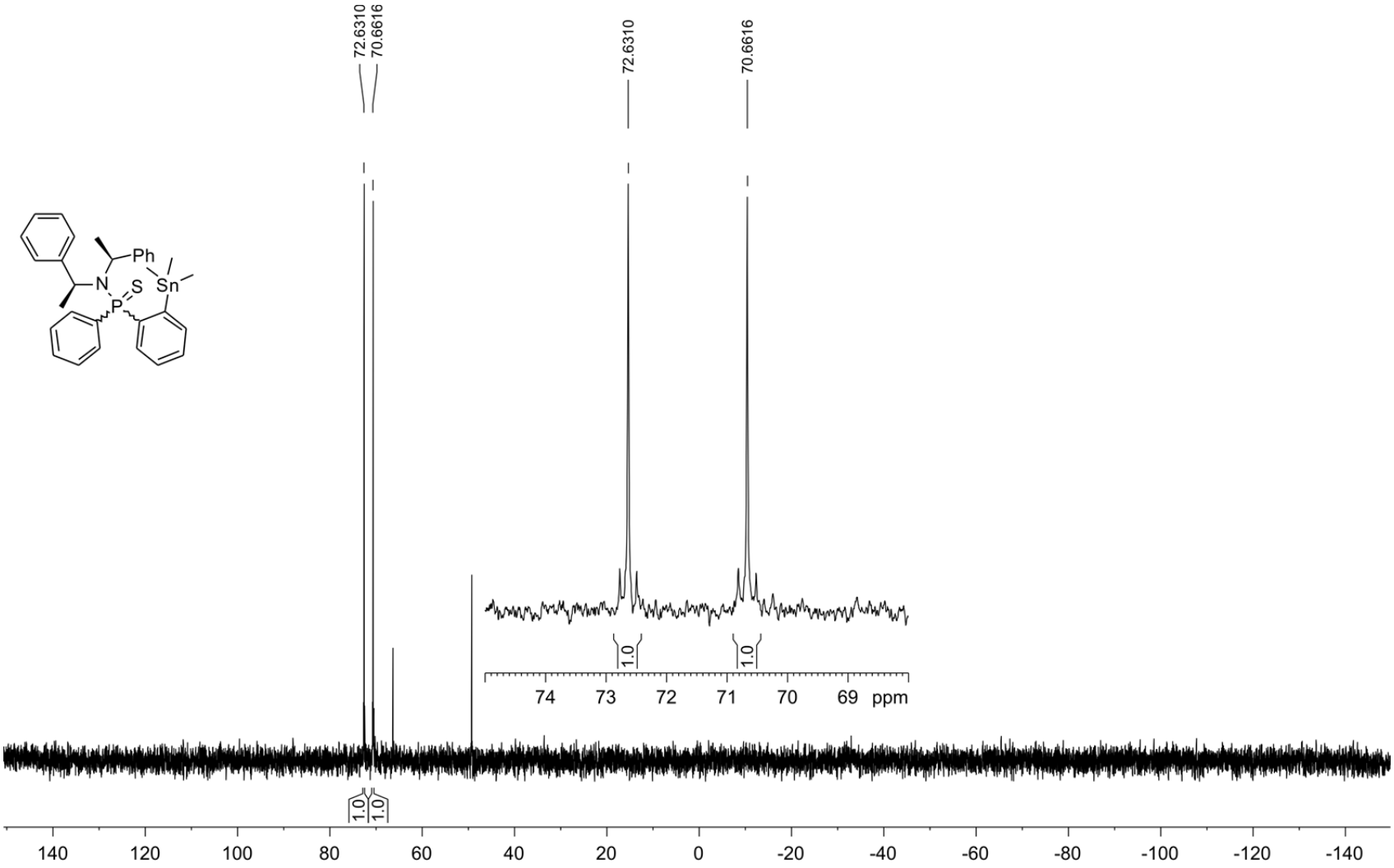

Figure S56. ^{31}P NMR spectrum (121.47 MHz) of **29** in $CDCl_3$.

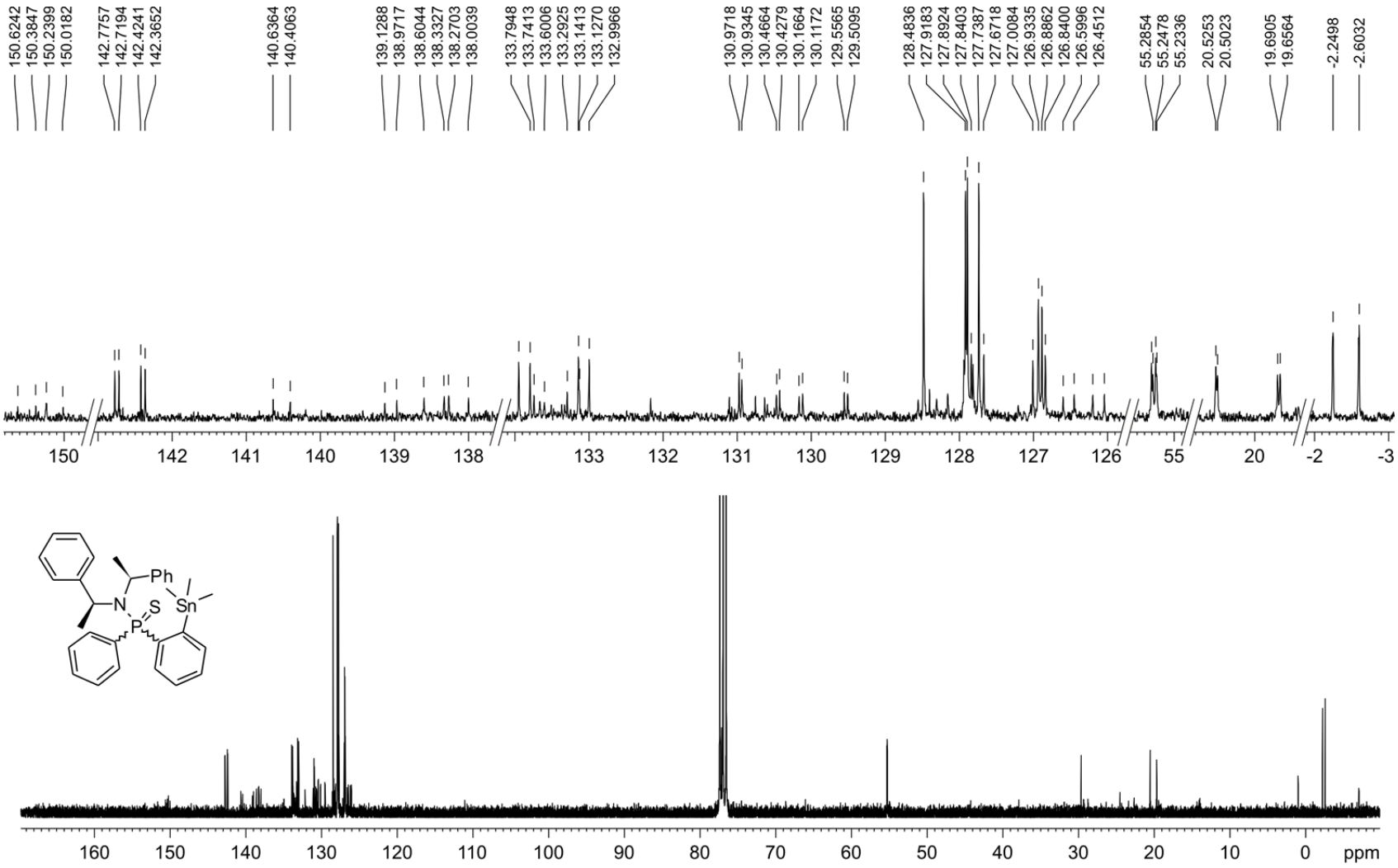

Figure S57. ^{13}C NMR spectrum (75.47 MHz) of **29** in $CDCl_3$.

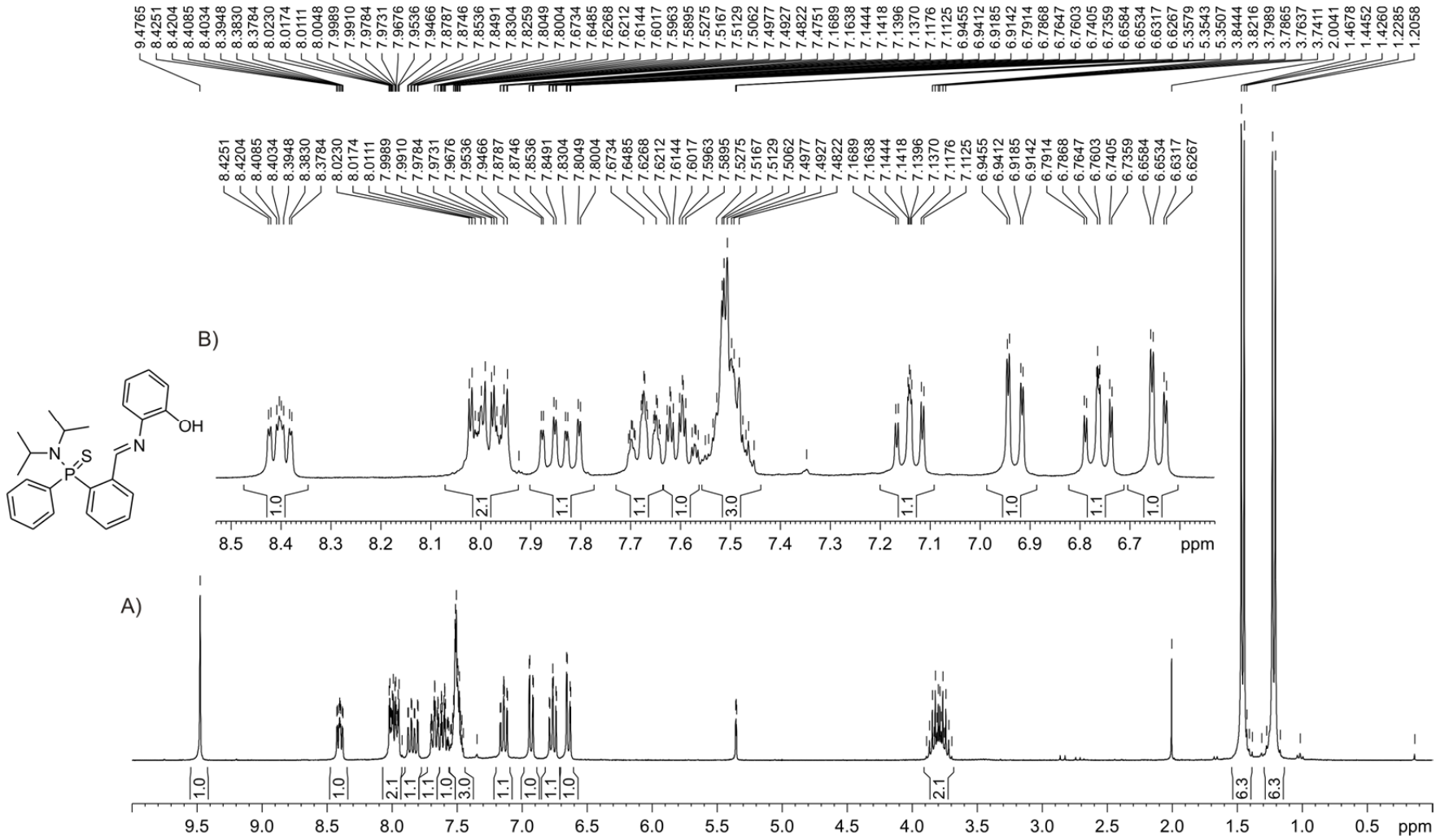

Figure S58. ^{1}H NMR spectrum (300.13 MHz) of **31** in CD_2Cl_2.

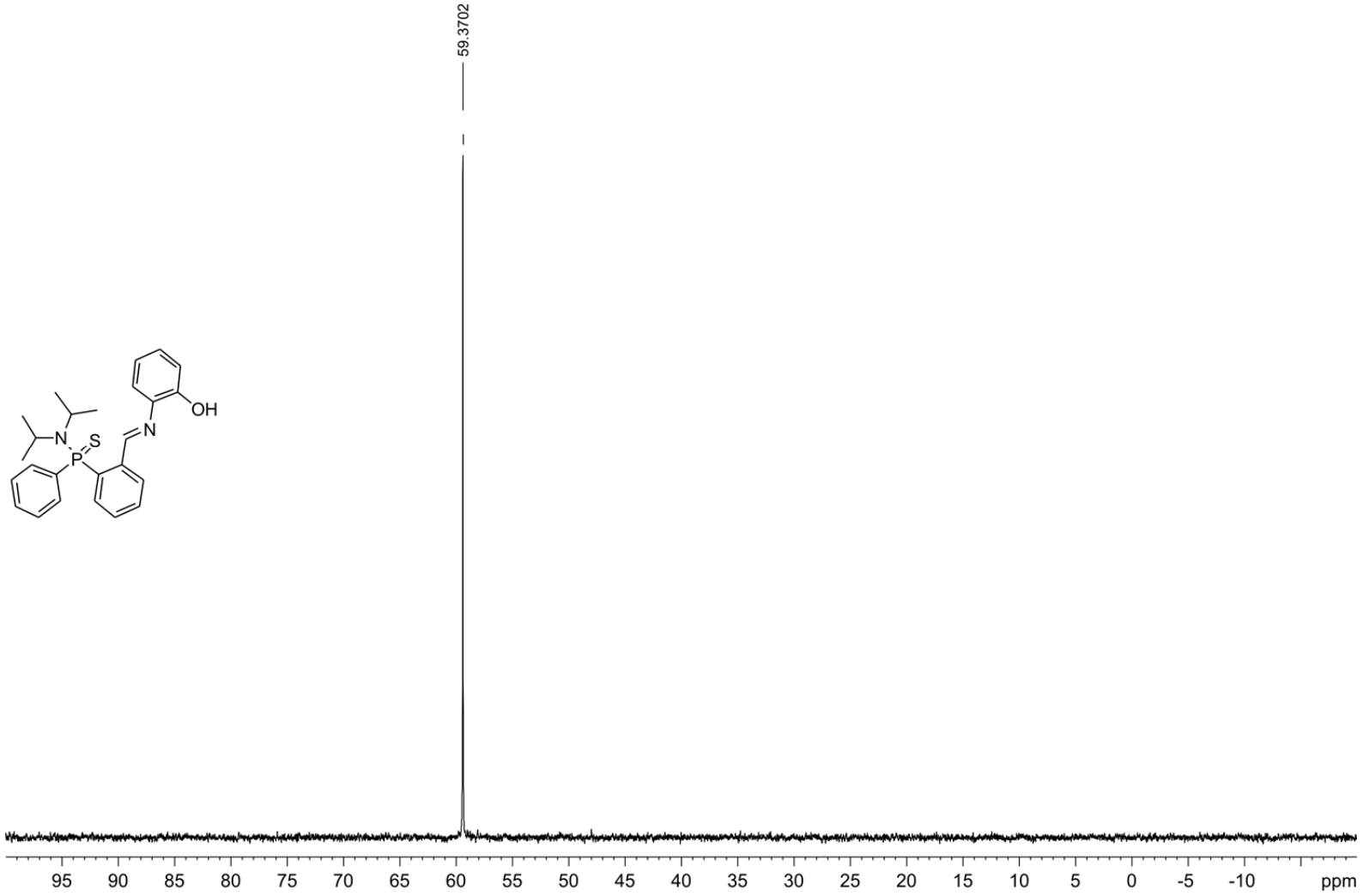

Figure S59. ^{31}P NMR spectrum (121.47 MHz) of **31** in CD_2Cl_2.

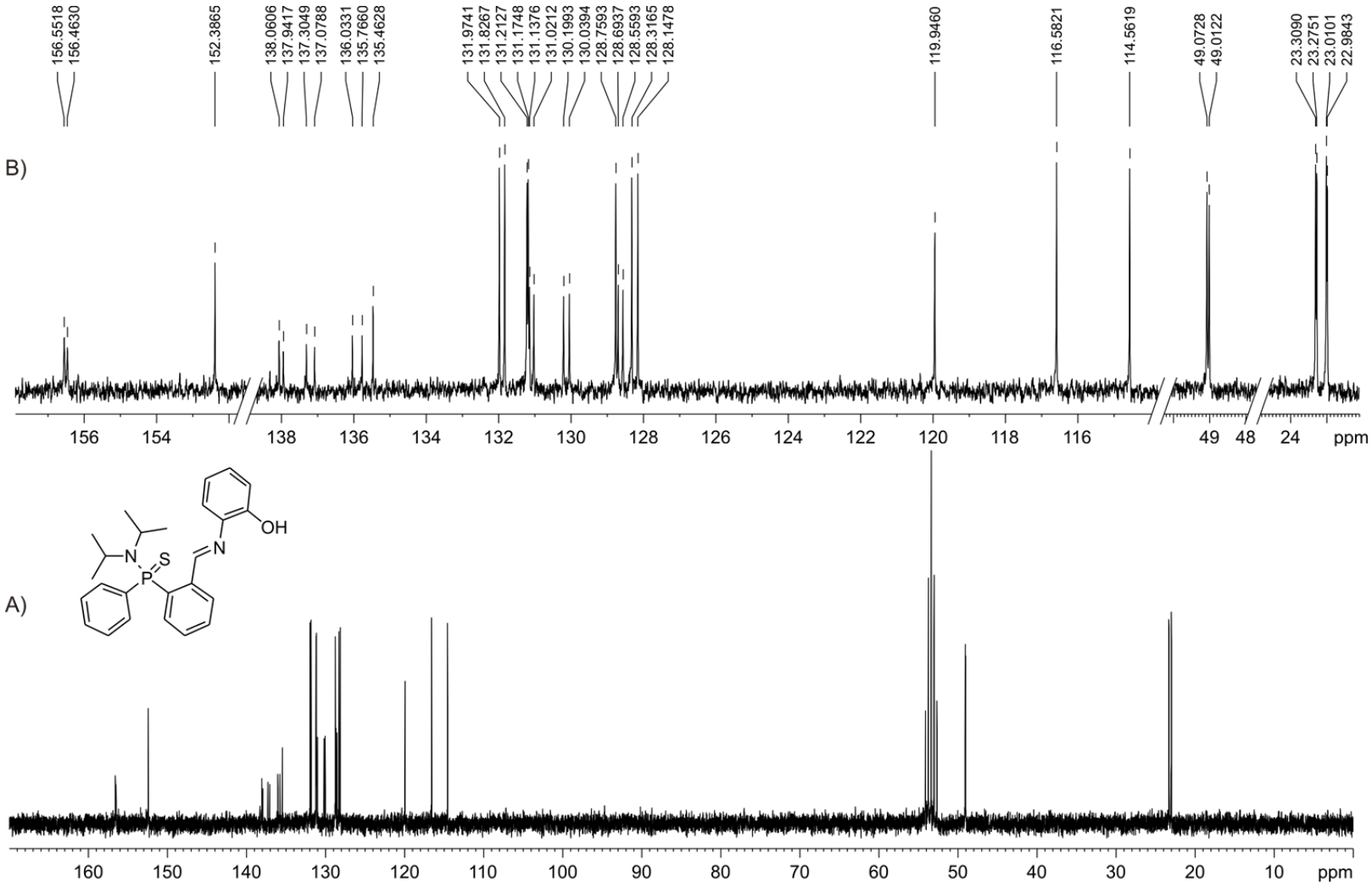

Figure S60. ^{13}C NMR spectrum (75.47 MHz) of **31** in CD_2Cl_2.

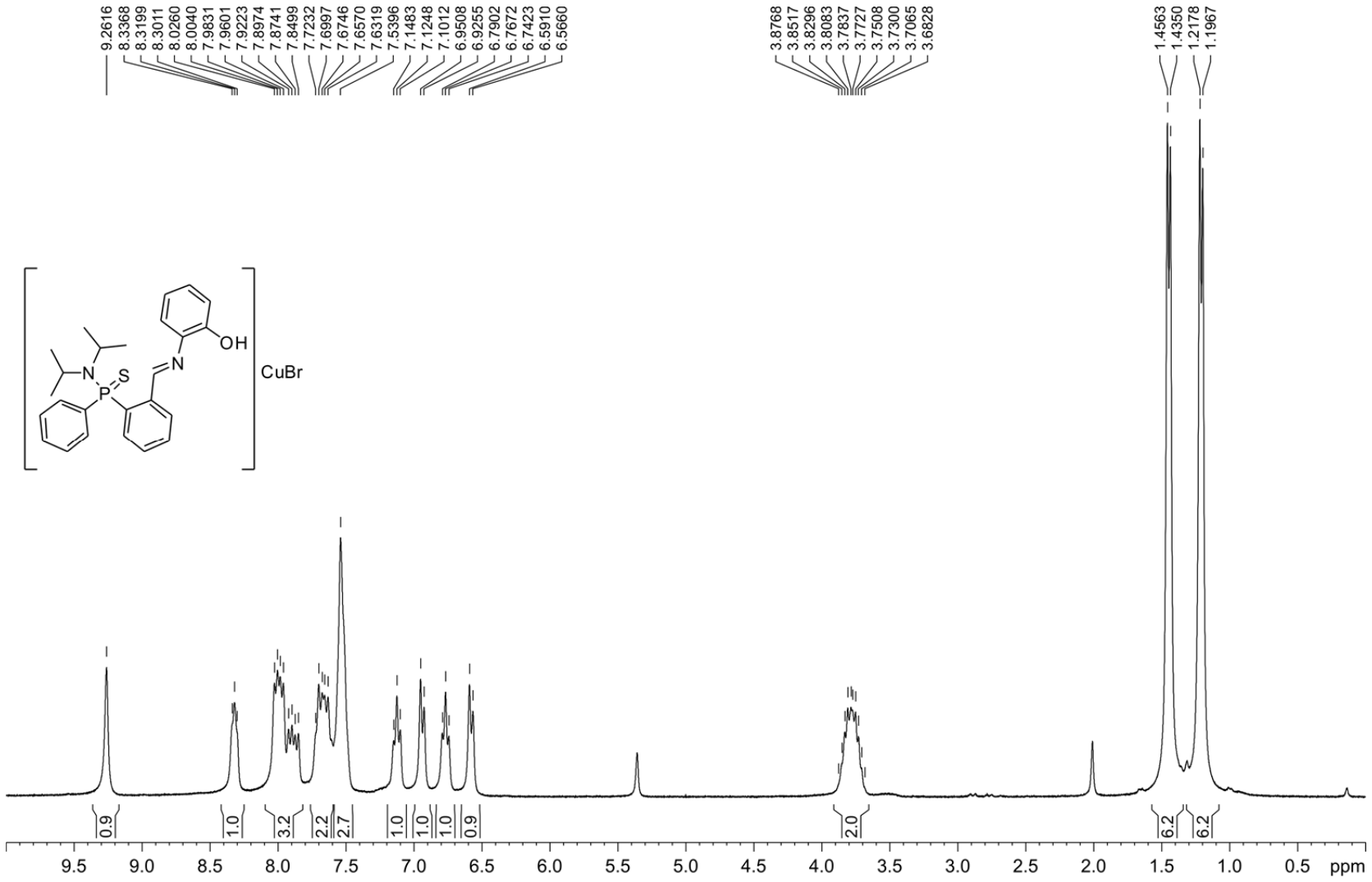

Figure S61. ^{1}H NMR spectrum (300.13 MHz) of **32** in CD_2Cl_2.

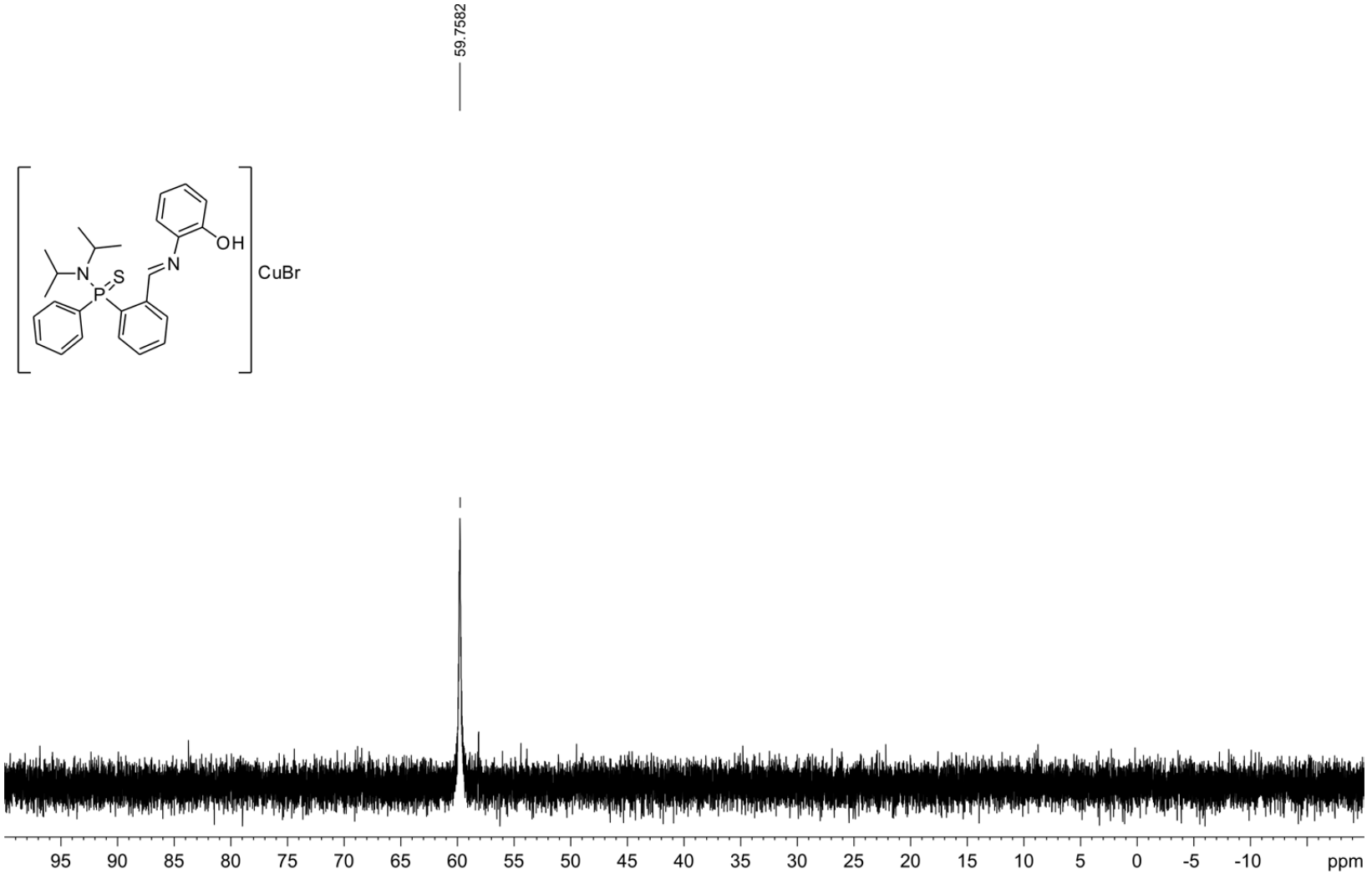

Figure S62. ^{31}P NMR spectrum (121.47 MHz) of **32** in CD_2Cl_2

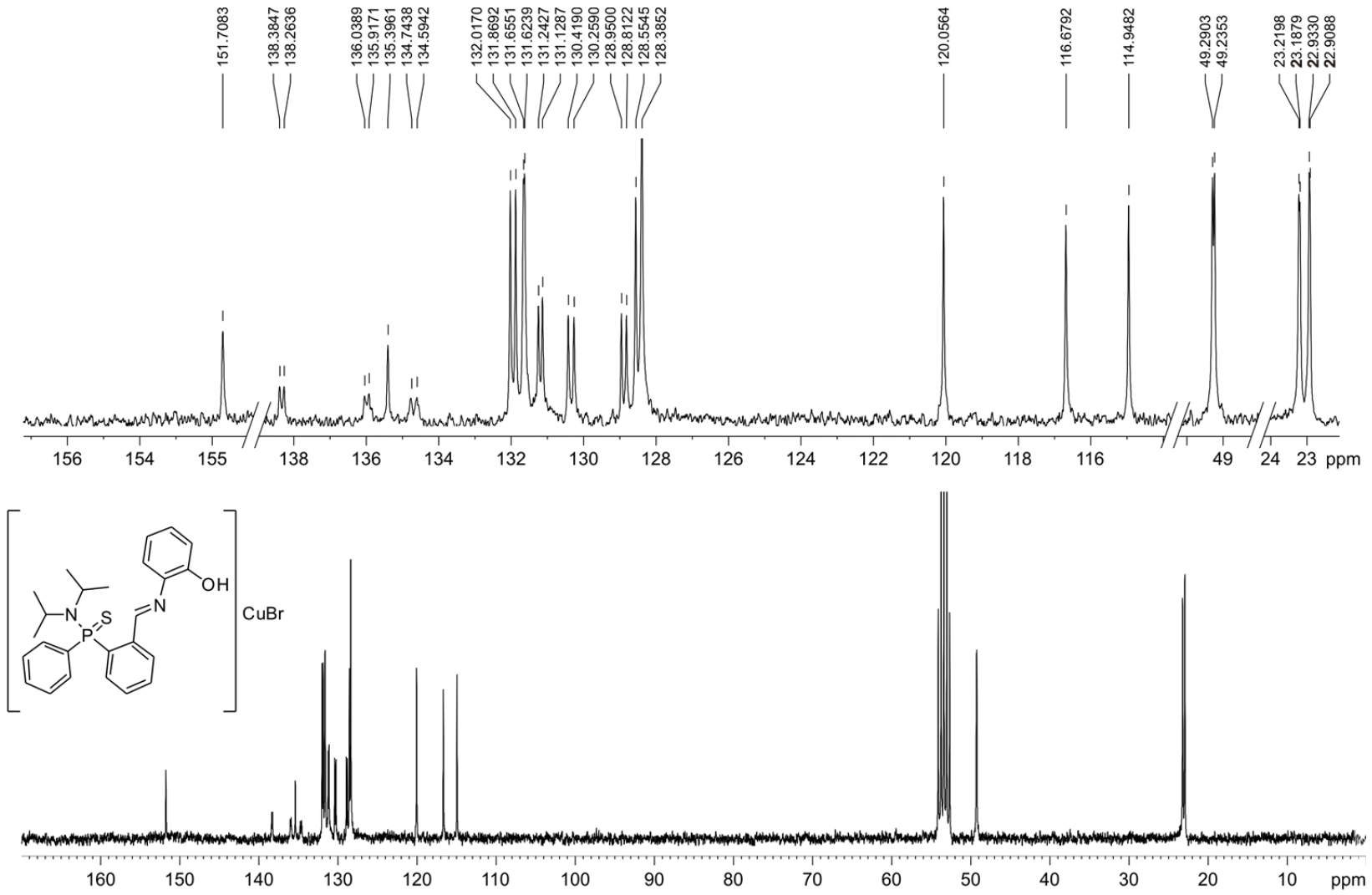

Figure S63. ^{13}C NMR spectrum (75.47 MHz) of **32** in CD_2Cl_2.

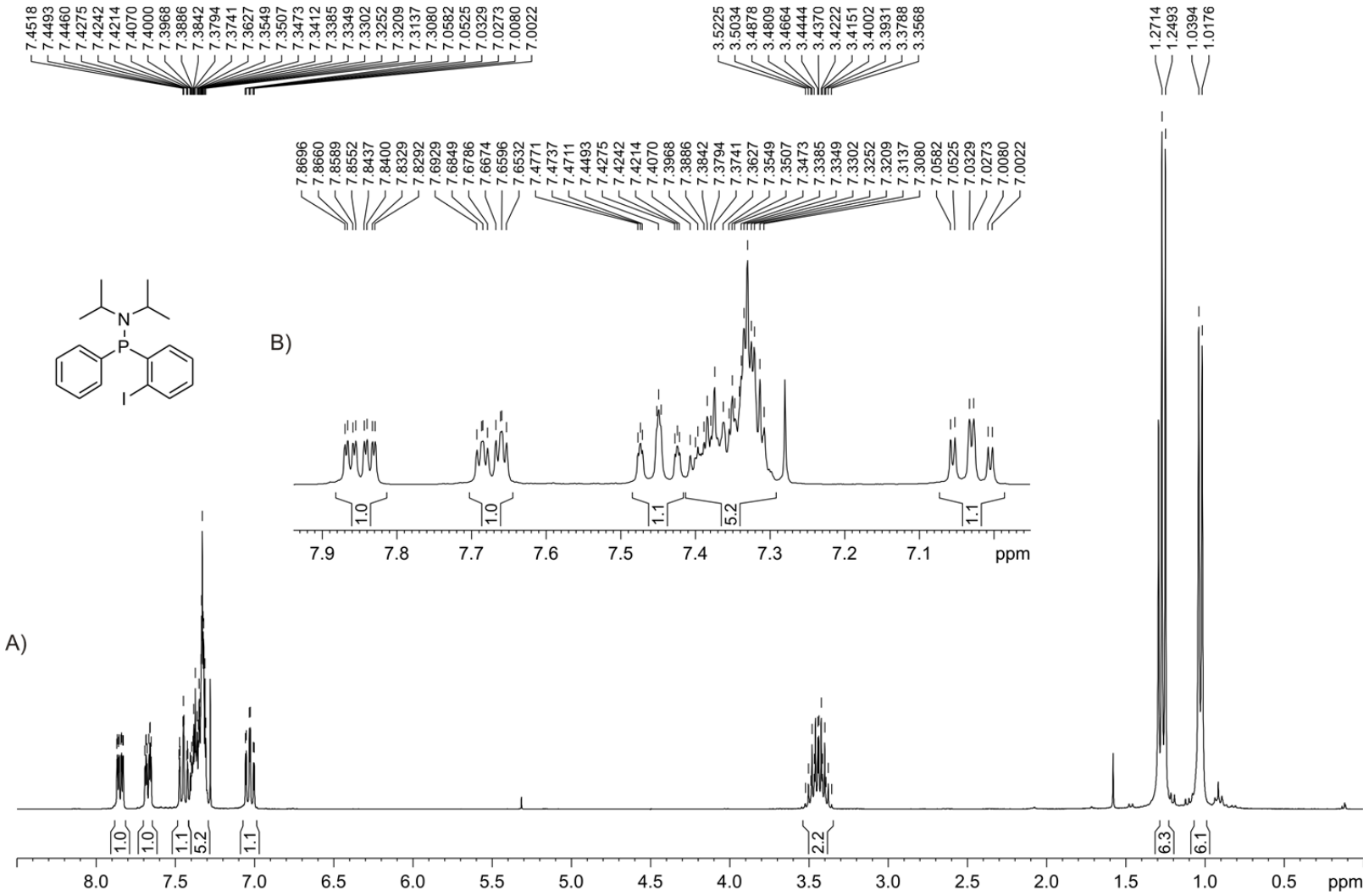

Figure S64. A) ^{1}H NMR spectrum (300.13 MHz) of **33** in $CDCl_3$. B) Expansion of the aromatic region of A).

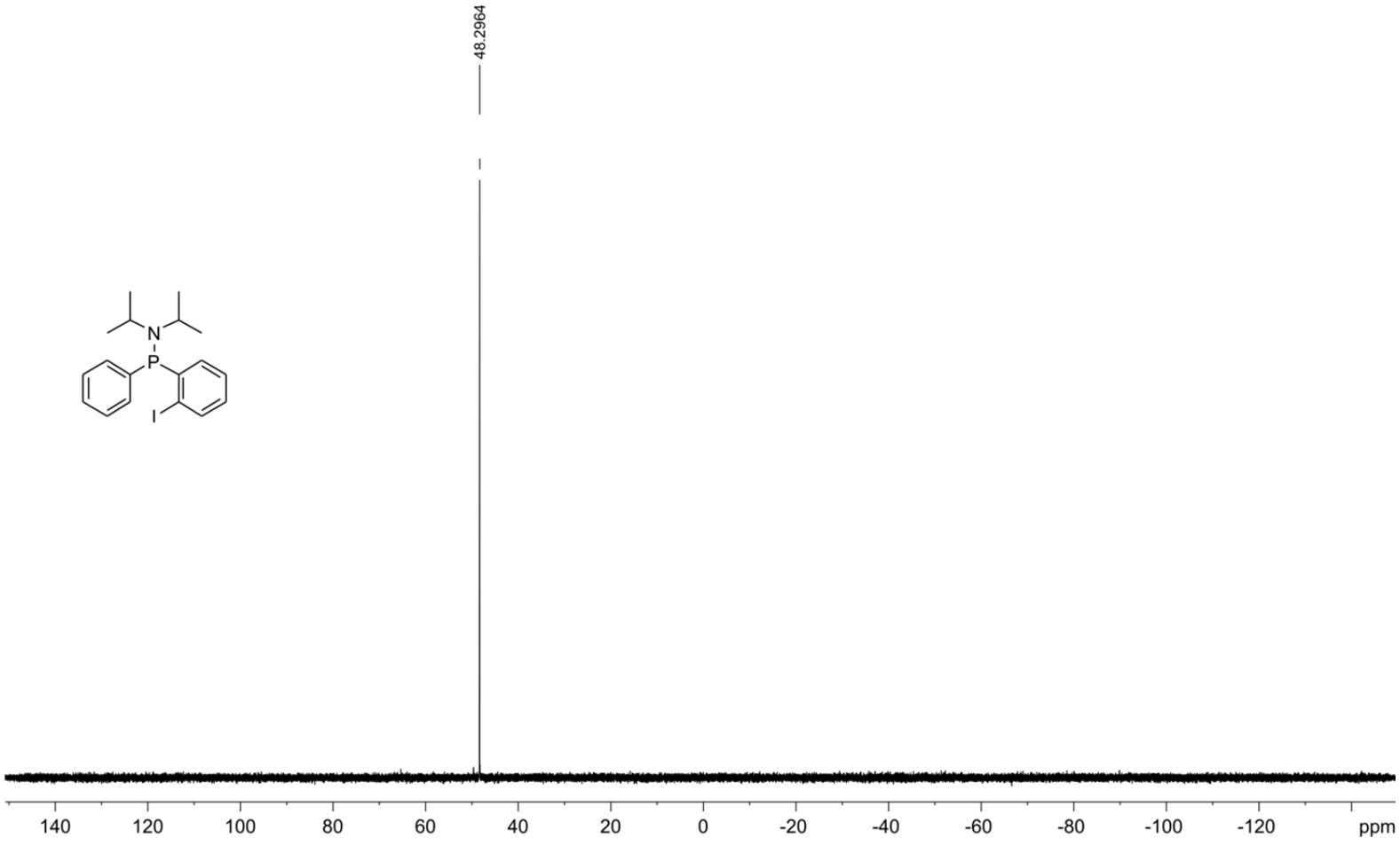

Figure S65. ^{31}P NMR spectrum (121.47 MHz) of **33** in $CDCl_3$.

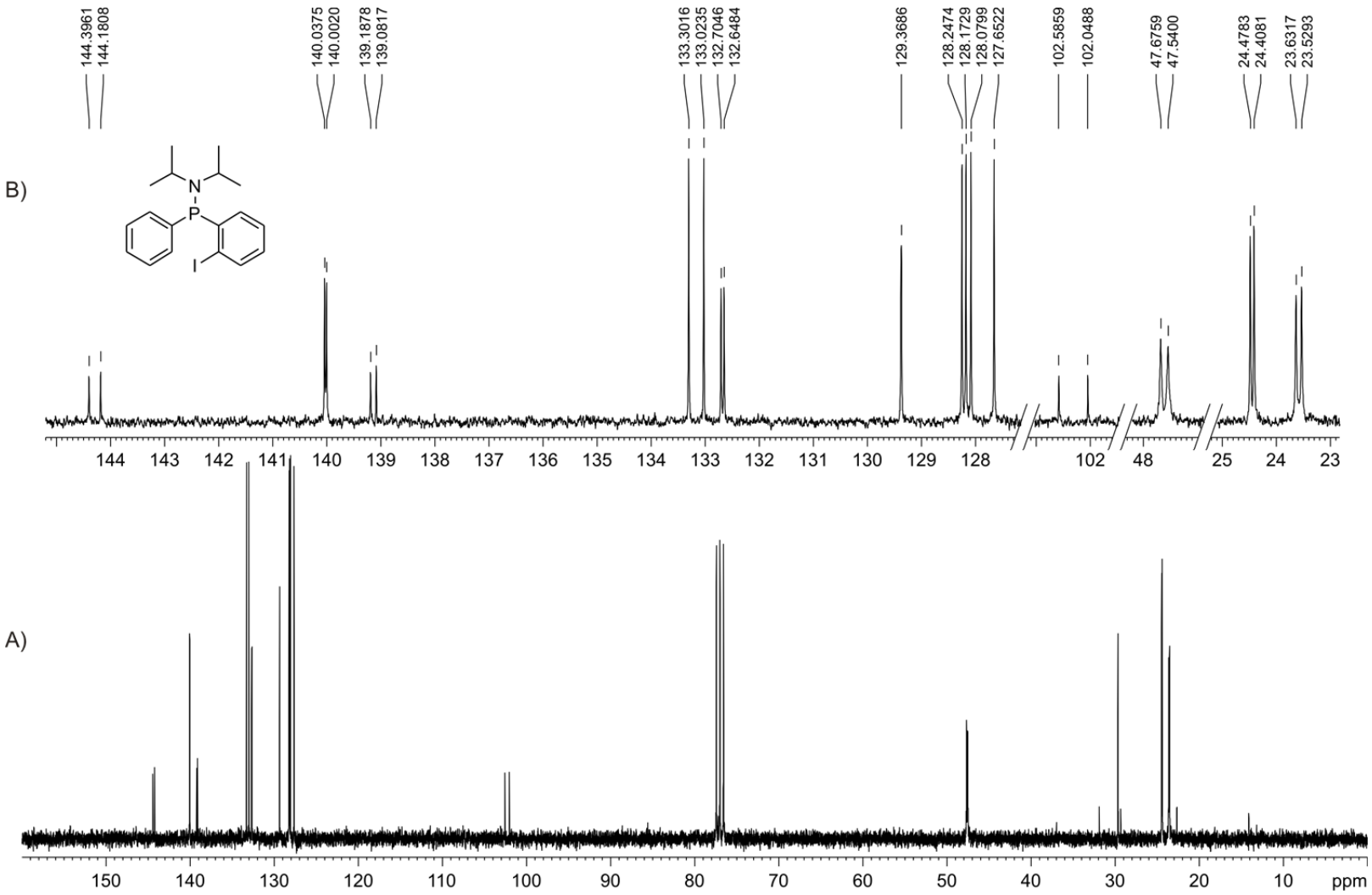

Figure S66. A) ^{13}C NMR spectrum (75.47 MHz) of **33** in $CDCl_3$. B) Expansion of A).

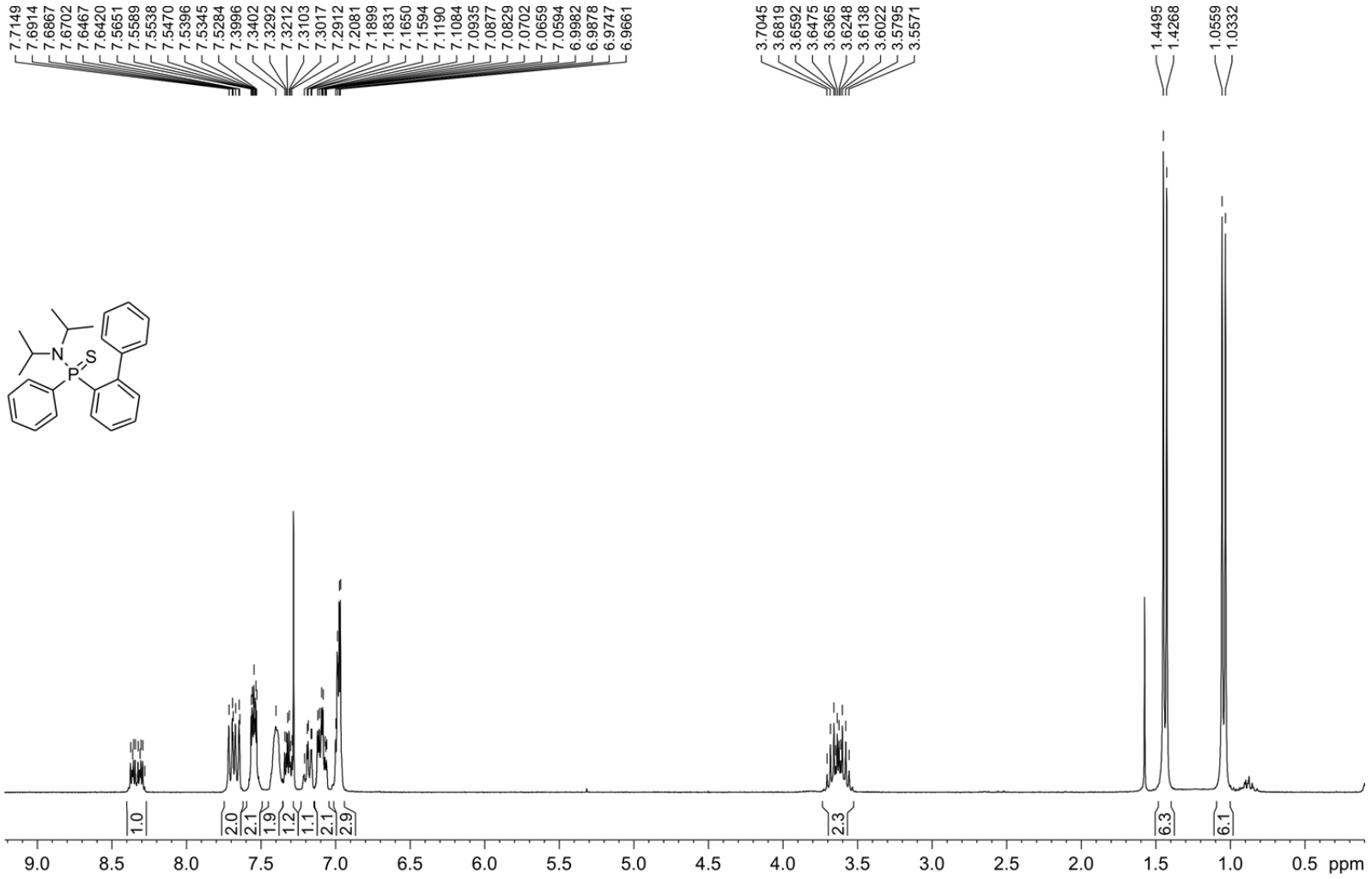

Figure S67. ^{1}H NMR spectrum (300.13 MHz) of **35** in $CDCl_3$.

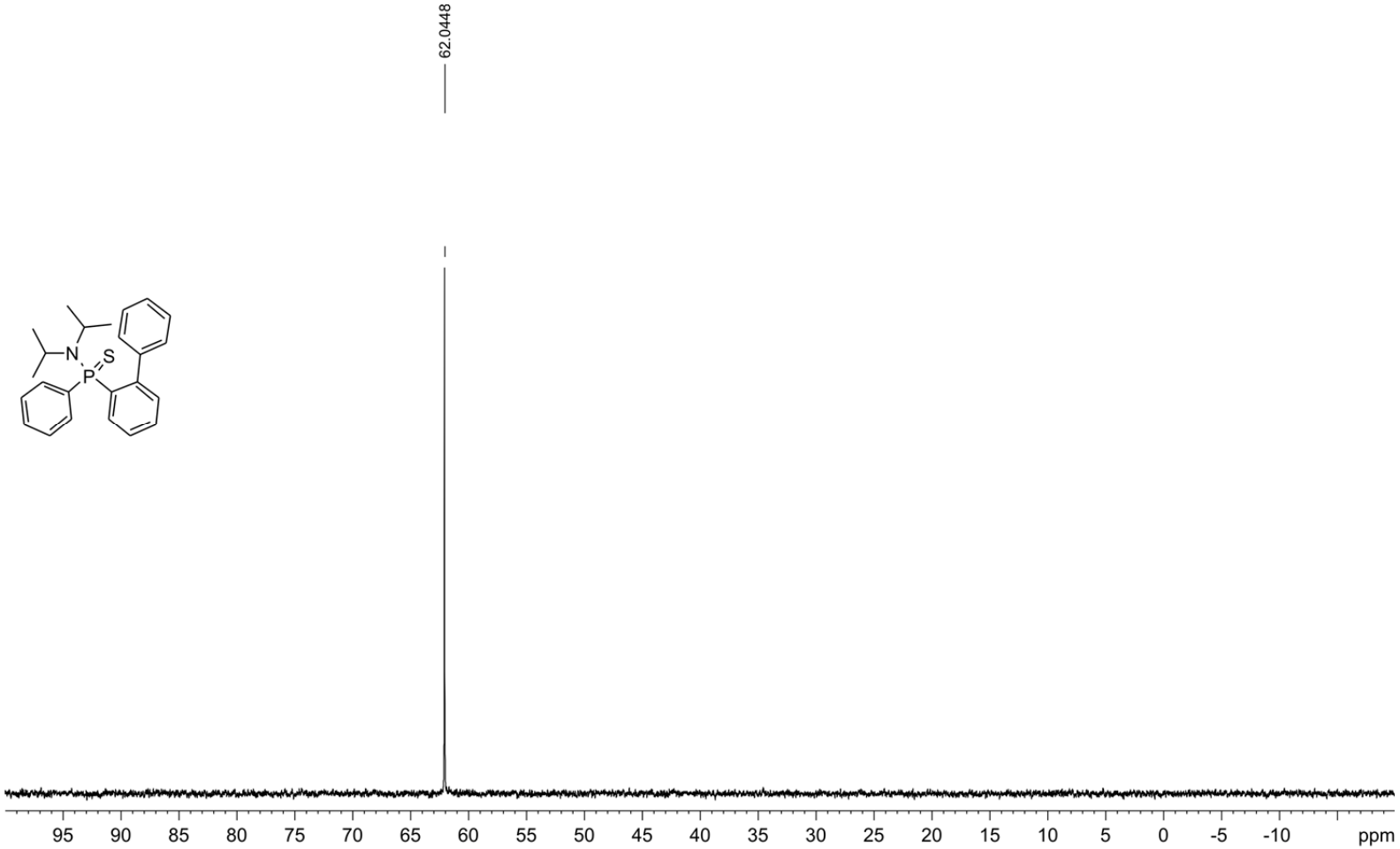

Figure S68. ^{31}P NMR spectrum (121.47 MHz) of **35** in $CDCl_3$.

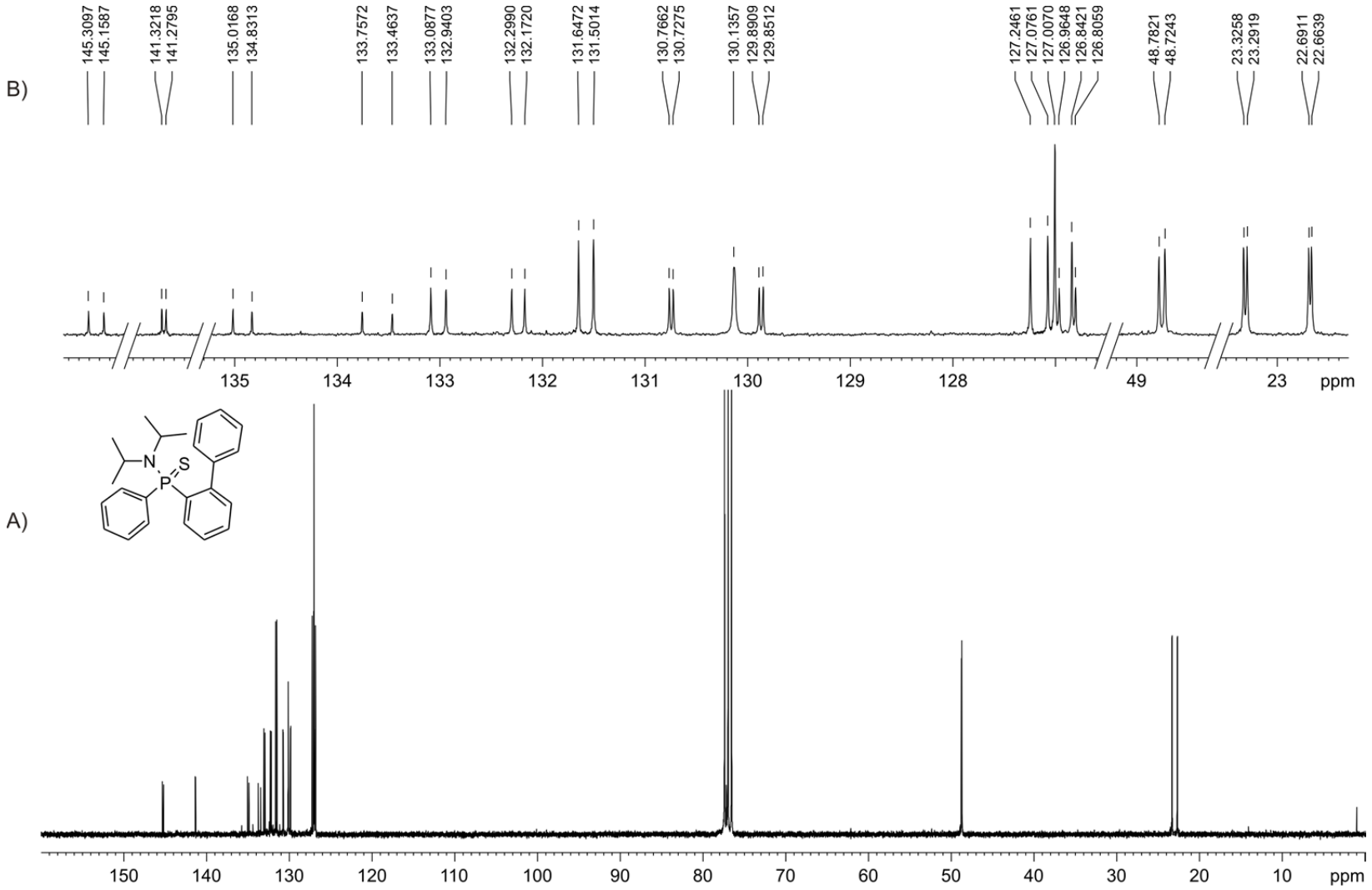

Figure S69. A) ^{13}C NMR spectrum (75.47 MHz) of **35** in $CDCl_3$. B) Expansion of A).

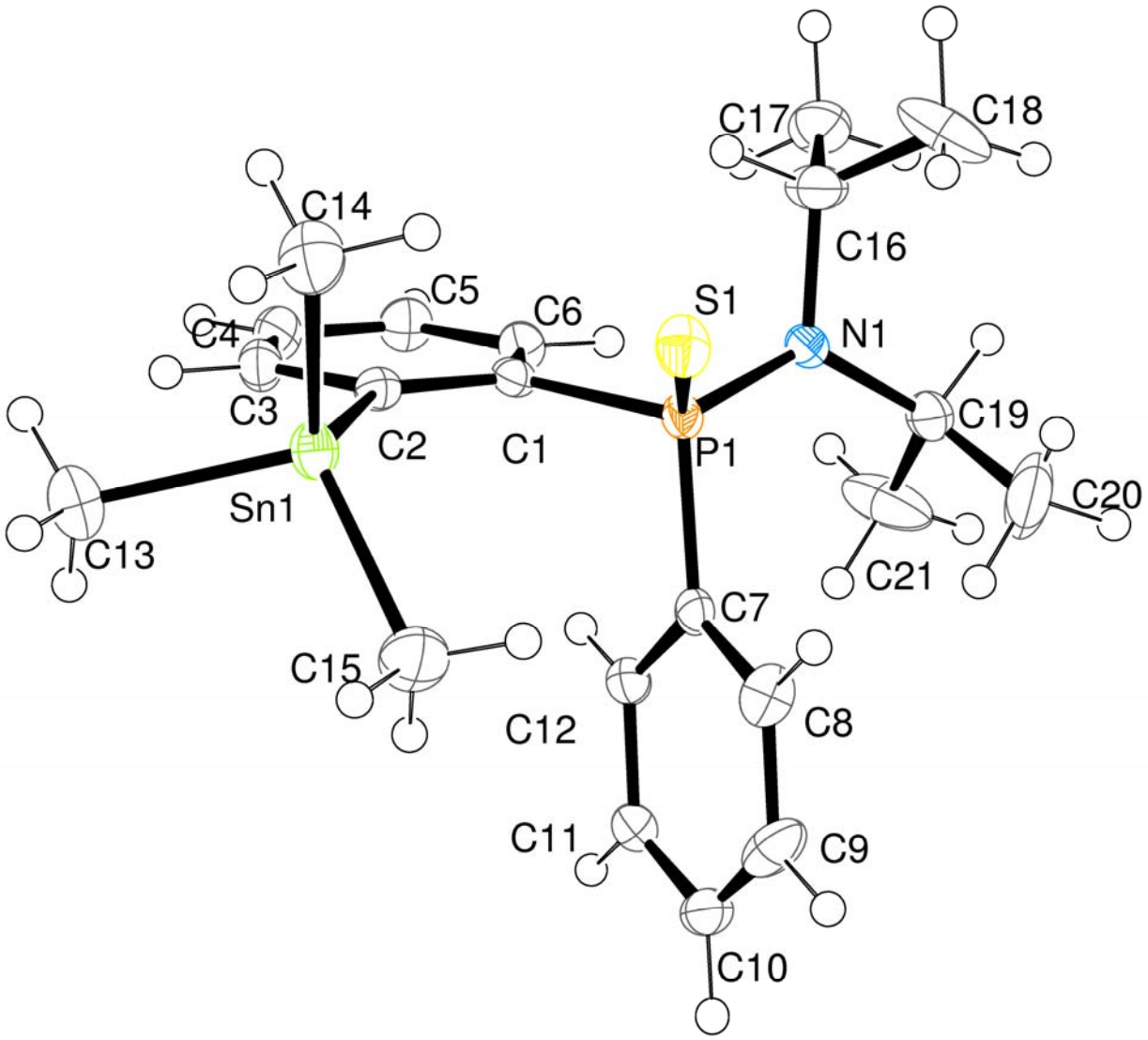

Figure S70. X-ray crystal structure of **9** (thermal ellipsoids shown at 50% probability) including atomic numbering.

Table S1. Crystal data and structure refinement for **9**.

Empirical formula	C21 H32 N P S Sn	
Formula weight	480.20	
Temperature	100(2) K	
Wavelength	1.54184 Å	
Crystal system	P21/c	
Space group	monoclinic	
Unit cell dimensions	a = 10.6237(1) Å	α= 90°.
	b = 16.3773(2) Å	β= 125.406(1)°.
	c = 15.8989(2) Å	γ = 90°.
Volume	2254.65(4) $Å^3$	
Z	4	
Density (calculated)	1.415 Mg/m^3	
Absorption coefficient	10.562 mm^{-1}	
F(000)	984	
Crystal size	0.27 x 0.14 x 0.13 mm^3	
Theta range for data collection	4.35 to 68.55°.	
Index ranges	-12<=h<=12, -18<=k<=19, -19<=l<=18	
Reflections collected	14406	
Independent reflections	4097 [R(int) = 0.0327]	
Completeness to theta = 67.50°	99.6 %	
Absorption correction	Empirical	
Max. and min. transmission	1.000 and 0.5559	
Refinement method	Full-matrix least-squares on F^2	
Data / restraints / parameters	4097 / 0 / 226	
Goodness-of-fit on F^2	1.045	
Final R indices [I>2sigma(I)]	R1 = 0.0272, wR2 = 0.0686	
R indices (all data)	R1 = 0.0301, wR2 = 0.0708	
Largest diff. peak and hole	0.439 and -0.931 $e.Å^{-3}$	

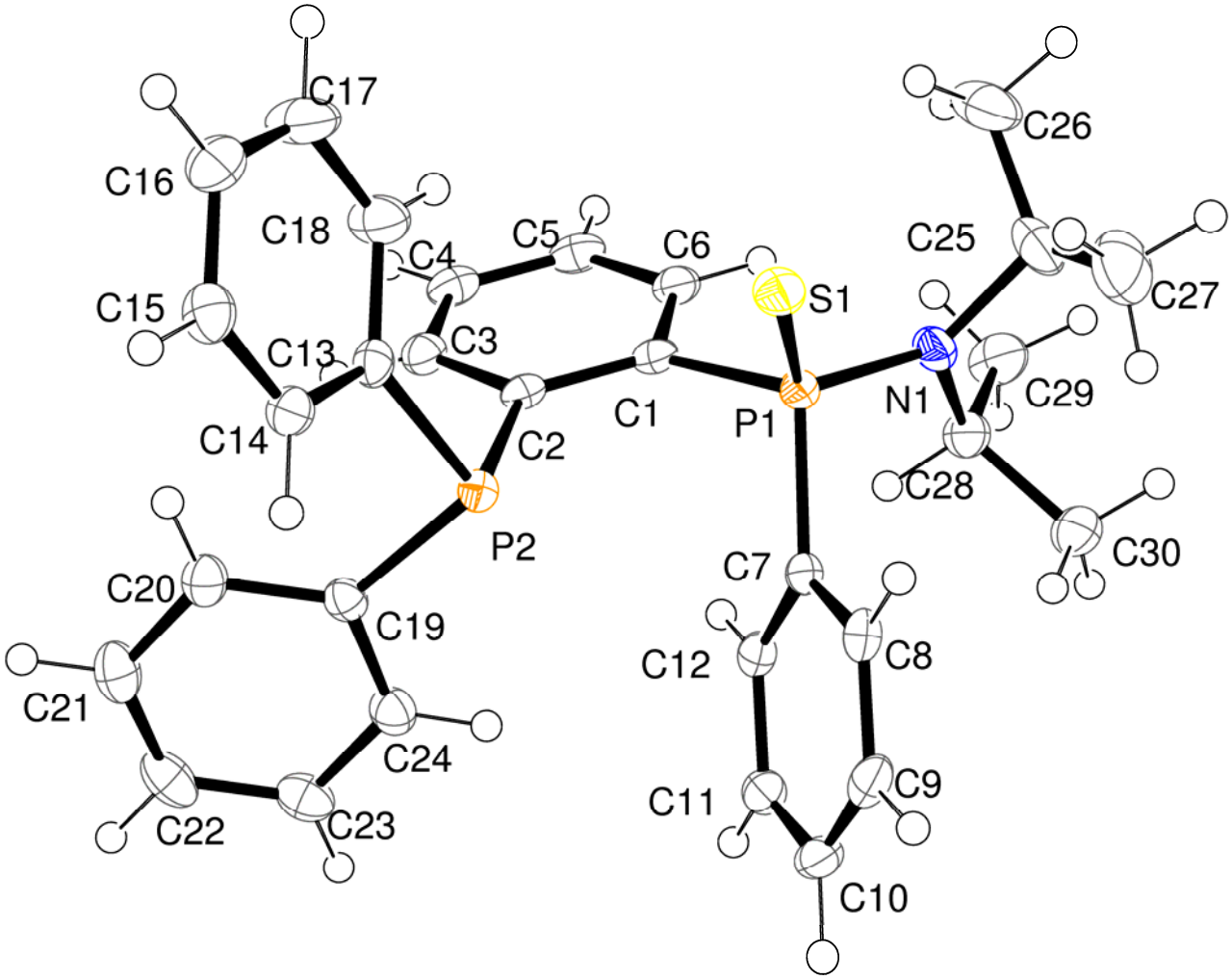

Figure S71. X-ray crystal structure of **12** (thermal ellipsoids shown at 50% probability) including atomic numbering.

Table S2. Crystal data and structure refinement for compound **12**.

Empirical formula	C30 H33 N P2 S	
Formula weight	501.57	
Temperature	100(2) K	
Wavelength	0.71073 Å	
Crystal system	Monoclinic	
Space group	P 21/c	
Unit cell dimensions	a = 13.6300(5) Å	α= 90°.
	b = 10.2681(3) Å	β= 119.548(2)°.
	c = 22.3237(6) Å	γ = 90°.
Volume	2717.96(15) $Å^3$	
Z	4	
Density (calculated)	1.226 Mg/m^3	
Absorption coefficient	0.256 mm^{-1}	
F(000)	1064	
Crystal size	1.41 x 0.429 x 0.339 mm^3	
Theta range for data collection	1.72 to 24.42°.	
Index ranges	-15<=h<=15, -11<=k<=11, -25<=l<=22	
Reflections collected	13903	
Independent reflections	4468 [R(int) = 0.0906]	
Completeness to theta = 24.42°	99.9 %	
Absorption correction	Refined	
Max. and min. transmission	1.0473 and 0.6756	
Refinement method	Full-matrix least-squares on F^2	
Data / restraints / parameters	4468 / 0 / 311	
Goodness-of-fit on F^2	1.027	
Final R indices [I>2sigma(I)]	R1 = 0.0423, wR2 = 0.1080	
R indices (all data)	R1 = 0.0443, wR2 = 0.1095	
Largest diff. peak and hole	0.620 and -0.377 $e.Å^{-3}$	